RECIPROCAL REGULATION OF GLUTAMINE METABOLISM AND REACTIVE OXYGEN SPECIES

by

Naniye Cetinbas

M.Sc., Simon Fraser University, 2009

B.Sc., Yildiz Technical University, 2003

A THESIS SUBMITTED IN PARTIAL FULFILLMENT OF

THE REQUIREMENTS FOR THE DEGREE OF

DOCTOR OF PHILOSOPHY

in

THE FACULTY OF GRADUATE AND POSTDOCTORAL STUDIES

(Pathology and Laboratory Medicine)

THE UNIVERSITY OF BRITISH COLUMBIA

(Vancouver)

December 2013

Abstract

Reactive oxygen species (ROS) are byproducts of normal cellular processes. While low or moderate levels of ROS promote and sustain oncogenic properties of cancer cells, excessive amounts are detrimental. Cancer cells counterbalance increased ROS production by engaging ROS-scavenging systems, which heavily rely on the antioxidants GSH and NADPH that can be synthesized from glutamine (GLN). Although GLN is not an essential amino acid, some cancer cells depend on exogenous GLN for survival, a phenotype known as GLN addiction. GLN plays versatile roles in cells from synthesis of macromolecules to redox balance. However, why GLN dependence for survival varies among different cancer cell types is not fully understood. This thesis tested the hypothesis that GLN addiction phenotype is ROS dependent. We first showed that loss of Hace1, a tumor suppressor that regulates ROS levels, results in increased GLN metabolism and GLN addiction. Inhibition of ROS reverses GLN addiction phenotype of Hace1 deficient cells, providing the first evidence that loss of a tumor suppressor leads to GLN addiction due to increased ROS levels. Using a panel of human cancer cell lines we established that GLN deprivation induces cell death in GLN addicted cells primarily by depleting intracellular antioxidant pools, resulting in increased ROS levels and oxidative damage. Furthermore GLN deprivation results in ROS-dependent elevation of glucose uptake in GLN addicted cells, which exacerbates oxidative stress causing cell death. Finally, we showed that GLN addicted cells are more sensitive to exogenous oxidants without GLN, and that AMPK mediated upregulation of ASCT2 expression and GLN uptake confers resistance to oxidative

stress in GLN addicted cells. These studies establish the reciprocal regulation of GLN metabolism and oxidative stress in cancer cells.

Preface

Contents of this thesis dissertation are novel and based on the research conducted by myself. Dihydroethidium staining and data analysis (Chapter 2, Figure 7A-D) was performed by Mads Daugaard, a postdoctoral fellow in Sorensen Laboratory. Alejandra Lopez, a research technician in Sorensen Laboratory, helped with In Cell data analysis (Chapter 2, Figure 1A-C, Figure 6C, Figure 7E). I was responsible for design and set up of these experiments. The metabolic tracing of glutamine carbons in Hace1 *wild type* and Hace1 *knock out* mouse embryonic fibroblasts (Chapter 2, Figure 4D-G) was done in collaboration with Dr. Ralph DeBerardinis Laboratory (University of Texas, South Western Medical Centre). I performed the metabolic labeling/metabolite extraction and Andrew Mullen, a PhD student in Dr. DeBerardinis Laboratory carried out mass spectrometry and data analysis.

Table of Contents

List of Tables

List of Figures

List of Abbreviations

ADP: Adenosine di-phosphate

AMP: Adenosine mono-phosphate

AMPK: AMP activated kinase

ATP: Adenosine tri-phosphate

CAT: Catalase

DCFDA: 5-(and-6)-chloromethyl-2', 7'-dichlorodihydrofluorescein diacetate, acetyl ester

DHE: Dihydroethidium

FDG: ^{18}F-2-deoxyglucose

GLN: Glutamine

GLS: Glutaminase

Glu: Glutamate

GPNA: Gamma-glutamyl-p-nitroanilide

GPX: Glutathione peroxidase

GR: Glutathione reductase

GRX: Glutaredoxin

GSH: Reduced glutathione

GSSG: Oxidized glutathione

Hace1: Hect domain and ankyrin repeat containing E3 ubiquitin protein ligase 1

HBSS: Hank's balanced salt solution

MEF: Mouse embryonic fibroblasts

NAC: N-acetyl cysteine

NADPH: Nicotinamide adenine dinucleotide phosphate

NAPA: Sodium phenyl acetate

Nox: NADPH oxidase

OAA: Oxaloacetate

PET: Positron emission tomography

PI: Propidium iodide

PL: Piperlongumine

ROS: Reactive oxygen species

SOD: Superoxide dismutase

TCA: Tricarboxylic acid

Trx: Thioredoxin

TXNIP: Thioredoxin interacting protein

α-KG: Alpha-keto glutarate

Glossary

GLN Addiction: Dependency on GLN for survival.

TCA cycle: A series of chemical reactions used by aerobic organisms to generate energy and intermediates that are used for biosynthesis of macromolecules.

Anaplerosis: Replenishment of the TCA cycle intermediates that are withdrawn from the cycle for biosynthesis of macromolecules.

Glutaminolysis: The stepwise conversion of GLN to lactate.

Acknowledgements

I would like to thank my senior supervisor Dr. Poul Sorensen and to my supervisory committee members Dr. Andrew Weng and Dr. Thibault Mayor for their valuable contributions to this work. I am grateful to my supervisory committee chair Dr. Susan Porter for her support throughout my PhD.

I cannot express the depth of my gratitude enough to Dr. DeBerardinis for his expertise, valuable suggestions, and support in this research.

I am indebted to my past and current fellow group members for teaching me the basics of cell biology techniques, without which I would not be able to pursue this work. Special thanks go to past and current members of Sorensen Lab; Dr. Barak Rotblat, Dr. Gabriel Leprivier, Dr. Cristina Tognon, Dr. Mads Daugaard, Amal El-Naggar, and Tony Ng for their support, encouragement and stimulating discussions, Amy Lee for all her support and help, and everyone else who helped me in one way or another in the lab.

Last but not least, I thank my husband and my daughter for their endless support, encouragement, and for their incredible tolerance to countless hours I spent in the lab at nights and in the weekends. I will be indebted to my daughter Ece Naz forever for her patience and understanding during the completion of my research and writing of this thesis. And finally I thank my parents, especially my father for teaching me to always aim high and strive for the best. I know he would be proud. To him I dedicate this thesis.

To my father…

Chapter 1: Introduction

1.1 Reactive Oxygen Species (ROS) in Normal and Cancer Cells

ROS can be defined as oxygen-containing chemically reactive molecules that are formed by incomplete reduction of oxygen (1, 2). Examples of ROS include; superoxide, nitric oxide, hydroxyl radicals, hydrogen peroxide, peroxynitrite, and hydroxide, which can all readily oxidize other molecules. There are several sources of ROS within the cell. They can be produced as by-products of normal biological processes. Mitochondrial respiration generates the majority of cellular ROS through electron leakage from electron transport chain, which then reacts with molecular oxygen producing highly reactive superoxide free radicals (3, 4). ROS are also produced to serve as microbicidal agents. In phagocytes, ROS, specifically superoxide production by NADPH oxidase is an essential component of innate immune response to invading microorganisms (5, 6). In non-phagocytic cells, ROS act as second messengers in promoting proliferation and survival upon growth factor stimulation. Receptor tyrosine kinases, such as platelet-derived growth factor receptor and epidermal growth factor receptor have been shown to signal through superoxide and subsequently hydrogen peroxide generation by NADPH oxidase (7-9). Hydrogen peroxide regulates the structure/activity of protein tyrosine phosphatases and the lipid phosphatase PTEN, by reversibly oxidizing the catalytic cysteine leading to activation of downstream signaling pathways, including activating protein 1 and Akt signaling for cell growth and survival respectively (10-13). Numerous studies have demonstrated that transformed cells produce more ROS than their normal counterparts (14-16). Oncogene activation,

abnormal cell metabolism, mutations in mitochondrial DNA, and loss of p53 and Hace1 tumor suppressor functions are so far the known sources of increased ROS associated with malignant transformation (17-21). Expression of the oncogenes *Ras* and *Bcr-Abl* increase ROS production by activating NADPH oxidase, whereas the expression of the oncogene *c-myc* has been linked to increased mitochondrial ROS production (22). One way to increase mitochondrial ROS production is the imbalanced expression of respiratory chain complex subunits, which results in inefficient transfer of electrons between electron transfer chain subunits and increased electron leakage (23). Mitochondrial DNA encodes approximately a dozen of mitochondrial proteins and the nuclear DNA encodes the remaining hundreds of mitochondrial proteins (24). c-myc is known to induce expression of nuclear encoded mitochondrial genes, which can disrupt the balance between proteins expressed from nuclear versus mitochondrial DNA leading to increased mitochondrial ROS (24, 25). Apart from oncogene driven transformation, mutations in mitochondrial DNA in certain cancers have been linked to elevated ROS levels via impaired expression/function of mitochondrial electron transport chain proteins encoded by mitochondrial DNA (20, 26-28). p53 is the critical protector of nuclear and mitochondrial DNA by sensing and eliminating oxidative stress (21, 29). Moreover, p53 regulates transcription of several genes involved in pro-oxidant and antioxidant response pathways (30, 31). Therefore loss of the tumor suppressor p53 impairs cellular redox homeostasis, resulting in ROS accumulation and genomic instability.

1.1.1 Cellular ROS scavenging systems

Accumulation of ROS in cells can result in loss of molecular functions and cell death by irreversible modifications of DNA, proteins, and lipids (32). Reactions between ROS and DNA can produce several different types of DNA damages. Perhaps the most common damage is caused by hydroxyl radical, which can react with sugar moieties of DNA bases resulting in sugar modifications and DNA double strand breaks (33). Hydroxyl radical can also damage DNA by oxidizing double bonds of DNA bases and by abstracting a hydrogen atom from the methyl group of thymine. DNA radicals can propagate further damage to DNA depending on their redox environment and reaction partners. Various types of ROS can oxidize proteins causing loss of function mainly by oxidation of critical amino acid residues (metal-binding sites, thiol groups on cysteine, methionine residues) (34). These modifications inactivate proteins or alter their localization, conformation or degradation rate. Protein oxidation can also cause accumulation of toxic protein aggregates. ROS are known to damage lipids by initiating an oxidation chain reaction of unsaturated lipids, a process known as lipid peroxidation (34). Both the superoxide anion and the hydroxyl radical can initiate this process and the resulting lipid products can eventually cause loss of membrane integrity and cell death.

Cells normally defend themselves against detrimental effects of ROS by engaging the antioxidative response pathways, involving superoxide dismutase enzymes, catalases, glutathione (GSH) and NADPH dependent peroxidases, and thioredoxins (Trx) (Fig. 1A) (1). Superoxide generated by mitochondria and NADPH oxidases is rapidly converted to hydrogen peroxide by superoxide dismutases. Catalase

degrades hydrogen peroxide to water and oxygen. Glutathione peroxidase can eliminate hydrogen peroxide using reduced glutathione (GSH). The oxidized glutathione (GSSG) can be reduced back to GSH by glutathione reductase in an NADPH dependent manner. Glutathione peroxidases are also the major lipid hydroperoxides (3) and their activities completely rely on GSH and NADPH. GSH is the most abundant antioxidant in the cell and in addition to its cofactor role in many antioxidant enzyme systems, it can directly scavenge hydroxyl radical, singlet oxygen, and regenerates other antioxidants vitamin C and E to their active forms (3). The glutaredoxin (Grx) system functions in the reduction of protein thiol groups. The reducing power of Grx is provided by GSH/glutathione reductase system, which is maintained by NADPH. The Trx system, comprised of Trx, NADPH, and Trx reductase is also indispensible for reducing oxidized protein thiol groups to maintain their proper function. When Trx reduces protein thiol groups, it becomes oxidized and can be reduced back again by NADPH dependent Trx reductase.

1.1.2 Adaptation to ROS in cancer cells

Accumulating evidence suggests that ROS increase is decisive for cellular transformation (35), proliferation (36), survival and disruption of cell death signaling (3). On the other hand, it was suggested that high ROS levels can induce and maintain senescence (37). Moreover, above a certain threshold, ROS can clash with survival pathways and are therefore cytotoxic (depicted in figure 1B). If unchecked, high amount of ROS results in oxidative damage to DNA, proteins, and lipids, eventually leading to

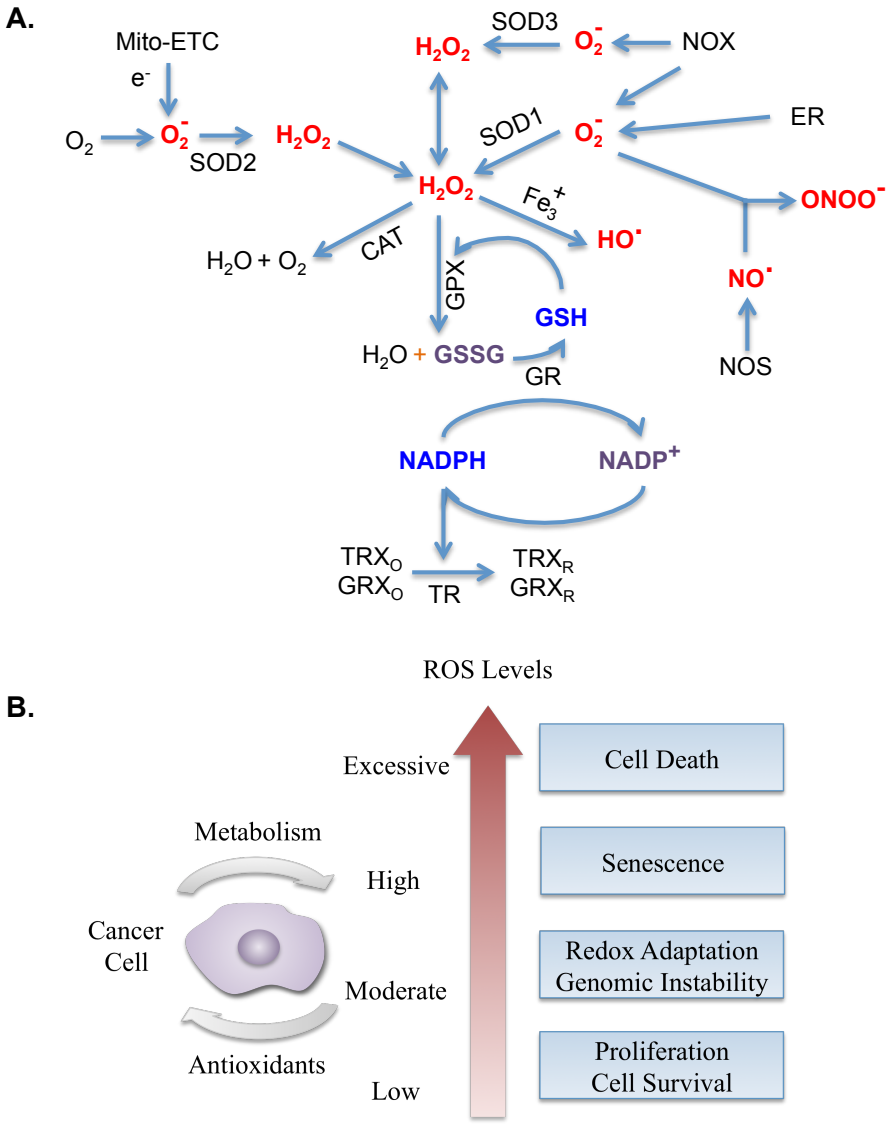

Figure 1. **ROS homeostatis. A.** Depiction of intracellular ROS scavenging pathways. O_2 (molecular oxygen), $O2^-$ (superoxide), e^- (electron), H_2O_2 (hydrogen peroxide), $HO^\cdot$ (hydroxyl radical), $NO^\cdot$ (nitric oxide), $ONOO^-$ (peroxynitrite), Mito-ETC (mitochondrial electron transport chain), NOX (NADPH oxidase), ER (endoplasmic reticulum), NOS (nitric oxide synthase), SOD (superoxide dismutase), CAT (catalase), GSH (reduced glutathione), GSSG (oxidized glutathione), TRX (thioredoxin), TR (TRX reductase), GPX (glutathione peroxiredoxidase), GR (glutathione reductase), GRX (glutaredoxin), **B.** Depiction of ROS adaptation in cancer cells.

cell death. Accordingly, a fine balance exists between ROS generation and ROS scavenging, which is crucial for cancer cell growth/survival.

In order to survive intrinsically produced ROS and oxidative stress, cancer cells must acquire adaptive mechanisms to counteract the toxic effects of elevated ROS and activate survival pathways. For example, oncogenic H-Ras-transformed cells upregulate superoxide and hydrogen peroxide levels with concomitant increase in the levels of antioxidants peroxiredoxin-3 and Trx peroxidase (38). Ras-transformed cells are more sensitive to GSH depletion, suggesting that increased ROS levels arising from oncogenic transformation renders the cells dependent upon antioxidants for survival (16). Another evidence comes from the studies with c-Myc-active melanoma cells. c-Myc was shown to control expression of GSH synthetase, and knockdown of c-Myc resulted in a significant decrease in GSH levels and led to apoptosis (39). Furthermore, Trx Reductase 1 is overexpressed in many cancers and its downregulation decreases tumorigenicity of cancer cells (40). A more recent study showed that physiological expression of oncogenic K-RAS, Myc, and B-RAF induces NRF2 expression to maintain low ROS levels, which confers growth advantage to tumors (41). All these data indicate that malignant transformation accompanies induction of ROS generation to promote cell proliferation through redox-sensitive signaling pathways, and in parallel, activation of adaptive ROS-scavenging pathways to minimize oxidative damage.

1.2 Cancer Cell Metabolism

Cancer cells exhibit high rate of growth and proliferation demanding accumulation of macromolecules and ample amount of energy. Rearrangement of cellular metabolism helps cancer cells meet these demands and confer growth and survival advantage under restricting conditions of tumor environment (42-44). Glucose and the non-essential amino acid glutamine (GLN) are the two major nutrient sources for cancer cells. Abnormal glucose metabolism in tumors has been an active area of research since the pioneering work by Otto Warburg was published in 1956 (45, 46). The seminal observation by Otto Warburg that tumors consume more glucose and secrete more lactate than normal tissue even in the presence of oxygen (the Warburg effect) has opened therapeutic opportunities that could benefit cancer patients. However, research in abnormal GLN metabolism gained momentum only recently by the findings that the oncogenic c-Myc can directly regulate expression of the genes involved in GLN metabolism (47, 48).

1.2.1 GLN metabolism in cancer cells

GLN is the most abundant amino acid in plasma and it is consumed by tumors at rates much greater than that of any other amino acid (49, 50). Akin to glucose, GLN is a major precursor for ATP synthesis. In addition to satisfying bioenergetic needs, GLN has many important functions in a variety of key processes in proliferating cells, including synthesis of proteins, nucleic acids, lipids, hexosamines, glutathione (GSH) and NADPH (50). Not surprisingly most proliferating cells require GLN for growth and

certain oncogenes has been shown to influence GLN metabolism (47, 51). GLN serves as both a carbon and nitrogen source for protein and DNA synthesis. It is the most abundant amino acid in plasma with a concentration reaching almost 1 mM, readily available to cancer cells (52). Although GLN is not an essential amino acid several types of cancer cells display GLN dependence for growth and survival, a phenotype known as GLN addiction. GLN addiction of cancer cells was initially thought to be an *in vitro* culture artifact (53). However, several studies revealed that tumors consume GLN avidly, evidenced by depleted GLN concentrations in blood samples from cancer patients (54, 55). GLN addiction of cancer cells is often attributed to the ability of GLN to support mitochondrial TCA cycle (tricarboxylic acid cycle) for energy production and synthesis of precursors used in DNA, protein and lipid synthesis. Recent studies revealed that GLN plays many more important roles in maintaining oncogenic phenotype of cancer cells than previously appreciated. Cells take up GLN by GLN transporters, of which ASCT2 is the major transporter in rapidly proliferating cells (53, 56). GLN is the primary nitrogen donor for purine and pyrimidine synthesis (57), and a substrate for protein synthesis. Its amine groups are used in the synthesis of most nonessential amino acids. The carbon skeleton of GLN is used in the replenishment of TCA cycle intermediates (anaplerosis) (52). When GLN enters the cell, it is converted to glutamate by Glutaminase (GLS), releasing ammonia as by product (Fig. 2). Glutamate is then converted to α-ketoglutarate (α-KG), which enters the TCA cycle to support anaplerosis for growth. A significant fraction of the GLN-derived carbon leaves the TCA cycle as malate and is converted to pyruvate by $NADP^+$ dependent malic enzyme producing NADPH (58). Lactate dehydrogenase then catalyses the lactate production

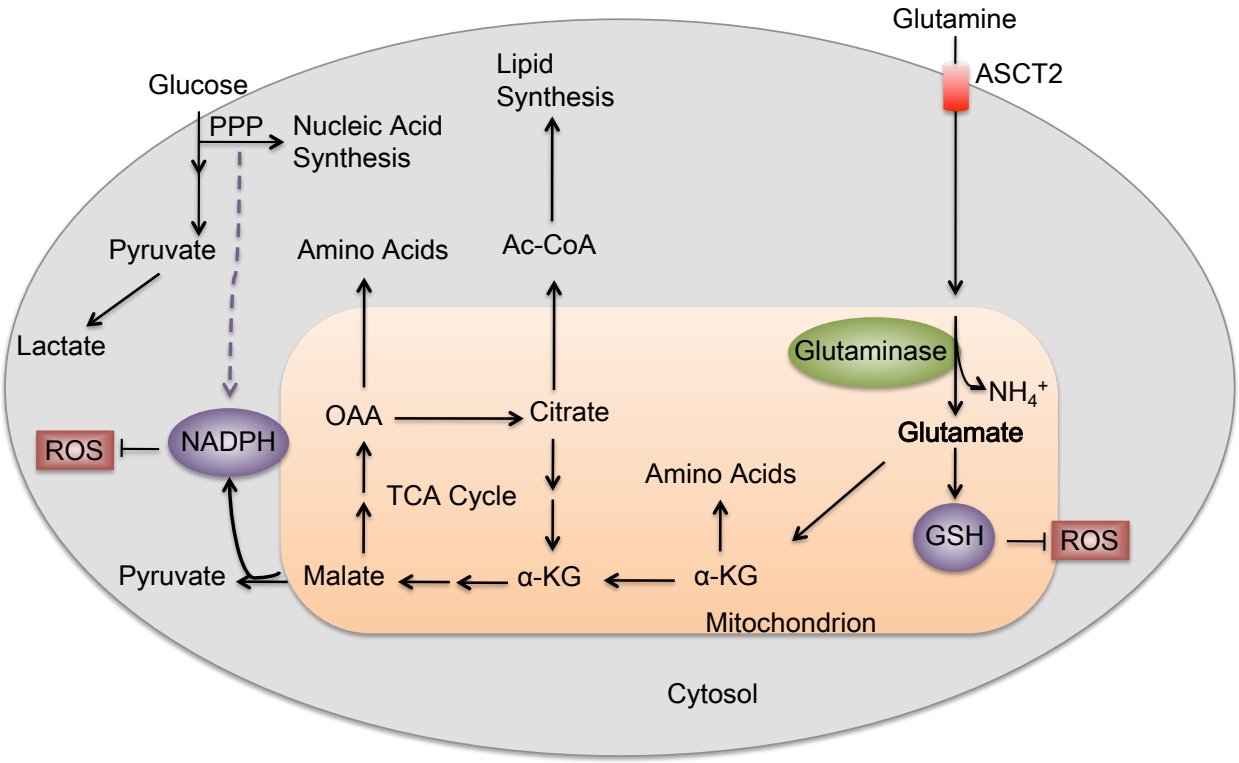

Figure 2. **GLN metabolism.** GLN is transported into cells by ASCT2 (major GLN transporter in rapidly proliferating cells) and converted to glutamate by the mitochondrial enzyme Glutaminase, releasing ammonia as by product. Glutamate then can be directly used in GSH synthesis or it can enter the TCA cycle to support anaplerosis and NADPH production. Glucose oxidation via the pentose phosphate pathway (PPP) also generates NADPH. α-KG (α-ketoglutarate).

from pyruvate. The stepwise conversion of GLN to lactate is known as ***glutaminolysis***, a process stimulated by malignant transformation (59). In addition to supporting the TCA cycle for growth and NADPH production, GLN-derived glutamate is directly used

for synthesis of GSH, a tripeptide of glutamate-cysteine-glycine. Therefore GLN metabolism is crucial for cancer cells to cope with the toxic effects of ROS.

1.2.2 Therapeutic targeting of GLN metabolism

Decades ago, GLN analogues with significant anti-cancer activities, such as L-DON (6-diazo-5-oxo-L-norleucine) and acivicin were used to target GLN metabolism in tumor cells. Both compounds were shown to primarily inhibit GLN-dependent enzymes involved in nucleotide biosynthesis (57). Their use was discontinued due to intolerable toxicities to central nervous system (60). Recently, Mueller et al. reported a phase II clinical study that L-DON has more tolerable side effects and is more effective when combined with polyethylene glycol-conjugated GLS (depletes GLN levels in plasma by 90%) in patients with advanced refractory solid tumors (61). Enzymatic lowering of blood GLN levels by L-asparaginase has also been explored in pancreatic cancer patients, but was determined to be significantly toxic in adults (62). Phenylacetate (PA), an aromatic fatty acid has been shown to have significant antitumor activity in mouse models of human cancers, including pancreatic cancer, breast cancer, and malignant gliomas (63-65). Mammalian circulation contains low concentrations of PA as a product of phenylalanine metabolism. PA is conjugated to GLN by the hepatic enzyme phenylacetyl-coenzyme A:glutamine acyltransferase, and the end product, phenylacetylglutamine, is excreted in urine (66). By depleting GLN, PA concomitantly reduces serum ammonia levels, and therefore is used to treat hyperammonemia in children with inborn urea cycle disorders (67). Because many cancer cell lines are GLN

dependent, PA is thought to exert its anti-proliferative effects in part by depleting plasma GLN. Phase I and II clinical studies showed that long-term administration of PA is well tolerated among all age groups. Central neurotoxicity (irritability, lethargy, and somnolence) was the major side effect observed, which was rapidly reversed with the discontinuation of the drug (68). In addition to therapeutic opportunities, differential GLN metabolism in cancer cells offers new possibilities for tumor imaging. Increased glucose consumption of tumors has been exploited for imaging using ^{18}F-2-deoxyglucose (FDG) and positron emission tomography (PET). In fact, a new, metabolically stable ^{18}Fluorine labeled 4-F-Glutamine analogues have been developed for PET imaging (69).

1.3 Combining GLN Metabolism Inhibition and Oxidative Stress in Cancer Cells as a Potential Therapeutic Approach

Intracellular ROS levels can determine cell fate. While low/moderate levels of ROS promote genomic instability and promote proliferation and survival, high levels of ROS induce senescence, and excessive ROS lead to cell death due to oxidative damage (Fig. 1B). Since cancer cells exhibit higher levels of ROS production as compared with the normal ones, overwhelming selectively the cancer cells by oxidative stress inducing drugs is an attractive treatment strategy. Although the idea of a ROS threshold concept-based cancer therapy has been proposed in 2000 (70), feasibility of this hypothesis has only recently gained momentum. Increasing ROS above the threshold can be achieved through exogenous ROS generating agents or inhibitors of ROS-scavenging pathways. Owing to their ability to mount an effective oxidative stress

response, cancer cells can become resistant to treatment with exogenous ROS generating agents. For instance, multidrug resistant HL-60 leukemia cells with elevated catalase levels and activity are remarkably resistant to cytotoxic effects of exogenous hydrogen peroxide (71). Hence, inhibiting the anti-oxidant pathways in cancer cells may be a more effective strategy. Within the last 7 years, several small molecule inhibitors of anti-oxidant pathways have been developed and shown to possess significant antitumor activity *in vitro* and *in vivo* (16, 72-75). Of interest, piperlongumine, a natural product isolated from the plant species *Piper Longum* L. was shown to selectively kill several different types of cancer cells by inhibiting antioxidant GSH pathway (74). Piperlongumine administration strikingly inhibited tumor growth in mouse xenograft models without any significant toxicity in normal mice. Despite its marked antitumor activity, a small number of cells can adapt to the oxidative stress induced by piperlongumine. While piperlongumine inhibits GSH system, Trx antioxidant pathway may remain unaffected, accounting for the residual cancer cell survival. Therefore a drug combination strategy may maximize the excessive ROS-mediated cancer cell death. Inhibition of GLN metabolism can potentially impair both the GSH and Trx antioxidant pathways by directly blocking GSH synthesis and NADPH production through glutaminolysis. Strategies using GLN analogues and glutamine-depleting enzymes have not been successful because of unacceptable toxicities (60, 62). GLN depletion by PA administration, in contrast, represents a relatively nontoxic approach and is clinically feasible. Indeed, phase II clinical studies using PA in patients with recurrent glioblastoma determined that PA was well tolerated with accepted side effects, however, further studies of single-agent phenylacetate were not warranted using the

same treatment schedule (68). Combining piperlongumine treatment with PA therefore has the potential for effective elimination of cancer cells.

1.4 Hypothesis and Significance

Although it is well known that transformed/cancer cells use GLN for synthesis of macromolecules and antioxidants, why dependency on GLN for survival varies among different cell types has not been well understood. This thesis study was undertaken to address the hypothesis that ***transformed/cancer cells with increased ROS levels depend on GLN to cope with oxidative stress, and are therefore GLN addicted.*** A detailed examination of the link between ROS and GLN addiction phenotype is important in our understanding of the oncogenic characteristics of cancer cells and can potentially lead to designing effective strategies that combine ROS induction and GLN depletion for treatment of human cancers.

1.5 Research Objectives

The studies in this thesis were designed to test and develop the above hypothesis and introduced in three research chapters, each focusing on different but related aspects of GLN metabolism and ROS. Chapter 2 demonstrates how increased ROS levels due to loss of the tumor suppressor Hace1 leads to altered GLN uptake/metabolism and GLN addiction, associating increased ROS levels with GLN addiction. In chapter 3, regulation of ROS levels by GLN metabolism was investigated in

a panel of human cancer cell lines and a correlation between GLN deprivation-induced ROS elevation and GLN addiction was established. Chapter 3 studies also identified a mechanism for GLN starvation-induced cell death, whereby increased glucose uptake due to the ROS elevation in the absence of GLN exacerbates ROS levels and leads to cell death. Moreover, the efficacy of combining GLN starvation with a pro-oxidant small molecule in elimination of GLN addicted cancer cells was demonstrated. Studies in chapter 4 investigated the possibility that GLN addicted cells may increase GLN uptake when exposed to exogenous oxidants and identified a mechanism for ROS-induced upregulation of GLN uptake.

Chapter 2: Loss of the Tumor Suppressor Hace1 Leads to GLN Addiction Due to Increased Cellular ROS Levels

2.1 Background and Rationale

Malignant transformation due to oncogene activation or loss of tumor suppressor genes is associated with altered cellular metabolism (42-44, 76). In addition to glucose, GLN serves as a major nutrient source for transformed cells *in vitro* and for tumors *in vivo* (54, 77). Although not an essential amino acid, many different types of cancer cells depend on extracellular GLN for survival, a phenomenon known as GLN addiction (53). Oncogenes such as Myc and K-Ras depend on GLN for cellular transformation and therefore upregulate GLN metabolism to meet the high demands of uncontrolled growth and proliferation (47, 48, 51). Recent studies reported that the loss of the tumor suppressor retinoblastoma protein (pRB) is also associated with increased GLN metabolism and renders the cells GLN addicted (78, 79). In addition to supporting the TCA cycle for growth, GLN-derived glutamate is directly used for GSH synthesis (52), and therefore GLN metabolism is crucial for cancer cells to cope with toxic effects of ROS. Interestingly, loss of pRB has been shown to be associated with increased ROS levels (78, 80). However, a direct link between increased cellular ROS levels and GLN addiction phenotype due to loss of a tumor suppressor gene has not been considered before.

Hace1 (*H*ECT domain and *A*nkyrin repeat *C*ontaining *E*3 ubiquitin-protein ligase 1) is a tumor suppressor gene that is inactivated in majority of the human Wilms'

tumors, the most common kidney cancer in children (81, 82). Recent studies demonstrated epigenetic inactivation of *Hace1* also in multiple other human tumors (83-88). Hace1 knockout mice develop spontaneous late onset tumors of diverse phenotypes, highlighting Hace1 as a *bona fide* tumor suppressor (82). To date, the only known target of Hace1 is the small Rho-GTPase, Rac1 (89, 90). In response to cytotoxic necrotizing factor-1 and hepatocyte growth factor, Hace1 ubiquitylates and targets GTP-bound Rac1 for proteosomal degradation reducing the Rac1-dependent bacterial invasion (91) and cell migration (90) respectively. Rac1 is involved in multiple regulatory processes, including ROS generation by NADPH oxidases (92, 93). Our laboratory demonstrated that Hace1 loss in mice, zebrafish, human Wilm's tumor tissues, and in human cancer cells is associated with increased ROS levels due to high Rac1 activity resulting in uncontrolled ROS production by NADPH oxidase (94). We hypothesized that increased ROS levels renders Hace1 deficient cells dependent on GLN.

In this chapter, we show that mouse embryonic fibroblasts (MEFs) derived from *Hace1*$^{-/-}$ (KO) mouse are more sensitive to GLN starvation as compared with the ones derived from the *Hace1*$^{+/+}$ (WT) littermates. Hace1 KO MEFs exhibit increased GLN uptake and metabolism, and depend on GLN for soft agar colony formation. We also show that GLN deprivation induces cell death in Hace1 KO MEFs by augmenting cellular ROS levels and the antioxidant compound N-acetyl cysteine (NAC) or the TCA cycle intermediate oxaloacetate (OAA) efficiently rescues GLN starvation-induced ROS elevation and cell death. Moreover, reduction of superoxide production by chemical inhibition of the NADPH oxidase subunit Nox1 in Hace1 KO MEFs inhibits

superoxide/ROS levels, and cell death in the absence of GLN. These findings implicate, for the first time, that increased ROS generation resulting from a loss of a tumor suppressor predisposes cells to GLN addiction.

2.2 Methods

Cell culture and reagents. Hace1 WT and KO MEFs were cultured in DMEM supplemented with 10% FBS and 1% streptomycin/penicillin (Invitrogen). For GLN starvation experiments, cells were seeded in regular DMEM and the following day the culture medium was changed into GLN-free medium (DMEM, without GLN, without pyruvate, without phenol red) (Gibco), supplemented with 10% dialyzed FBS (Invitrogen) and 1% streptomycin/penicillin (Invitrogen). NAC, OAA, and gamma-L-glutamyl-p-nitroanilide hydrochloride (GPNA) were purchased from Sigma. Sodium phenyl acetate (NaPA) was from Santa Cruz. ML171 (NOX1 inhibitor) was from EMD Millipore.

Soft agar colony formation assay. 8000 cells/well were mixed with 1 mL of 0.4% agar (top layer) in DMEM without GLN, supplemented with GLN, OAA, NaPA, or GPNA where indicated, and layered on 6-well plates covered with 0.8% agar in DMEM in triplicates. Wells were supplemented with 2-4 drops of the corresponding medium every 2 days. After 2 weeks, wells were imaged and colony numbers were counted using

ImageJ. Results are given as percentages of colonies per number of events (colonies + single cells) counted.

Cell death assays. Cell death analyses were performed using either IN Cell imaging or propidium iodide (PI) staining. For In Cell analysis, cells seeded in triplicates in 96 well plates. After 24 hours or 72 hours of GLN starvation, cells were co-stained with 150 μM Hoechst 33342 (Molecular Probes) for nuclear segmentation and 10 μM ethidium homodimer-1 (Molecular Probes) to identify dead cells, incubated at 37 °C for 20 minutes and imaged using IN Cell Analyzer (GE Healthcare). Cells with overlapping staining were also considered non-viable. The Images were analyzed (by Alejandra Lopez) using IN Cell Developer software (GE Healthcare). For PI staining, cells were seeded in 6-well plates in triplicates and the next day the culture medium was exchanged to GLN-free medium with/without 2 mM GLN. After 72 hours, both detached and attached cells were pooled, centrifuged, resuspended in cold PBS containing 1 μg/mL propidium iodide (PI, Molecular Probes), and analyzed immediately using FACSCalibur flow cytometer (BD Biosciences) in FL-3 channel.

ROS measurements. ROS were measured by either using the general ROS indicator DCFDA (5-(and-6)-chloromethyl-2',7'-dichlorodihydrofluorescein diacetate, acetyl ester) (Molecular Probes) or the superoxide indicator DHE (dihydroethidium) (Molecular Probes). Cells were seeded in 6-well plates in triplicates and the next day the culture medium was exchanged to GLN-free medium with/without 2 mM GLN. After 48 hours, ROS levels were measured. Cells were incubated with 5 μM DCFDA for 40 minutes.

Medium was removed and the cells were washed with PBS. After trypsinizing, cells were centrifuged and resuspended in PBS containing 1µg/mL PI, and analyzed immediately by flow cytometry using FL-1 channel for DCFDA and FL-3 channel for PI fluorescence. PI was included for exclusion of dead cells. Superoxide levels were measured using DHE (by Dr. Mads Daugaard) as described before (94). Superoxide anion O_2^- rapidly oxidizes DHE yielding oxyethidium, which then binds DNA and emits light in the 570-580 nm ranges when excited at 488 nm. After indicated treatments, cells were washed in Hank's Balanced Salt Solution (HBSS), incubated for 30-60 minutes in HBSS containing 10 µM DHE, washed in HBSS and directly analyzed for oxyethidium fluorescence with an epi- fluorescence HAL100 microscope (Zeiss).

^{14}C-GLN uptake assay. Cells were seeded in triplicates in 6-well plates and GLN uptake was determined as in (95) with modifications. Cells were incubated in GLN-free medium for 20 minutes and 0.2 µCi/mL [U-^{14}C]GLN was added. After 15 minutes incubation at room temperature, cells were washed 3x with PBS, lysed with 250 µL of 0.2% SDS in 0.2 N NaOH, incubated for 30 minutes at room temperature, transferred into eppendorf tubes and incubated in a heating block at 60 ^{o}C for another 20 minutes. 25 µL of 1 N HCl was added into each tube to neutralize NaOH. 200 µL of the lysate was transferred into scintillation vials containing 6 mL scintillation liquid (Scintisafe Econo, Fisher Scientific), and the total radioactivity was determined using a β-scintillation counter (Perkin Elmer). Protein concentration was determined using DC (detergent compatible) protein assay kit (BioRad) and radioactivity was normalized to protein concentration.

Ammonia assay. Cells were seeded in triplicates in 6-well plates. 2 days later culture media from the wells were collected, spun down to remove any floating cells, and ammonia levels were analyzed using an ammonia assay kit (BioVision) according to the kit instructions.

Metabolic labeling. ^{13}C labeling experiments were performed essentially as described (96). Cells were cultured in regular media to 80-90% confluence in 10 cm dishes, and after rinsing with ice-cold PBS, overlaid with medium containing 25 mM glucose and 4 mM [U-^{13}C]GLN. After 8 hours incubation, labeled cells were rinsed with ice-cold PBS, lysed in cold 50% methanol, and subjected to three freeze-thaw cycles. The lysates were centrifuged to remove precipitated protein, then evaporated and derivatized by trimethylsilylation (Tri-Sil HTP reagent, Thermo). Three μL of the derivatized material were injected onto an Agilent 6970 gas chromatograph equipped with a fused silica capillary gas chromatography column (30 m length, 0.25 mm diameter) and networked to an Agilent 5973 Mass Selective Detector. The abundance of the following ions was monitored: m/z 245-249 for fumarate; m/z 335-339 for malate; and m/z 465-471 for citrate. The measured distribution of mass isotopomers was corrected for natural abundance of ^{13}C (97). Gas chromatography and mass spectrometry analyses were performed by Andrew Mullen in Dr. Ralph DeBerardinis laboratory (University of Texas-Southern Medical Centre).

Statistical analysis. Statistical significance was determined using a two-tailed student's t-test.

2.3 Results

2.3.1 Hace1 deficient cells are sensitive to GLN starvation.

As indicated earlier, we proposed that increased ROS levels may lead to GLN addiction. To test this hypothesis, we compared the GLN dependency of Hace1 WT and KO MEF since loss of Hace1 leads to increased ROS levels. We stained the cells with Hoechst or Ethidium after 24 hours and 72 hours GLN starvation and quantified the number of live and dead cells using IN Cell Analyzer. Both cell lines exhibited similar numbers of live and dead cells after 24 hours of GLN starvation, whereas after 72 hours, Hace1 KO MEFs had significantly higher number of dead cells (Fig. 3A-C). GLN starvation did not increase cell death in Hace1 WT MEFs after 72 hours (Fig. 3B), however the number of live cells was increased (Fig. 3A) suggesting that the Hace1 WT MEFs do not depend on GLN for growth or survival. To support these findings, we also quantified cell death by measuring propidium iodide (PI) incorporation into dead cells using flow cytometry analysis. Consistent with the results given above, GLN starvation induced significant cell death only in the Hace1 KO MEFs (Fig. 3D). These data establish that loss of Hace1 renders the cells dependent on GLN for survival.

2.3.2 Hace1 loss leads to increased GLN uptake and metabolism

Since Hace1 KO MEFs depend on GLN for survival, we predicted that these cells might have increased GLN uptake and metabolism as compared to their WT counterparts. Using a radioactively labeled glutamine (U-^{14}C-Gln), we measured GLN

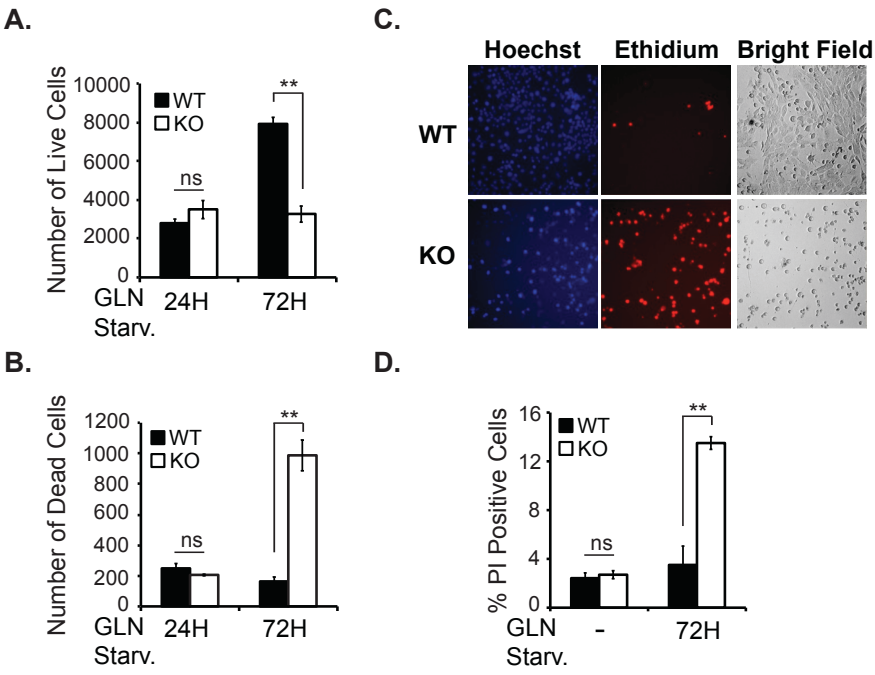

Figure 3. **Hace1 KO MEFs are sensitive to GLN starvation.** Number of live (**A**) and dead (**B**) cells was determined using Hoechst or ethidium staining respectively after 24 hours and 72 hours of GLN starvation. **C.** Representative images of Hace1 WT and KO MEFs stained with Hoechst and ethidium 72 hours after GLN starvation. **D.** GLN starvation-induced cell death determined was by PI staining followed by flow cytometry. Error bars represent S.D. (n=3). $^{**}p < 0.005$. In Cell analysis was performed by Alejandra Lopez.

uptake and found that Hace1 KO MEFs take up significantly more GLN than the WT MEFs (Fig. 4A). Conversion of GLN to glutamate is the first step of GLN metabolism and is associated with ammonia production. Consistent with increased GLN uptake, Hace1 KO MEFs generate significantly higher levels of ammonia (Fig. 4B). Many transformed cell lines use GLN as the major anaplerotic precursor for synthesis of TCA cycle intermediates. Since Hace1 KO MEFs take up more GLN, we investigated

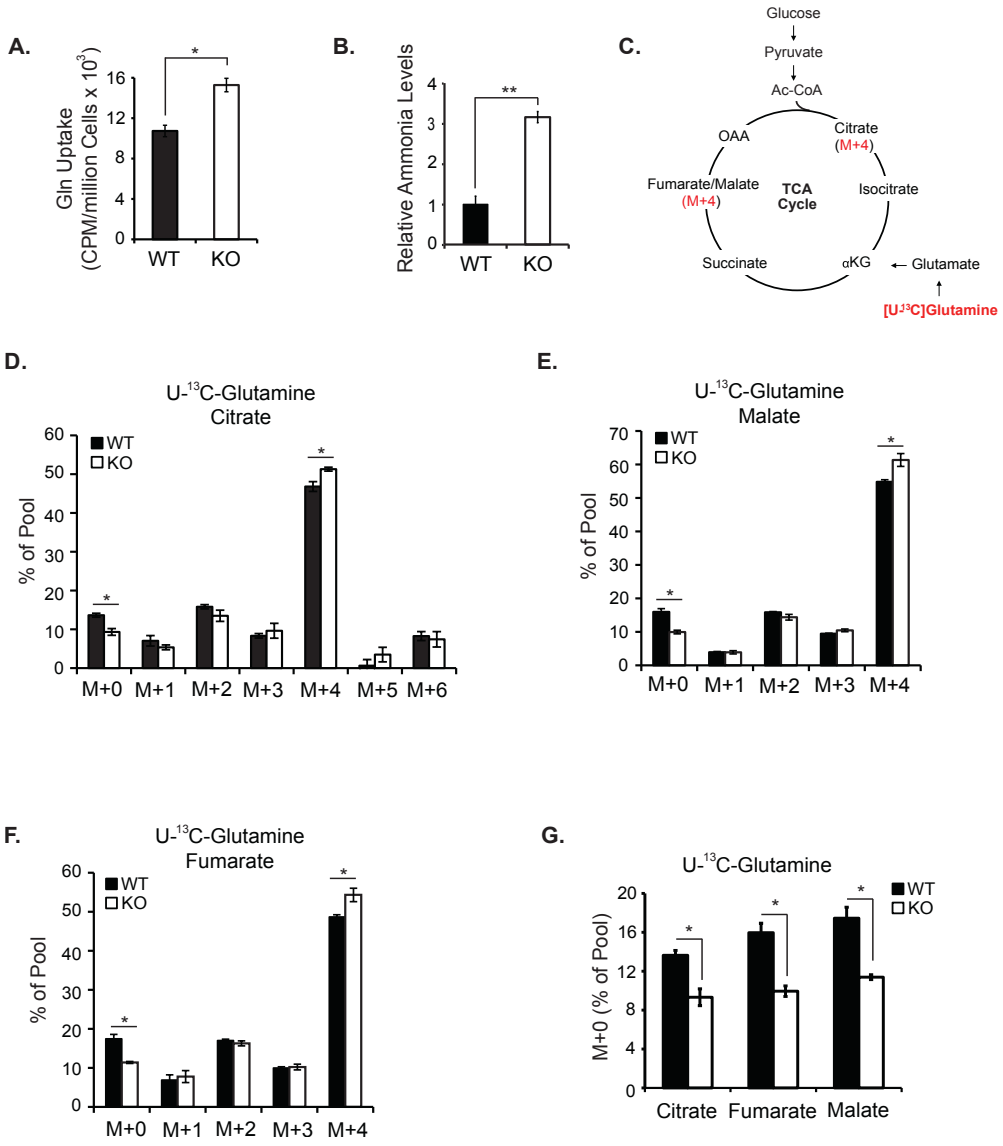

Figure 4. **Hace1 loss leads to increased GLN uptake and metabolism. A**. Hace1 KO MEFs take up more GLN. GLN uptake was determined using radiolabeled GLN. **B**. Hace1 KO MEFs secrete more ammonia. **C.** Schematic of incorporation of GLN carbons into the TCA cycle intermediates. Enrichment analysis of ^{13}C-GLN-derived citrate (**D**), malate (**E**), and fumarate (**F**) in Hace1 WT and KO MEFs labeled with U-^{13}C-GLN. **G.** Comparison of non-GLN derived (M+0) TCA cycle intermediate pools in Hace1 WT and KO MEFs. Error bars represent S.D. (n=3). * $p < 0.05$, ** $p < 0.005$. Mass spectrometry analysis of ^{13}C-labeled samples was performed by Andrew Mullen in Dr. Ralph DeBerardinis Laboratory (University of Texas).

whether GLN is metabolized differently in the Hace1 WT and KO MEFs. We cultured the cells in media containing [U-^{13}C]-GLN and analyzed the incorporation of GLN carbons into the TCA cycle intermediates citrate, malate, and fumarate using mass spectrometry. Processing of [U-^{13}C]-GLN in the TCA cycle generates M+4 isotopomers (Fig. 4C), whereas non-GLN sources (e.g. glucose) produce M+0 isotopomers (un-labeled) of these intermediates. We found that both cell lines efficiently incorporated GLN carbons into the TCA cycle intermediates (Fig. 4D-F) suggesting that Hace1 loss does not cause a major change in the pathways by which these cells use GLN. However, Hace1 KO MEFs displayed significantly higher levels M+4 isotopomers of citrate, malate, and fumarate. In contrast, the levels of unlabeled intermediates (M+0 isotopomers) were higher in Hace1 WT MEFs (Fig. 4G), suggesting a modest enhancement in the fraction of the TCA cycle intermediate pools labeled by GLN in Hace1 KO MEFs over this time course. This data implies that loss of Hace1 results in a slight but significant shift towards GLN as more favored anaplerotic precursor.

2.3.3 Hace1 KO MEFs depend on GLN for transformation activity

Transformed cells feed GLN into the TCA cycle to maintain sufficient pools of biosynthetic precursors to support oncogenic processes (58). We therefore tested if GLN withdrawal could block the ability of Hace1 KO MEFs to form colonies in soft agar medium, which is a well-established assay for transformation activity of cells. As expected, Hace1 KO MEFs formed strikingly higher number of colonies in the presence of GLN, whereas it was completely inhibited without GLN (Fig. 5A). Addition of the

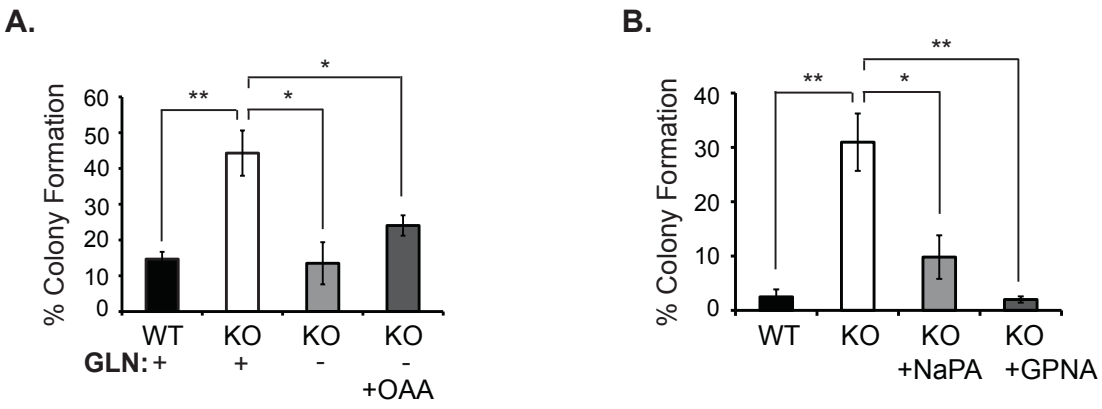

Figure 5. **Hace1 KO MEFs depend on GLN for transformation activity. A**. Soft agar colony formation assay. Hace1 KO MEFs cannot form colonies in the absence of GLN. OAA (10 mM) does not restore the transformation ability of Hace1 KO MEFs without GLN. **B.** Inhibition of GLN uptake by NaPA or GPNA blocks soft agar colony formation by Hace1 KO MEFs. Error bars represent S.D. (n=3). * $p < 0.05$, ** $p < 0.005$.

anaplerotic OAA in soft agar medium did not restore colony formation efficiency of the Hace1 KO cells in the absence of GLN. This is expected because in addition to its role as anaplerotic precursor for biosynthesis of the TCA cycle intermediates, GLN is also directly used for hexosamine and nucleotide biosynthesis, which are essential for proliferation (95, 98). We also evaluated chemical inhibitors of cellular GLN uptake to assess the potential use of chemical GLN depletion techniques to inhibit growth of Hace1 deficient tumors. Two such inhibitors are sodium phenylacetate (NaPA) and gamma-L-glutamyl-p-nitroanilide hydrochloride (GPNA). NaPA is known to block tumor growth *in vivo* by depleting GLN in circulation (99). NaPA was also reported to block growth of cancer cells *in vitro* (100) although how NaPA works in cell culture is

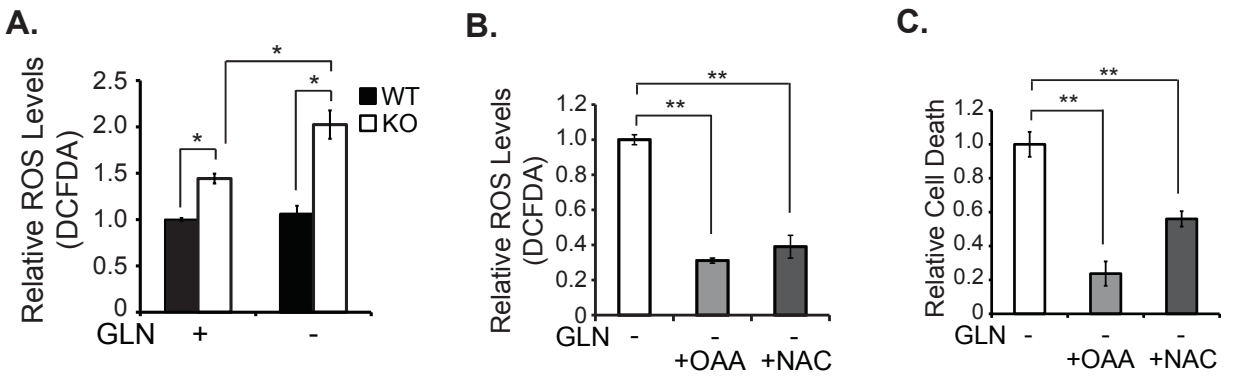

Figure 6. **Hace1 loss leads to ROS-dependent GLN addiction. A**. GLN starvation augments ROS levels in Hace1 KO MEFs. ROS levels were measured using DCFDA staining followed by flow cytometry. OAA and NAC rescue GLN starvation-induced ROS (**B**) and cell death (**C**). Cell death was measured by Hoechst/ethidium staining followed by IN Cell analysis. Error bars represent S.D. (n=3). * $p < 0.05$, ** $p < 0.005$.

unknown. GPNA is an inhibitor of the GLN transporter ASCT2 and therefore reduces cellular GLN uptake (101). Both NaPA and GPNA effectively blocked soft agar colony formation of Hace1 KO MEFs (Fig. 5B). Together these results suggest that Hace1 KO MEFs uptake and metabolize more GLN and depend on GLN for cellular transformation, and that GLN depletion may be an effective strategy to block growth of Hace1 deficient tumors.

2.3.4 GLN starvation induces cell death in Hace1 KO MEFs by augmenting cellular ROS levels

Because Hace1 loss leads to increased ROS levels both *in vitro* and *in vivo* (94) and GLN is a precursor for the synthesis of the antioxidant GSH, we investigated the

possibility that GLN is required for survival of Hace1 KO MEFs to overcome the toxic effects of increased ROS production. We compared ROS levels in the Hace1 WT and KO MEFs with/without GLN starvation using the general ROS indicator CM-H_2DCFDA followed by flow cytometry analysis. We found that Hace1 KO MEFs have significantly higher ROS compared with the WT MEFs, and that GLN starvation augments the ROS levels in Hace1 KO MEFs but not in WT MEFs (Fig. 6A). GLN is converted to glutamate, which is used as substrate for glutathione synthesis for cellular ROS clearance. Accordingly, we predicted that glutamine starvation-induced cell death may be due to elevated ROS levels in Hace1 KO MEFs and that a ROS scavenger, or a TCA cycle intermediate that can be converted to glutamate and eventually to glutathione should rescue cell death in the absence of GLN. Indeed, addition of OAA or NAC to the culture medium efficiently reduced GLN starvation-induced ROS increase and cell death in Hace1 KO MEFs (Fig. 6B, 6C), suggesting that GLN starvation induces cell death in Hace1 KO MEFs by augmenting cellular ROS levels.

2.3.5 Increased ROS generation by NADPH oxidase mediates GLN starvation-induced cell death in Hace1 KO MEFs.

To determine whether increased superoxide generation by NADPH oxidase is the source of ROS augmentation and cell death in Hace1 KO MEFs after GLN withdrawal, we first analyzed the superoxide levels in Hace1 WT and KO MEFs with/without GLN starvation using the superoxide specific dye dihydroethidum (DHE). As expected, Hace1 KO MEFs had significantly higher superoxide levels as compared

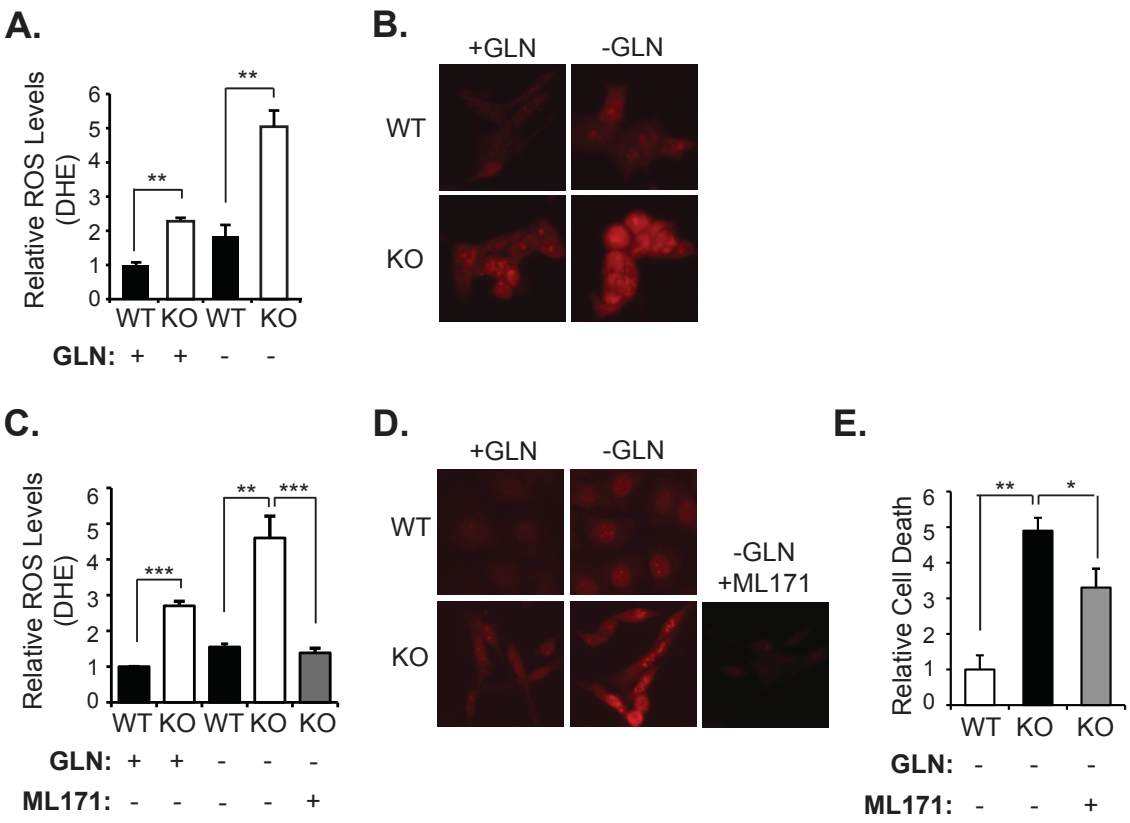

Figure 7. Inhibition of superoxide generation by NADPH oxidase subunit Nox1 reduces GLN starvation-induced ROS and cell death in Hace1 deficient cells. A. GLN starvation augments superoxide levels in Hace1 KO MEFs. Superoxide levels were measured using DHE staining. **B.** Representative images of DHE stained Hace1 WT and KO MEFs with/without 30 hours GLN starvation. **C.** Inhibition of NADPH oxidase subunit Nox1 by ML171 (5 μM) blocks GLN starvation (30 hours)-induced superoxide augmentation in Hace1 KO MEFs as measured by DHE staining. **D.** Representative images of DHE stained cells from C. **E.** Inhibition of NADPH oxidase subunit Nox1 by ML171 (5 μM) blocks GLN starvation (72 hours)-induced cell death in Hace1 KO MEFs Error bars represent S.D. (n=3). ***$p < 0.001$, **$p < 0.005$, *$p < 0.05$. DHE staining and data analysis was performed by Dr. Mads Daugaard.

with the WT MEFs (Fig. 7A, 7B). GLN starvation only modestly increased superoxide levels in Hace1 WT MEFs, whereas it caused a marked increase in Hace1 KO MEFs (Fig. 7A, 7B). Inhibition of NADPH oxidase subunit Nox1 using ML171 (a Nox1 inhibitor) reduced GLN starvation-induced superoxide levels (Fig. 7C, 7D) and cell death in Hace1 KO MEFs (Fig. 7E). These results strongly indicate that Hace1 deficiency leads to increased superoxide generation by NADPH oxidase and therefore Hace1 deficient cells depend on GLN to cope with increased cellular ROS levels and to avoid oxidative stress.

2.4 Discussion

Aberrant growth and proliferation is a highly demanding process that requires ample amount of energy and accumulation of macromolecules. Therefore activation of oncogenes or loss of tumor suppressor genes is accompanied by altered metabolism of glucose and GLN to meet these demands. Along with metabolic changes, increased ROS generation also facilitates cellular transformation. However, due to their toxic effects, cellular ROS levels are subject to tight regulation. Thus, several oncogenes have been shown to increase ROS generation and concomitantly activate anti-oxidant pathways to maintain cellular redox balance, which confers growth and survival advantages to cancerous cells. Beyond its role in supporting energetic requirements of oncogenic activity, GLN is also a key element in the maintenance of cellular redox balance. Yet, it is not known whether increased ROS generation resulting from activation of an oncogene or loss of a tumor suppressor can render cells dependent on

GLN for survival. Our data suggest that loss of the tumor suppressor Hace1 leads to GLN addiction due to increased ROS generation. In the absence of GLN, ROS levels are augmented, resulting in further increase in ROS eventually causing cell death. These results also imply GLN metabolism as a potential therapeutic target for treatment of cancers in which Hace1 is inactivated.

Hace1 KO MEFs are less complex genetically compared to the cells derived from patient tumors and offer a relatively straightforward system to study the effects of increased ROS levels on GLN metabolism. Hace1 reduces ROS levels by inhibiting NADPH-mediated superoxide generation both *in vitro* and *in vivo* (94). NADPH oxidases function at the cell membranes to generate superoxide, which is rapidly converted to H_2O_2 spontaneously in an acidic pH environment or catalytically by the superoxide dismutases (6). Superoxide generation by NADPH oxidase holoenzyme is carried out by the Nox catalytic subunits, of which the Nox1, Nox2 and Nox3 require recruitment of active form of the small GTPase Rac1 to the NADPH oxidase sites at the membrane (102). Hace1 ubiquitinates and targets active form of Rac1 for proteosomal degradation (89, 90) and thereby inhibits NADPH oxidase-mediated ROS generation (94). Rac1 is currently the only known E3 ligase target of Hace1. Hace1 tumor suppressor activity seems to have evolved to control ROS generation by inhibiting Rac1-dependent NADPH oxidases. The results of this chapter studies demonstrate that Hace1 KO MEFs depend on GLN for survival to cope with uncontrolled ROS generation by NADPH oxidase.

Although high levels of ROS generation can justify the dependency on GLN for survival, it does not completely explain the increased GLN uptake observed in Hace1

KO MEFs. Increased need for synthesis of antioxidants and/or building blocks, due to increased ROS generation and proliferation respectively, could both lead to this phenotype. As revealed by the metabolic labeling studies, both Hace1 WT and KO MEFs metabolize GLN similarly via the TCA cycle, although Hace1 KO MEFs seem to have only a slightly higher preference for GLN as precursor for the synthesis of the TCA cycle intermediates. Therefore these results do not address the above-mentioned issue. It may be informative to test whether treatment with antioxidant compounds could decrease GLN uptake and metabolism by Hace1 KO MEFs to the levels observed with Hace1 WT MEFs. This may help determine the role of intracellular ROS levels, if any, in the regulation of GLN uptake and metabolism.

A precedent of GLN addiction due to loss of a tumor suppressor has been described with $pRB^{-/-}$ MEFs. pRB deficient MEFs increase GLN uptake and metabolism and are dependent on GLN for survival (78), but the mechanism by which pRB loss leads to GLN addiction remain unclear. Curiously, pRB deficient cells exhibit high levels of ROS as compared with their pRB proficient counterparts (80) for reasons yet to be elucidated. Based on our findings, it is likely that GLN addiction of pRB deficient cells may also be ROS dependent. Nevertheless, the study herein is the first description of increased ROS due to loss of a tumor suppressor leading to GLN addiction.

Chapter 3: ROS-Dependent GLN Addiction of Human Cancer Cells

3.1 Background and Rationale

Results of the studies given in chapter 2 provide substantial evidence that increased ROS levels lead to GLN addiction, supporting our hypothesis. While it is relatively straightforward to probe the contribution of increased ROS levels on GLN addiction phenotype in a simple system, in which a tumor suppressor gene with a ROS-inhibiting function is deleted, it is challenging to test this in cancer cells with much more complex genetic background. Moreover, ROS can be generated by several different mechanisms in cells, including mitochondrial electron transport chain, NADPH oxidases, endoplasmic reticulum, nitric oxide synthases, and xanthine oxidases (1, 3). It is therefore difficult to estimate the contribution of each of these ROS generating pathways to GLN addiction phenotype of a given cancer cell line. Instead, we aimed to determine the mechanism of GLN starvation-induced cell death, which we predicted to be ROS mediated.

The role of GLN in maintaining cellular GSH pools has been described more than a decade ago (103-105). Recently, GLN starvation was shown to deplete GSH, increase ROS, and lead to cell death in a GLN addicted human cancer cell line (47). Based on these studies, several reviews of GLN metabolism introduced GLN as the precursor for GSH synthesis, and therefore GLN starvation is expected to deplete GSH and increase ROS in general (42, 50, 52, 59). Most proliferating cells depend on GLN for growth, however, dependency on GLN for survival (GLN addiction) varies among cancer cell lines. Yet, it has not been defined whether GLN addicted cells depend on

GLN for survival in order to manage cellular ROS levels. We hypothesized that GLN addiction phenotype of cancer cells is ROS dependent; GLN starvation depletes antioxidants and increases ROS only in the cells that require GLN for survival.

In this chapter, using several human cancer cell lines we first show that GLN withdrawal does not cause ROS elevation or antioxidant depletion in all cell types. Instead, GLN deprivation-induced ROS increase and antioxidant depletion correlates with dependency of the cells on GLN for survival. Unlike GLN independent cells, GLN addicted cells increase glucose uptake in the absence of GLN in a ROS dependent manner. Surprisingly, reducing glucose concentration to very low levels rescues GLN starvation induced ROS elevation and cell death in GLN addicted cells, and inhibition of mitochondrial metabolism by rotenone reverses this effect. GLN independent cells prevent the increase in glucose uptake upon GLN starvation by upregulating TXNIP, a negative regulator of glucose uptake. Furthermore, inhibition of mitochondrial pyruvate transport renders GLN independent cells GLN addicted. Collectively, these results suggest that GLN addicted cells solely rely on GLN for redox balance, whereas GLN independent cells compensate for GLN loss by diverting glucose into antioxidant generating pathways via mitochondrial metabolism.

3.2 Methods

Cell culture, siRNA transfection. All cell lines, except HCT116, were cultured in high glucose DMEM (Sigma) containing 2 mM GLN and supplemented with 10% FBS

(Sigma) and 1% penicillin/streptomycin (Invitrogen). HCT116 cells were maintained in McCoy's 5A medium (Sigma). 1 μg/mL insulin (Sigma) was added into culture medium for MCF7 cells. For GLN starvation experiments, cells were seeded in regular media and the next day it was replaced by high glucose DMEM without GLN and pyruvate (Gibco) supplemented with 10% dialyzed FBS (Invitrogen) and 1% penicillin/streptomycin. 2-4 mM glutamine was added where stated. Cells were transfected with 20 μM siRNAs (ON-TARGETplus, Dharmacon) using Lipofectamine RNAiMAX transfection reagent (Invitrogen).

TXNIP siRNA sequence: GCAAACAGACUUCGGAGUA

Cell death and ROS measurements. Cells were seeded in 6-well plates in triplicates. Cell death and ROS were measured as described in Chapter 2.2 using PI and DCFDA staining respectively.

Glutathione and NADPH assays. Intracellular reduced and oxidized glutathione levels were measured using a commercial kit (BioVision). ~ 1.0 x 10^6 cells were seeded in 6-cm dishes, and after indicated treatments cells were washed twice with ice-cold PBS, and lysed with 100 μL of glutathione assay buffer and glutathione was measured according to the manufacturer's protocol. Intracellular NADPH levels were measured using previously described enzymatic cycling methods (106, 107). 1.0×10^6 cells were plated in 6-cm dishes in triplicates, after treatments the cells were lysed in 150 μL of extraction buffer (20 mM nicotinamide, 20 mM NaHCO3, 100 mM Na_2CO_3), passed

several times through a 25-gauge needle and centrifuged. To destroy NADP+, 100 µL of the supernatant was incubated at 60 °C for 30 min. 160 µL of NADP-cycling buffer (100 mM Tris-HCl pH 8.0, 0.5 mM thiazolyl blue, 2 mM phenazine ethosulfate, 5 mM EDTA) containing 1.3 U of G6PD was added to a 96-well plate containing 20 µL of the cell extract, and the plate was incubated for 1 minute in the dark at 30 °C. Next, 20 µL of 10 mM glucose 6-phosphate was added into each well, and the change in absorbance at 570 nm was measured every 30 s for 4 min at 30 °C with a Tecan microplate reader.

^{14}C-Glucose uptake. ^{14}C-Glucose uptake was measured using a method similar to ^{14}C-Glutamine Uptake assays as described before (48, 95) with modifications. 2 – 3 x 10^5 cells were seeded on 6-well plates in triplicates and treated as described in the main text. The media was removed and the cells were overlaid with 800 µL of glucose-free DMEM, incubated at 37 ^{o}C for 10-15 minutes. 2 µL (0.2 µCi/µL) of D-[U-$^{14}C_6$]glucose (Perkin Elmer) was added into each well and incubated at 37 ^{o}C for 2 minutes. After washing 3 times with 1 mL PBS, 250 µL of lysis buffer (0.2% SDS, 0.2 N NaOH) was added on the cells and incubated for 30 minutes at room temperature, transferred into eppendorf tubes and incubated in a heating block at 60 ^{o}C for another 20 minutes. 25 µL of 1 N HCl was added into each tube to neutralize NaOH. 200 µL of the lysate was transferred into scintillation vials containing 6 mL scintillation liquid (Scintisafe Econo, Fisher Scientific), and the total radioactivity was determined using a β-scintillation counter (Perkin Elmer). Radioactivity was normalized to protein concentration.

Cell proliferation assay. Cell proliferation assay was performed using BrdU cell proliferation chemiluminescent assay kit (Cell Signaling Technology) in 96 well plates according to the kit instructions.

Measurement of lipid synthesis. Lipid synthesis assay was performed as described before (108, 109). 3 x 10^6 cells were seeded in 6-well plates in triplicates and the next day cells were incubated in 1 mL media with/without glutamine for 20 hours. 1.5 µCi [1,2-^{14}C]acetate added and cells were incubated for another 4 hours. Labeled cells were washed three times in PBS and lysed in 0.4 mL Triton-X 100 (0.5% in H_2O). Lipids were extracted by sequential addition of 1 mL methanol, 2 x 1 mL chloroform and 1 mL H_2O with vortexing. Samples were centrifuged at 4500 rpm using a bench top centrifuge for 20 minutes and the organic phase was transferred to a new 15 mL falcon tube, evaporated to dryness using nitrogen gas and resuspended in 50 µL chloroform. Samples were then transferred to scintillation vials with 6.5 mL Scintisafe Econo scintillation liquid, and the total radioactivity was determined using a β-scintillation counter.

Cell lysis, Western blots and antibodies. Cells were lysed with 2x SDS-sample buffer, boiled at 90 °C for 10 minutes, and ran on NuPAGE (Invitrogen) 4-12% bis-tris precast gels. Proteins then transferred on to nitrocellulose membrane and analyzed by Western blots. Antibodies used were; Cleaved Parp (BD Biosciences), phospho-H2AX, GAPDH, Akt (Cell Signaling) and TXNIP (MBL International).

Statistical analysis. Statistical significance was determined using a two-tailed student's t-test.

3.3 Results

3.3.1 GLN starvation-induced cell death correlates with ROS Elevation

Because GLN is a precursor for GSH and NADPH antioxidant synthesis and effective ROS management is vital for cancer cell survival, we hypothesized that GLN starvation-induced cell death correlates with increased ROS. To test this, we measured ROS and cell death after GLN starvation using the general ROS indicator DCFDA and propidium iodide (PI) staining respectively in several human cancer cell lines. GLN starvation induced significant cell death only in the cell lines that exhibited increased ROS levels after GLN withdrawal (Fig. 8A). On the other hand ROS levels were not affected in the cell lines that did not require GLN for survival (Fig. 8B). We designated the GLN withdrawal sensitive cells as GLN addicted (shown in red font) and insensitive cells as GLN independent (shown in blue font). These results establish a clear correlation (Fig. 8C) between GLN starvation-induced cell death and ROS increase.

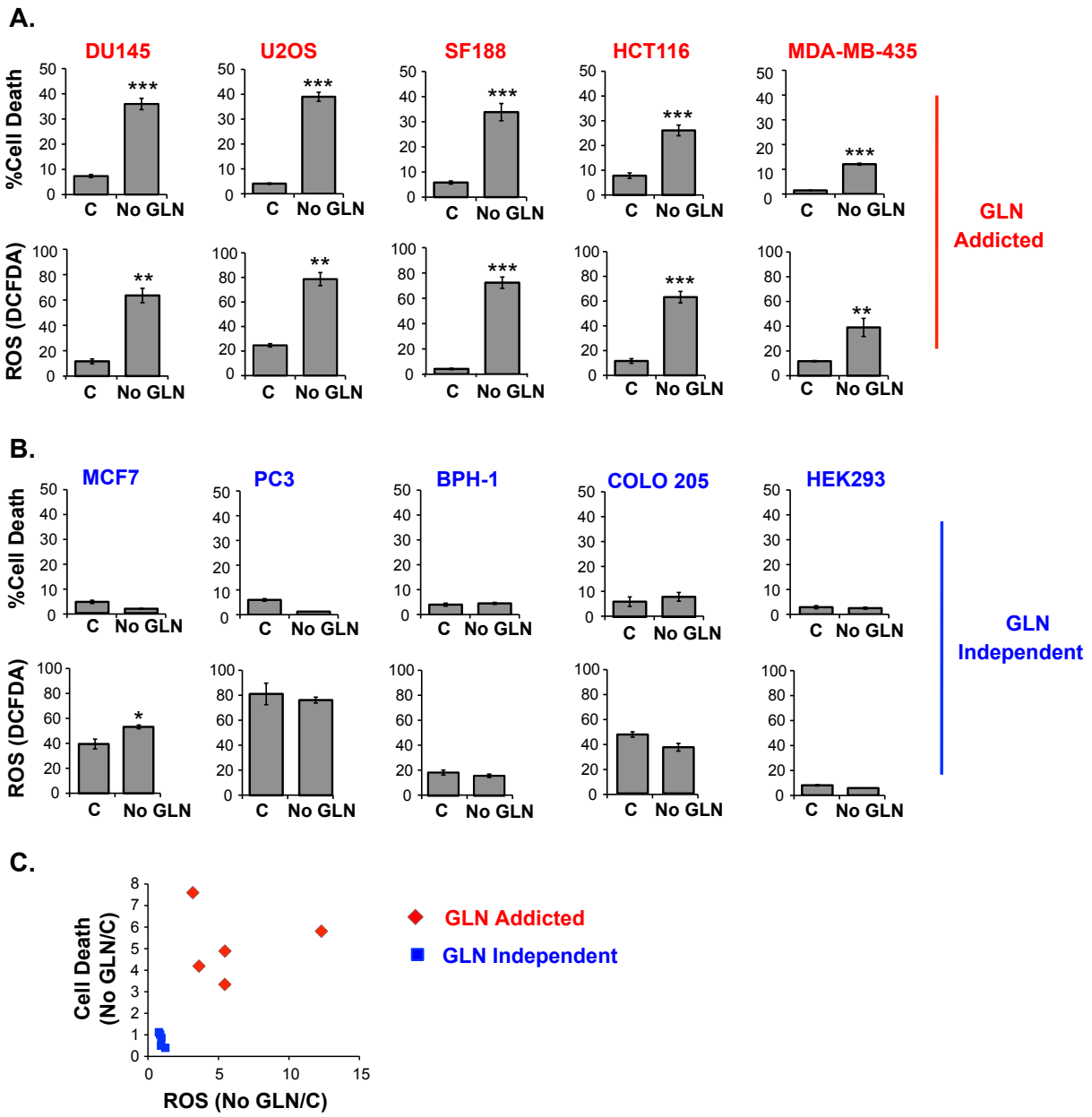

Figure 8. **GLN starvation-induced cell death correlates with increased ROS levels.** Cells were categorized as **(A)** GLN addicted (red font) and **(B)** GLN independent (blue font) based on their sensitivity to GLN starvation. Cell death was measured after 48-72 hours GLN starvation by PI staining followed by flow cytometry. ROS levels were measured after 24-48 hours GLN starvation by DCFDA staining followed by flow cytometry. **C.** Correlation analysis of ROS vs cell death in GLN addicted and GLN independent cells. Error bars represent S.D. (n=3). *$P < 0.05$, **$P < 0.005$, ***$P < 0.001$.

3.3.2 GSH or Glu inhibit GLN starvation-induced cell death and ROS elevation

To determine the contribution of GLN starvation-induced ROS increase to cell death, we tested the ability of Glu or the antioxidant GSH to rescue GLN starvation-induced cell death in two GLN addicted cell lines, U2OS and DU145. Glu is the downstream product of GLN, which can be directly used in GSH synthesis, or after conversion to α-KG, it can enter the TCA cycle to increase NADPH generation (Fig. 2). Both Glu and GSH addition inhibited GLN starvation-induced cell death and ROS increase (Fig. 9A, 9B). Addition of the antioxidant NAC also inhibited GLN starvation-induced cell death and ROS in DU145 cells (Fig. 9C). To complement these findings, we assessed the GLN starvation-induced cell death and oxidative stress by Western blot analysis of the apoptotic cell death marker cleaved-PARP (110), and the DNA damage marker phospho-H2AX (111). Oxidative stress causes damage to DNA, which mounts a DNA damage response that can be marked by increased phospho-H2AX levels (111). Consistent with above results, GLN starvation increased cleaved-PARP and phospho-H2AX levels in the GLN addicted cells (Fig. 10A). In parallel, cleaved-PARP and phospho-H2AX levels were suppressed by addition of GSH (Fig. 10A*)*. In marked contrast, GLN starvation caused only a marginal increase in cleaved-PARP and phospho-H2AX levels in the two GLN independent cell lines, PC3 and BPH-1 (Fig. 10B), showing that GLN starvation does not cause oxidative stress in these cells. We used etoposide as a positive control for functional DNA damage response, as it causes DNA strand breaks and leads to increased H2AX phosphorylation (112, 113). Etoposide treatment markedly increased phospho-H2AX levels in both PC3 and BPH-1 cells,

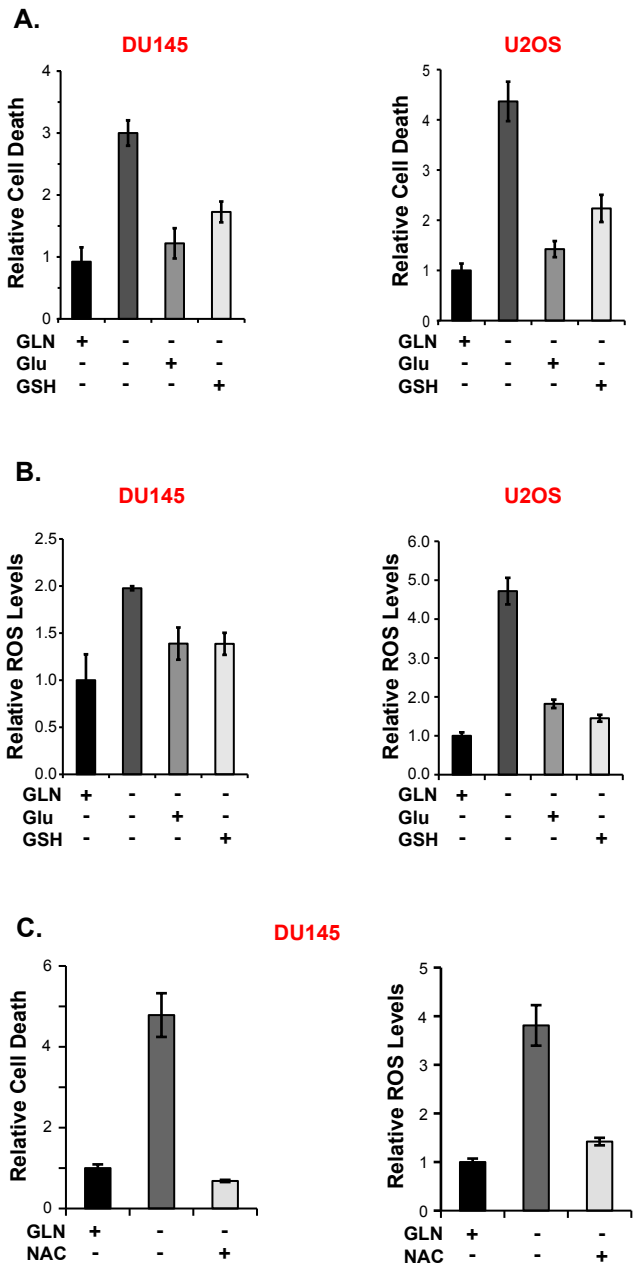

Figure 9. Glu and GSH inhibit GLN starvation-induced cell death and ROS increase. Effect of Glu (5 mM) and GSH (3 mM) on GLN starvation-induced **(A)** cell death, (**B)** ROS in GLN addicted DU145 and U2OS cells. **C.** Effect of NAC (3 mM) on GLN starvation-induced cell death and ROS in DU145 cells. Cell death and ROS were measured after 48 hours and 30 hours of GLN starvation respectively by PI or DCFDA staining. Error bars represent S.D. (n=3).

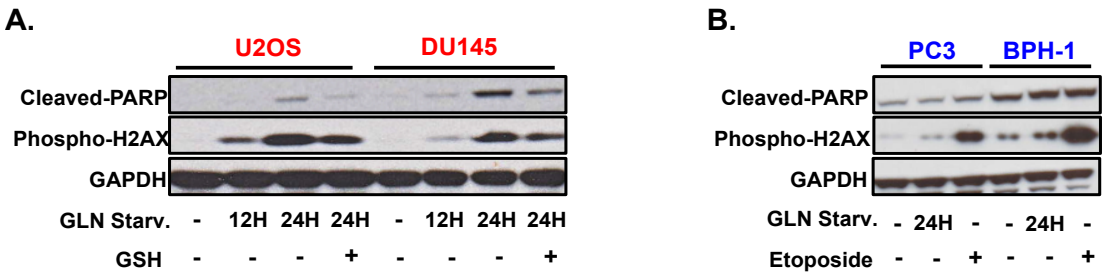

Figure 10. GLN starvation induces DNA damage response and cell death specifically in the GLN addicted cells. A. Western blot analysis of cleaved-PARP and phospho-H2AX levels in GLN addicted DU145 and U2OS cells after 12 and 24 hours GLN starvation. 3 mM GSH was used to assess its effect on GLN-starvation-induced induction of cleaved-PARP and phospho-H2AX. **B.** Western blot analysis of cleaved-PARP and phospho-H2AX levels in GLN independent PC3 and BPH-1 cells after 24 hours GLN starvation. 10 μM etoposide was used as positive control for phospho-H2AX induction.

ensuring that there are no defects in H2AX phosphorylation in these cells. Together these results demonstrate that GLN starvation induces cell death predominantly by increasing cellular ROS and oxidative stress.

3.3.3 GLN starvation depletes antioxidant pools in GLN addicted cells

GLN is a precursor for production of GSH and NADPH, which are the two crucial intracellular ROS scavengers. Because GLN withdrawal increases ROS only in the GLN addicted cells, we predicted that GSH and NADPH pools should be depleted only in the GLN addicted cells after GLN withdrawal. As predicted, both GSH and NADPH levels were reduced by more t han 50% in the GLN addicted DU145 and U2OS cells

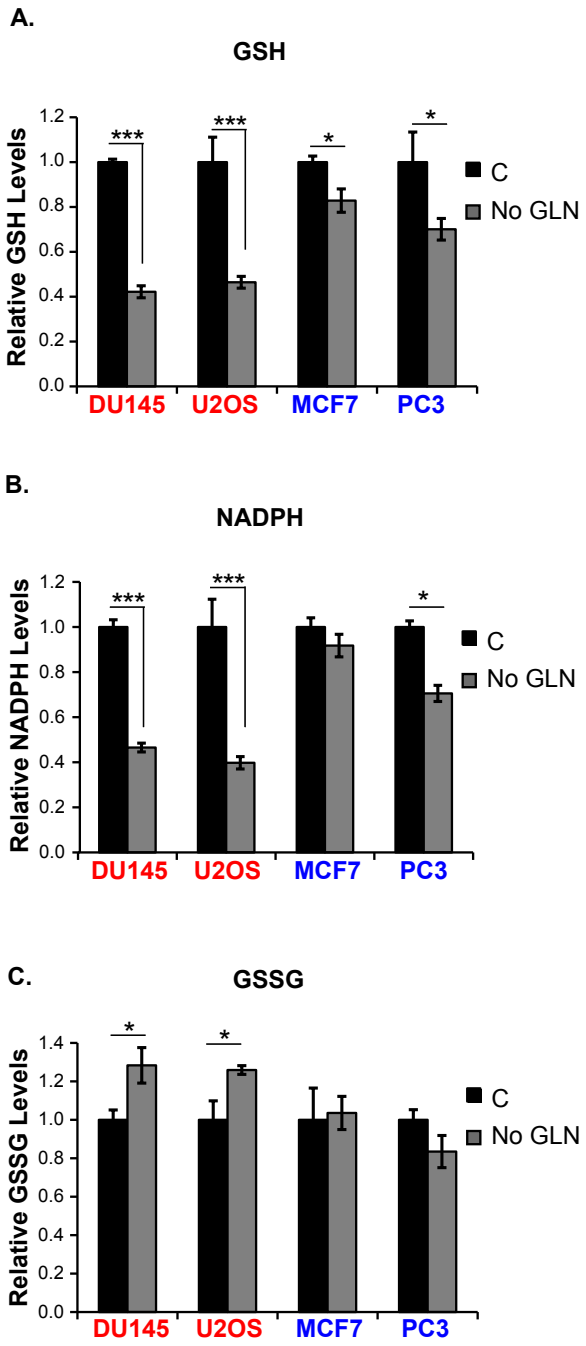

Figure 11. GLN starvation depletes antioxidant pools in GLN addicted cells. GSH **(A)**, NADPH **(B)**, and GSSG **(C)** levels were measured in GLN addicted (DU145, U2OS) and GLN independent (MCF7, PC3) cells after 20 hours of GLN starvation. Data are the average ± SD of three independent cultures. *$P < 0.05$, **$P < 0.005$, ***$P < 0.001$.

after 24 hours of GLN starvation, whereas only a modest change was observed in the GLN independent MCF7 and PC3 cells (Fig. 11A, 11B). We also measured oxidized glutathione (GSSG) levels in the same cell extracts that were used in the GSH measurements and found that GLN starvation significantly increases GSSG levels on in the GLN addicted cells after 24 hours of GLN starvation, whereas no significant change was observed in the GLN independent MCF7 and PC3 cells (Fig. 11C), suggesting that the GLN independent cells maintain sufficient levels of GSH and NADPH after GLN starvation as there is no increase in the GSSG levels.

3.3.4 Glu replenishes antioxidant pools in the GLN addicted cells in the absence of GLN

In Chapter 3.3.2 we showed that Glu inhibits GLN starvation-induced ROS increase and cell death (Fig. 9A, 9B). In order to test if this is by replenishing the antioxidant pools, we added Glu into GLN-free culture medium and measured GSH and NADPH levels in the GLN addicted DU145 and U2OS cells. Consistent with the earlier results shown in Chapter 3.3.3, GLN starvation markedly reduced both GSH and NADPH pools and addition of Glu partially rescued this effect (Fig. 12 A, 12B).

3.3.5 Glucose starvation does not deplete NADPH or induce ROS

NADPH is in general thought to be produced mainly through glucose oxidation in the pentose phosphate pathway (59, 114), and therefore glucose starvation of cells is

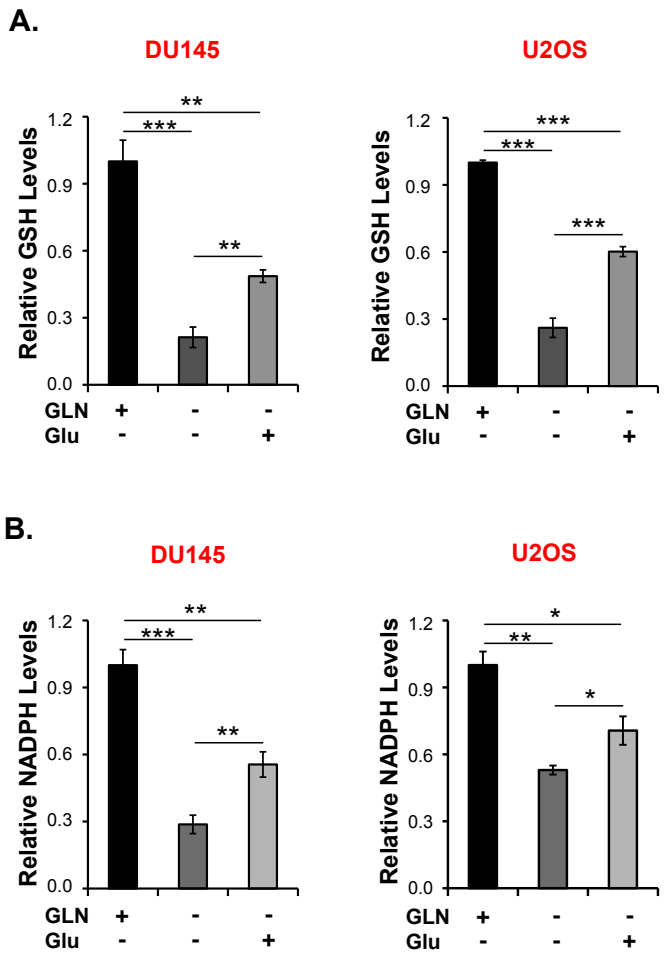

Figure 12. Glu partially rescues GLN starvation-induced depletion of antioxidant pools. Effect of Glu (5 mM) on **(A)** GSH levels **(B)** NADPH levels in GLN addicted DU145 and U2OS cells after 20 hours of GLN starvation. Data are the average ± SD of three independent cultures. *$P < 0.05$, **$P < 0.005$, ***$P < 0.001$.

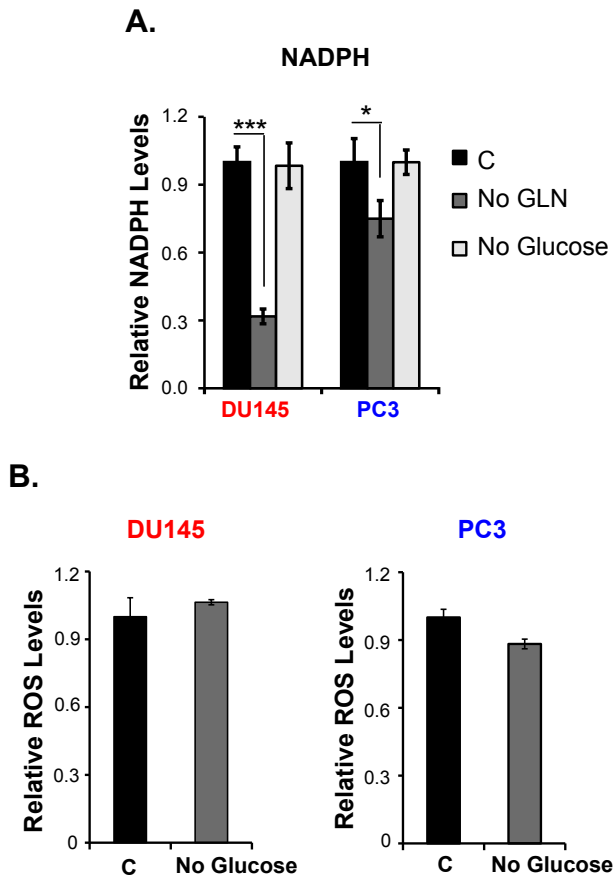

Figure 13. Glucose starvation does not deplete NADPH or increase ROS. NADPH (**A)** and ROS (**B**) levels in DU145 and PC3 cells were measured after 20 hours of GLN or glucose starvation. Results were given relative to control values in each cell line. Error bars represent SD (n=3). **P*<0.05, ****P*<0.001.

expected to increase ROS. GLN starvation-induced NADPH depletion specifically in the GLN addicted cells implied a GLN dependent vs. a GLN independent (e.g. glucose dependent) NADPH production in GLN addicted cells and GLN independent cells respectively. To test this idea, we starved the GLN addicted DU145 cells and GLN

independent PC3 cells from either GLN or glucose for 20 hours and measured NADPH levels. In keeping with the results shown in the previous sections of this chapter, GLN starvation led to a severe depletion of NADPH in DU145 cells whereas it was modestly changed in PC3 cells (Fig. 13A). Interestingly, glucose starvation did not cause any significant reduction in the NADPH pools in neither cell lines. In parallel, glucose starvation did not increase cellular ROS levels in these cells (Fig. 13B). This suggests that GLN addicted cells completely rely on GLN for NADPH synthesis, whereas GLN independent cells may employ different precursors and pathways to compensate NADPH levels.

3.3.6 GLN starvation increases glucose uptake in GLN addicted cells in a ROS dependent manner

Because the antioxidant levels are not reduced as much after GLN withdrawal in the GLN independent cells, we wondered whether these cells are able to use other means to replenish their GSH and NADPH pools in the absence of GLN. Glucose has been recognized as the major source of NADPH production via pentose phosphate pathway (59, 114). Therefore we anticipated that the GLN independent cells might increase glucose uptake in the absence of GLN to generate more NADPH, which would increase recycling of the GSSG back to GSH, preventing oxidative stress. Unexpectedly, glucose uptake was remarkably elevated in GLN addicted DU145 and U2OS cells 24 hours after GLN withdrawal, whereas it was reduced or unchanged in the GLN independent MCF7 and PC3 cells respectively (Fig. 14A). We then tested if increased glucose uptake in the GLN addicted cells is due to increased ROS after GLN

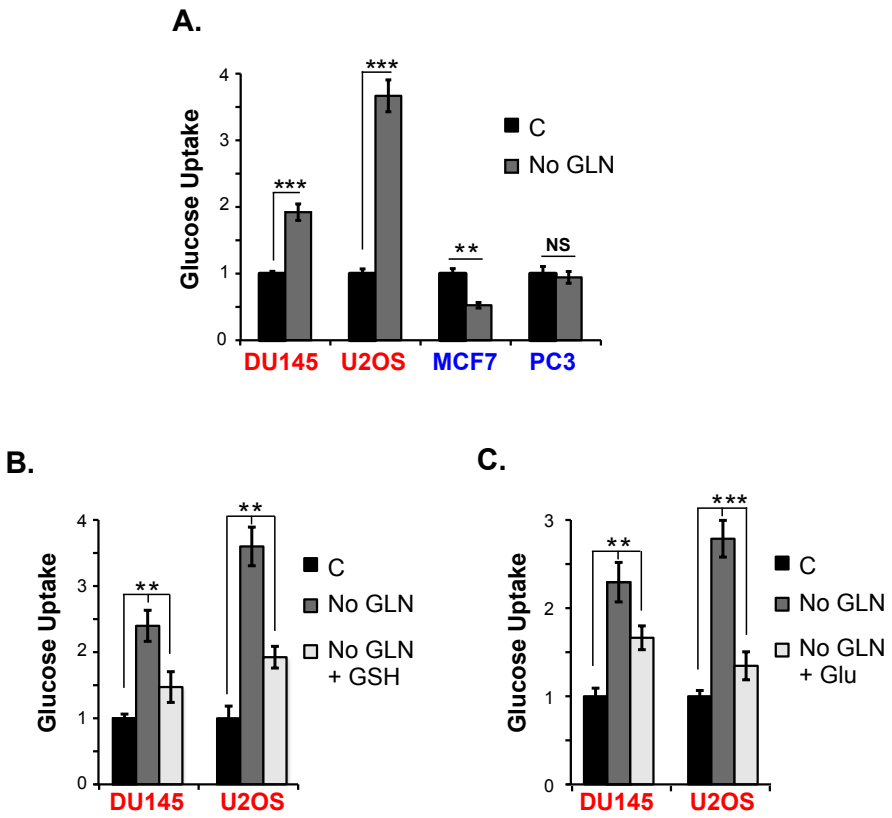

Figure 14. GLN starvation increases glucose uptake in GLN addicted cells in a ROS dependent manner. A. ^{14}C-glucose uptake by GLN addicted (DU145, U2OS) and GLN independent (MCF7, PC3) cells after 18-20 hours of GLN starvation. **B**. ^{14}C-glucose uptake by GLN addicted DU145 and U2OS cells after 20 hours of GLN starvation with/without 3 mM GSH or 5 mM Glu (**C**). Data is average ± SD of 3 independent cultures. **P*<0.05, ***P*<0.005, ****P*<0.001.

withdrawal. Addition of Glu or GSH into the culture medium blocked GLN starvation induced elevation of glucose uptake in both DU145 and U2OS cells (Fig. 14B, 14C), which places GLN starvation-induced ROS upstream of increased glucose uptake.

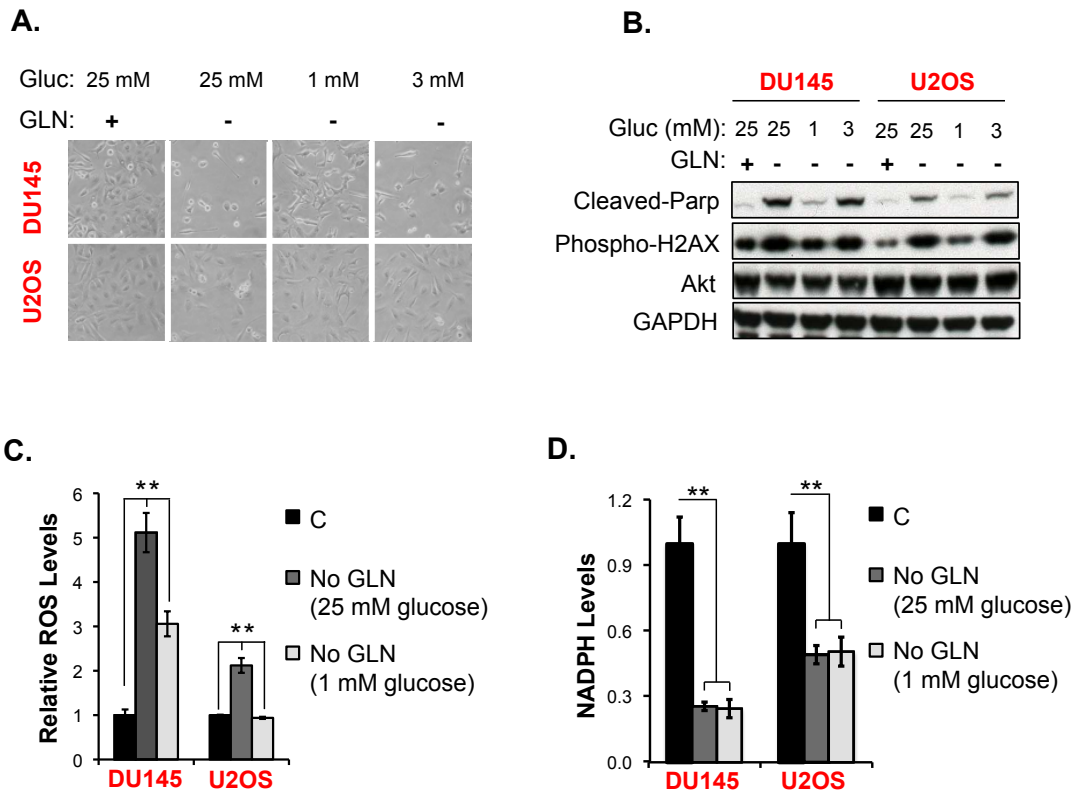

Figure 15. **GLN addicted cells survive GLN starvation in low glucose medium. A** Images of DU145 and U2OS cells cultured in GLN-supplemented or GLN-free medium containing high (25 mM) or low (1 mM, 3 mM) concentrations of glucose. **B.** Western blot analysis of cleaved PARP and phospho-H2AX levels in cells treated as in A. **C.** ROS were measured in DU145 and U2OS cells cultured for 20 hours in GLN-free media containing either 25 mM or 1 mM glucose using DCFDA staining. **D.** NADPH levels were measured in DU145 and U2OS cells cultured for 20 hours in GLN-free media containing either 25 mM or 1 mM glucose. Error bars represent SD (n=3). **P*<0.05, ***P*<0.005, ****P*<0.0005.

3.3.7 Increased glucose uptake in the absence of GLN aggravates ROS and leads to cell death in GLN addicted cells

To determine if high levels of glucose uptake in the absence of GLN causes oxidative stress and cell death in GLN addicted cells, we cultured the cells in GLN-free high glucose (25 mM), or low glucose (1 mM and 3 mM) media and compared the cell death and oxidative stress by Western blot analysis of the cleaved-PARP and phosho-H2AX levels. Reducing glucose concentration to 1 mM rescued GLN starvation induced cell death and oxidative stress evident from the low levels of cleaved-PARP and phospho-H2AX comparable to basal levels (Fig. 15A, 15B). Moreover, DCFDA measurements revealed that ROS induction by GLN starvation was efficiently inhibited by reducing glucose concentration down to 1 mM in the culture medium (Fig. 15C, 15D), but did not change NADPH levels (Fig. 15D). Combined with above results, these findings demonstrate that GLN starvation-induced oxidative stress elevates glucose uptake in GLN addicted cells, which in return aggravates oxidative stress in the absence of GLN and leads to cell death.

3.3.8 Increased glucose uptake in the absence of GLN does not cause increased proliferation or lipid synthesis

Above results indicate that increased glucose uptake in the absence of GLN is detrimental for GLN addicted cells. We inferred that increased concentration of intracellular glucose when GLN concentration is low might serve as a signal to continue or increase proliferation, which would magnify the stress and lead to a catastrophic cell death. To test this idea, we measured DNA synthesis using the thymidine analog 5-

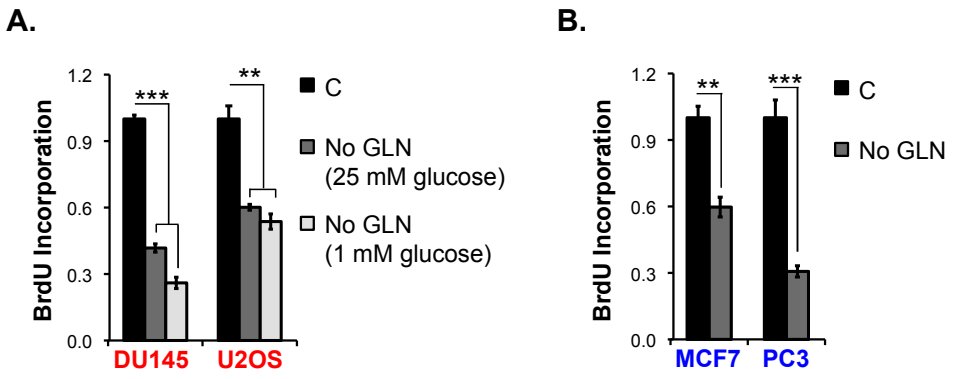

Figure 16. GLN starvation inhibits proliferation in both GLN addicted and GLN independent cells. A. Effect of GLN starvation in high (25 mM) or low (1 mM) glucose medium on cell proliferation in GLN addicted DU145 and U2OS cells. **B.** Effect of GLN starvation on cell proliferation in GLN independent cells. Cells were cultured for 24 hours and proliferation was measured using BrdU incorporation assay. Error bars represent SD (n=3). **P*<0.05, ***P*<0.005, ****P*<0.0005.

bromo-2'-deoxyuridine (BrdU) in both GLN addicted and GLN independent cells with/without GLN starvation. Proliferating cells incorporate BrdU into newly synthesized DNA (during S-phase of cell cycle) in place of thymidine. As shown in figure 16A, 16B, all four cell lines exhibited significantly reduced BrdU incorporation after GLN starvation. Reducing glucose concentration down to 1 mM in the absence of GLN did not cause further decrease in BrdU incorporation in GLN addicted cells, suggesting that GLN starvation-induced cell death is not due to continuous or increased proliferation.

Lipid synthesis is one of the major processes that consume NADPH (43, 59). As mentioned earlier, NADPH is generated by oxidation of glucose through pentose phosphate pathway, and by partial oxidation of GLN through glutaminolysis. Since GLN

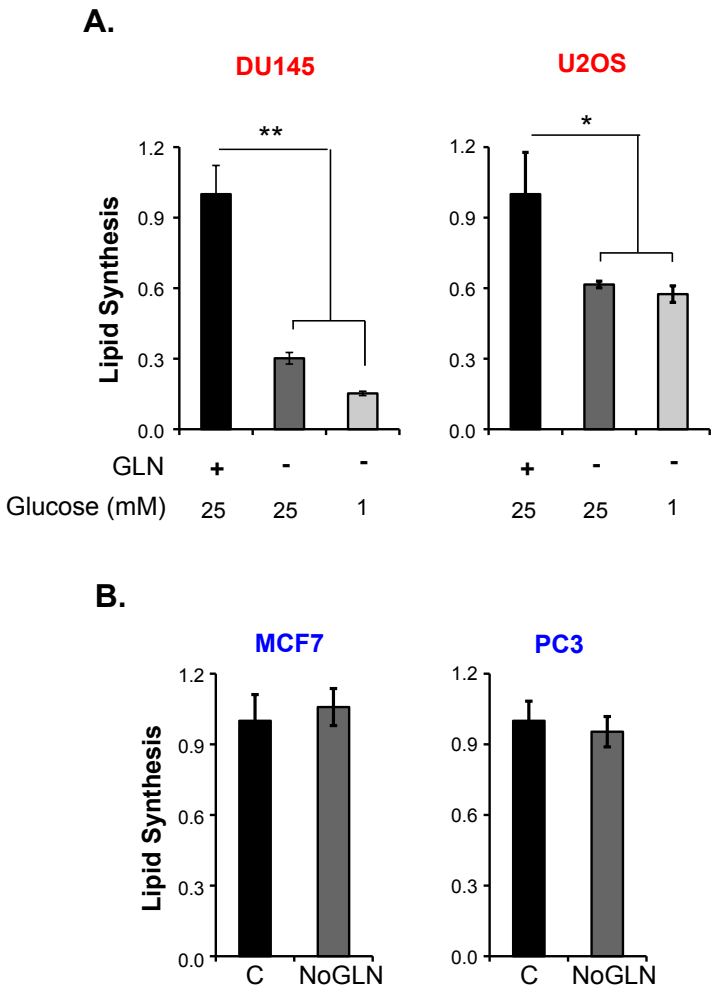

Figure 17. GLN starvation inhibits lipid synthesis in GLN addicted cells. A. Effect of GLN starvation in high (25 mM) or low (1 mM) glucose medium on lipid synthesis in GLN addicted DU145 and U2OS cells. **B.** Effect of GLN starvation on lipid synthesis in GLN independent cells. Cells were starved from GLN for 18 hours and incubated with $^{14}C_2$-acetate for another 5 hours. Lipids were extracted and quantified as described in materials and methods. Error bars represent SD (n=3). *P<0.05, **P<0.005.

starvation depletes NADPH pools in GLN addicted cells, we predicted that due to high glucose uptake, GLN addicted cells might synthesize more NADPH but continue or

increase lipid synthesis, leading to increased NADPH consumption that exceeds the rate of NADPH synthesis. However, the rate of lipid synthesis was reduced in GLN addicted cells after GLN starvation, whereas it was not changed in GLN independent cells (Fig. 17A, 17B). Together these results suggest that increased glucose uptake in the absence of GLN does not cause cell death due to sustained DNA or lipid synthesis.

3.3.9 Mitochondrial metabolism contributes to survival of GLN addicted cells under GLN starvation and low glucose condition

Above findings suggested that high glucose concentration might block a process that helps cells compensate for the loss of GLN, a major nutrient source. Apart from glucose and GLN, which serve as main fuel supply for proliferating cells, mitochondria can also metabolize other nutrients, such as amino acids and lipids (43). Therefore we presumed that mitochondrial metabolism might contribute to survival of GLN addicted cells under GLN starvation and low glucose condition, by making use of other nutrients. Treatment of the GLN addicted U2OS cells with very low concentration of rotenone, a well-established inhibitor of mitochondrial metabolism, resulted in significant ROS increase under no GLN/1 mM glucose (low glucose) condition (Fig. 18), suggesting that GLN addicted cells rely on residual mitochondrial metabolism in the absence of GLN and high glucose concentration completely abrogates it. Interestingly, rotenone significantly increased ROS levels also when cells were cultured in 25 mM glucose and GLN replete medium, but it did so to a lesser extend in the absence of GLN. Hence, inhibition of mitochondrial metabolism under basal conditions appears to mimic GLN starvation.

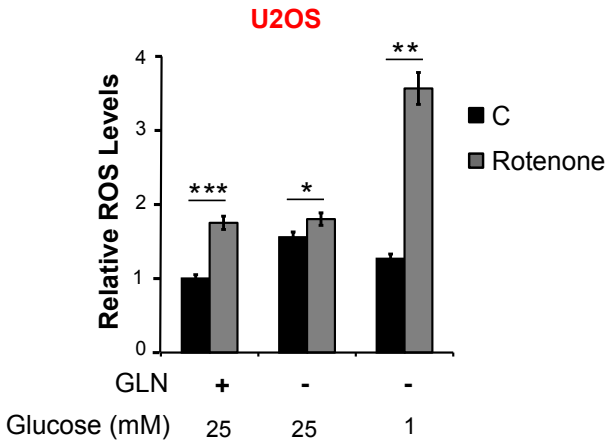

Figure 18. Inhibition of mitochondrial metabolism increases ROS levels in GLN addicted cells under GLN starvation/low glucose condition. Cells were GLN starved in high glucose (25 mM) or low glucose (1mM) medium for 20 hours. 0.5 μg/μL rotenone was used where indicated. Error bars represent SD (n=3). **P*<0.05, ***P*<0.005, ****P*<0.001.

3.3.10 GLN independent cells block elevation of glucose uptake by increasing TXNIP expression in the absence of GLN

GLN levels were previously shown to regulate glucose uptake in a TXNIP (thioredoxin interacting protein) dependent manner (115). TXNIP is a well-characterized inhibitor of TRX antioxidant activity (116, 117). Independent from its TRX inhibitory function, TXNIP directly binds to the glucose transporter Glut1 via its α-arrestin domain and inhibits glucose transport (118). When GLN is present, TXNIP expression is suppressed and cellular glucose transport is maintained. GLN withdrawal upregulates TXNIP expression and thereby inhibits glucose uptake to ensure growth arrest (115). Based on these reports, we hypothesized that GLN independent cells might block GLN

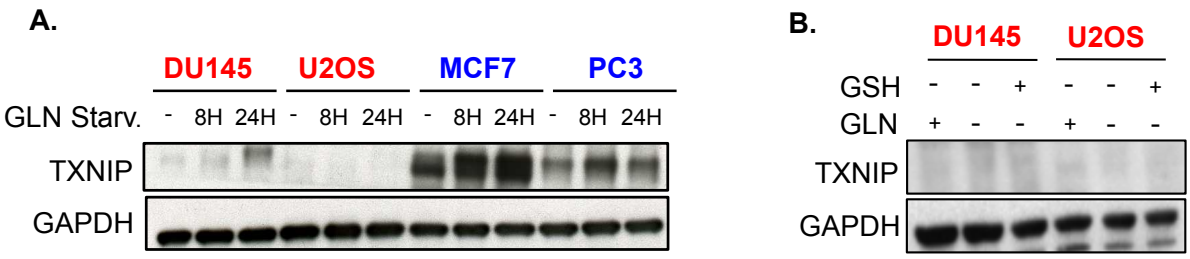

Figure 19. GLN addicted cells cannot induce TXNIP expression under GLN starvation. A Comparison of TXNIP protein expression in GLN addicted (DU145, U2OS) and GLN independent (MCF7, PC3) cells under control and GLN starvation conditions by Western blot analysis. **B.** Effect of GSH on TXNIP protein levels in GLN addicted cells under GLN starvation (24 hours).

starvation-induced elevation of glucose uptake by upregulating TXNIP expression. We therefore compared TXNIP protein levels in GLN addicted and GLN independent cells with/without GLN starvation. As shown in figure 19A, GLN starvation did not induce TXNIP protein in GLN addicted DU145 and U2OS cells, whereas it resulted in a marked increase in the GLN independent MCF7 and PC3 cells. Interestingly, TXNIP levels were vanishingly low in the GLN addicted cells as compared to the GLN independent cells under basal conditions. Since GLN starvation increases ROS levels only in the GLN addicted cells, we suspected that TXNIP induction by GLN starvation might be inhibited by ROS. However, treatment of the GLN addicted DU145 and U2OS cells with the antioxidant GSH did not effect an increase in TXNIP levels in the absence of GLN (Fig. 19B). These findings suggest that contrary to the GLN independent cells, GLN addicted

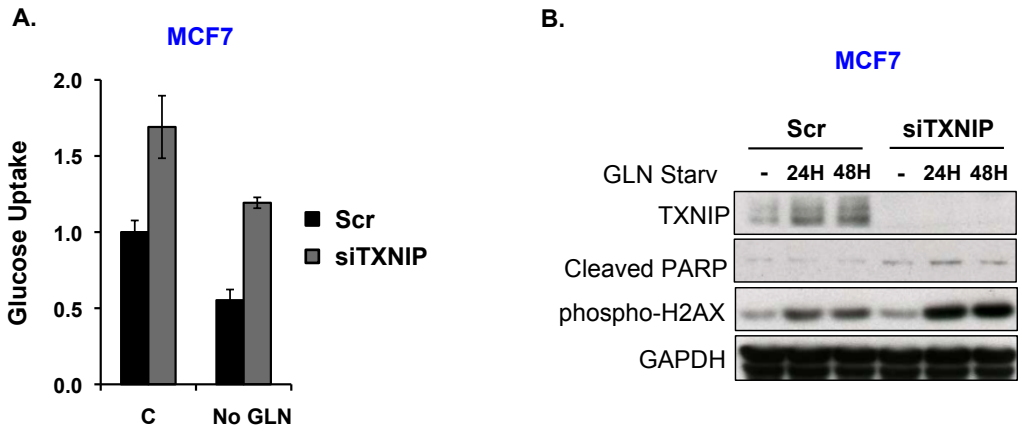

Figure 20. Reducing TXNIP expression increases glucose uptake in GLN independent MCF7 cells. A Comparison of glucose uptake in GLN independent MCF7 cells treated with 20 nM scrambled (Scr) or TXNIP siRNAs (siTXNIP) cultured in normal or GLN-free medium (24 hours). **B.** Effect of TXNIP knock down on cell death (cleaved PARP) and oxidative damage (phospho-H2AX) in MCF7 cells cultured in normal or GLN-free media. Error bars represent SD (n=3).

cells have very low TXNIP levels and are somehow not able to induce it, as they should upon GLN starvation.

We next tested if down regulation of TXNIP could increase glucose uptake in GLN independent cells in the absence of GLN. Knock down of TXNIP using specific siRNAs resulted in increased glucose uptake in MCF7 cells under both basal and GLN starvation conditions (Fig. 20A). This prompted us to hypothesize that down regulation of TXNIP may render GLN independent cells GLN addicted due to increased glucose uptake. However, despite the increased glucose uptake, down regulation of TXNIP expression in MCF7 cells induced only a marginal increase in ROS levels and cell death

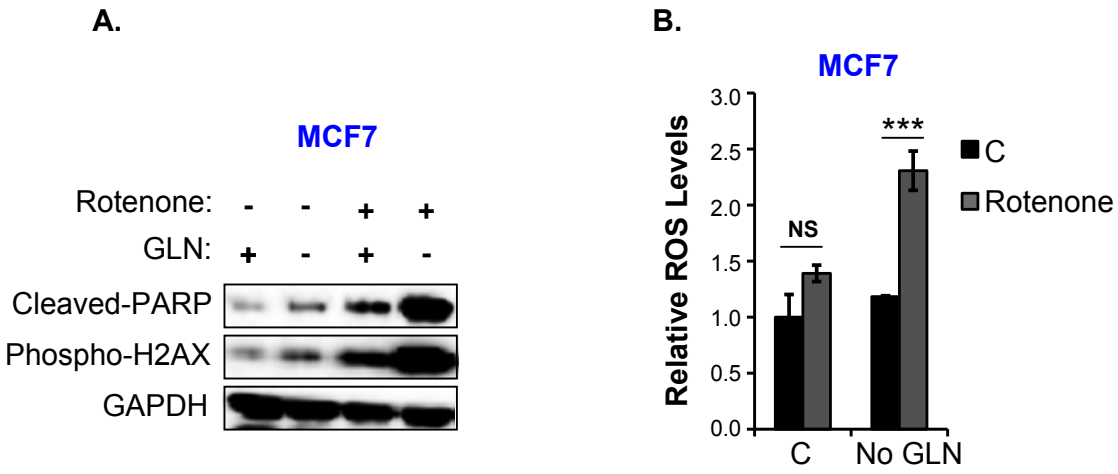

Figure 21. Inhibition of mitochondrial metabolism renders GLN independent cells GLN addicted. A. Effect of mitochondrial metabolism inhibitor (rotenone) on oxidative stress and cell death in GLN independent MCF7 cells cultured in the presence or absence of GLN. Cell death and oxidative stress were determined by western blot analysis of cleaved PARP and phospho-H2AX levels respectively. GAPDH was used as loading control. **B.** Effect of rotenone treatment on ROS levels in MCF7 cells. 0.5 μg/μL rotenone was used. GLN starvation was carried out for 24 hours. Error bars represent SD (n=3). $^{***}P < 0.001$.

as measured by phospho-H2AX and cleaved-PARP levels (Fig. 20B), implying that increased glucose uptake alone is not sufficient to sensitize GLN independent cells to GLN starvation and there may be other factors contributing GLN addiction phenotype.

3.3.11 Inhibition of mitochondrial metabolism renders GLN independent cells GLN addicted

The results of the studies given in this chapter so far established that GLN independent cells do not rely on GLN for redox balance. Unlike the GLN addicted cells,

they maintain or even decrease glucose uptake under GLN starvation. This hinted the possibility that these cells may use glucose efficiently and are able to divert it into the antioxidant generating pathways. Oxidation of glucose-derived pyruvate by mitochondrial metabolism can compensate for GLN loss to produce NADPH and Glu, and eventually reduced GSH. To test this idea, we first used rotenone to inhibit mitochondrial metabolism in GLN independent MCF7 cells and analyzed oxidative stress and cell death under GLN starvation. Rotenone markedly increased oxidative stress and cell death in MCF7 cells under GLN starvation as evidenced by the increased cleaved PARP and phospho-H2AX levels (Fig. 21A). We confirmed the induction of oxidative stress by rotenone treatment in the absence of GLN by ROS measurements (Fig. 21B).

To test specifically the importance of glucose derived pyruvate metabolism in mitochondria for survival of GLN independent cells under GLN starvation, we used UK-5099, a specific inhibitor of mitochondrial pyruvate transport (Fig 22), and examined whether GLN starvation induces oxidative stress and cell death, and depletes GSH in GLN independent MCF7 cells when pyruvate entry to mitochondria is inhibited. Similar to rotenone, UK-5099 also markedly increased oxidative stress and cell death in the absence of GLN apparent from the increased phospho-H2AX levels and cleaved PARP levels (Fig. 23A). In parallel, UK-5099 treatment caused a significant reduction in GSH in the absence of GLN (Fig. 23B). Of note, both rotenone and UK-5099 treatment increased phospho-H2AX and cleaved PARP levels also in the presence of GLN, however to a much lesser extend. These results support the premise that GLN independent cells adopted a mechanism that can alternate between the nutrients

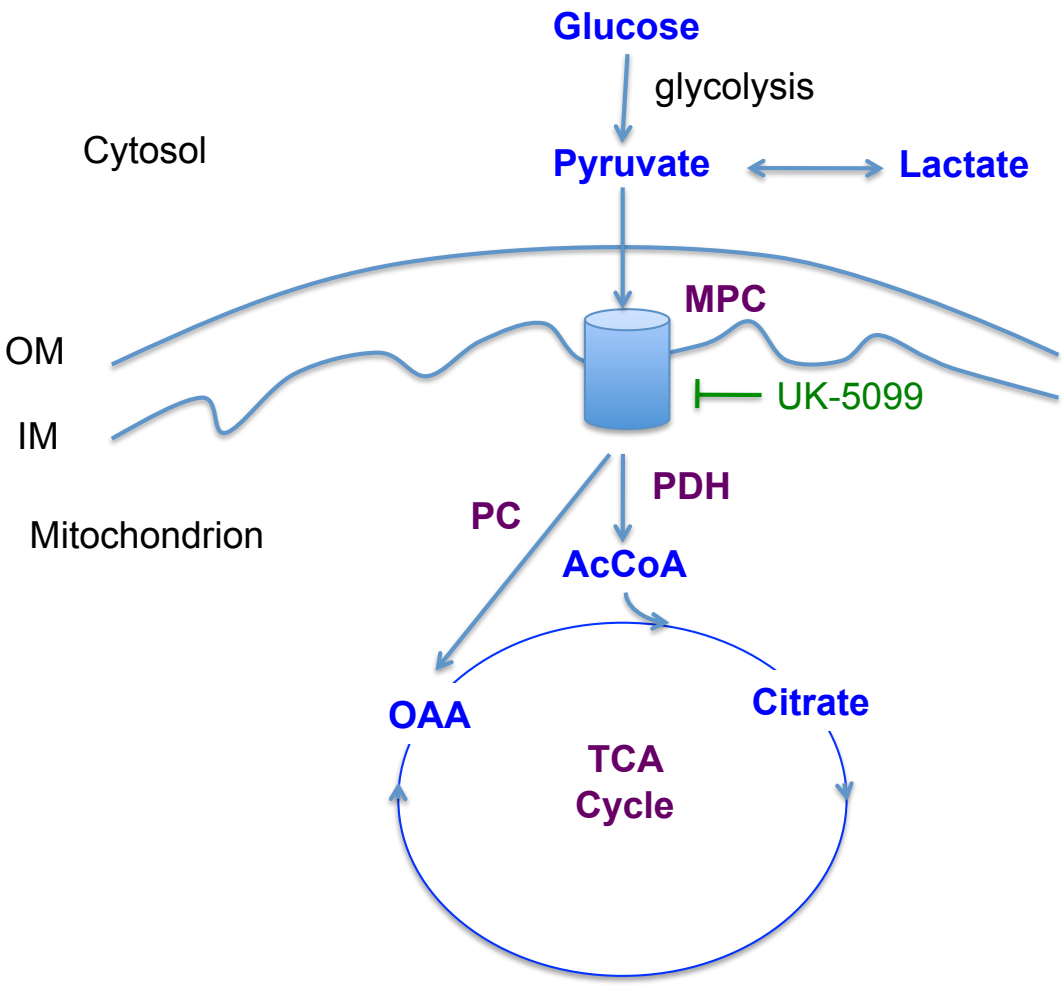

Figure 22. **Pyruvate transport and oxidation by mitochondria.** Pyruvate is synthesized from glucose via glycolysis and transported into mitochondria by mitochondrial pyruvate carrier (MPC). Pyruvate carboxylase (PC) or pyruvate dehydrogenase (PDH) oxidize pyruvate producing the TCA cycle precursors oxaloacetate (OAA) or Acetyl Co-A (AcCoA) respectively. UK-5099 is a specific inhibitor of MPC. OM (outer mitochondrial membrane), IM (inner mitochondrial membrane).

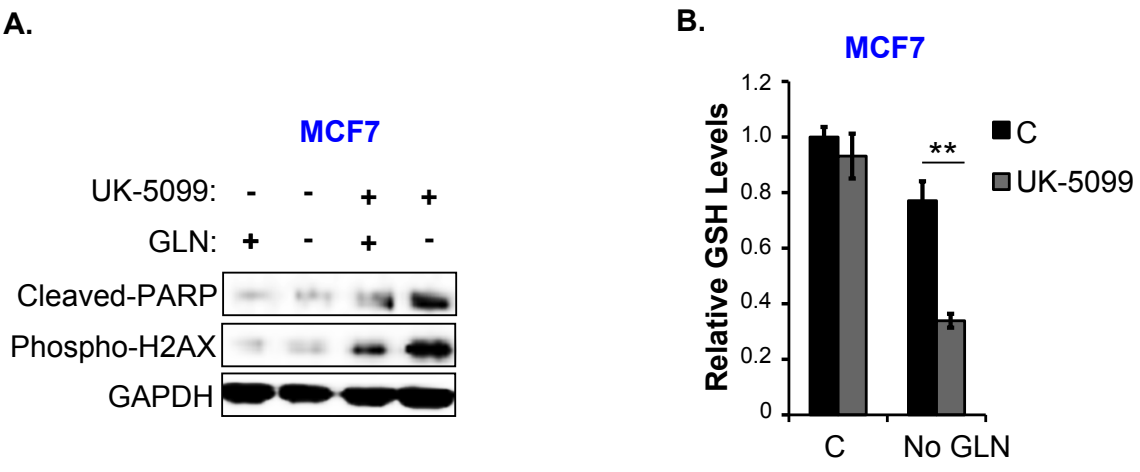

Figure 23. Inhibition of mitochondrial pyruvate transport renders GLN independent cells GLN addicted. A. Effect of mitochondrial pyruvate transport inhibitor (UK-5099) on oxidative stress and cell death in GLN independent MCF7 cells cultured in the presence or absence of GLN. Cell death and oxidative stress were determined by western blot analysis of cleaved PARP and phospho-H2AX levels respectively. GAPDH was used as loading control. **B.** Effect of UK-5099 treatment on GSH levels in MCF7 cells. 100 μM UK-5099 was used. GLN starvation was carried out for 24 hours. Error bars represent SD (n=3). $^{**}P < 0.005$.

depending on their availability, which allows them to control their redox state and survive.

3.3.12 Combination of GLN starvation with oxidative stress inducing agents effectively kills GLN addicted cells

The above studies clearly demonstrate that GLN addicted cells depend on GLN to maintain sufficient pools of antioxidants and manage ROS levels. Accordingly, we

predicted that treatment of the GLN addicted cells with pro-oxidant reagents while depriving them from their antioxidant precursor GLN may efficiently kill them by exacerbating oxidative stress. One such pro-oxidant reagent is piperlongumine (PL), which was shown to increase oxidative stress by both generating intracellular ROS and inhibiting antioxidant pathways (74, 119). We tested the efficiency of PL treatment alone at a low concentration or in combination with GLN starvation in inducing cell death in a number of GLN addicted and GLN independent human cancer cell lines. PL treatment did not cause significant cell death when the cells were supplied with GLN, however it induced marked cell death in GLN addicted cells in the absence of GLN (Fig. 24A). Consistent with the results shown earlier in this chapter, PL treatment did not synergize with GLN starvation to kill GLN independent cells (Fig. 24B), indicating that these cells can use other means to clear ROS in the absence of GLN whereas GLN addicted cells completely depend on GLN to cope with ROS. ROS levels also correlated with cell death as shown in GLN addicted DU145 cells, in which PL treatment amplified GLN starvation-induced ROS levels (Fig. 24C).

3.4 Discussion

Most cancer cell types depend on GLN for survival, but how GLN starvation induces cell death remains elusive. The findings presented in this chapter corroborate a GLN starvation induced cell death mechanism whereby increased ROS levels, triggered by GLN starvation, signal for increased glucose uptake, which surprisingly exacerbates the deleterious effects of GLN starvation in GLN addicted cells. GLN independent cells

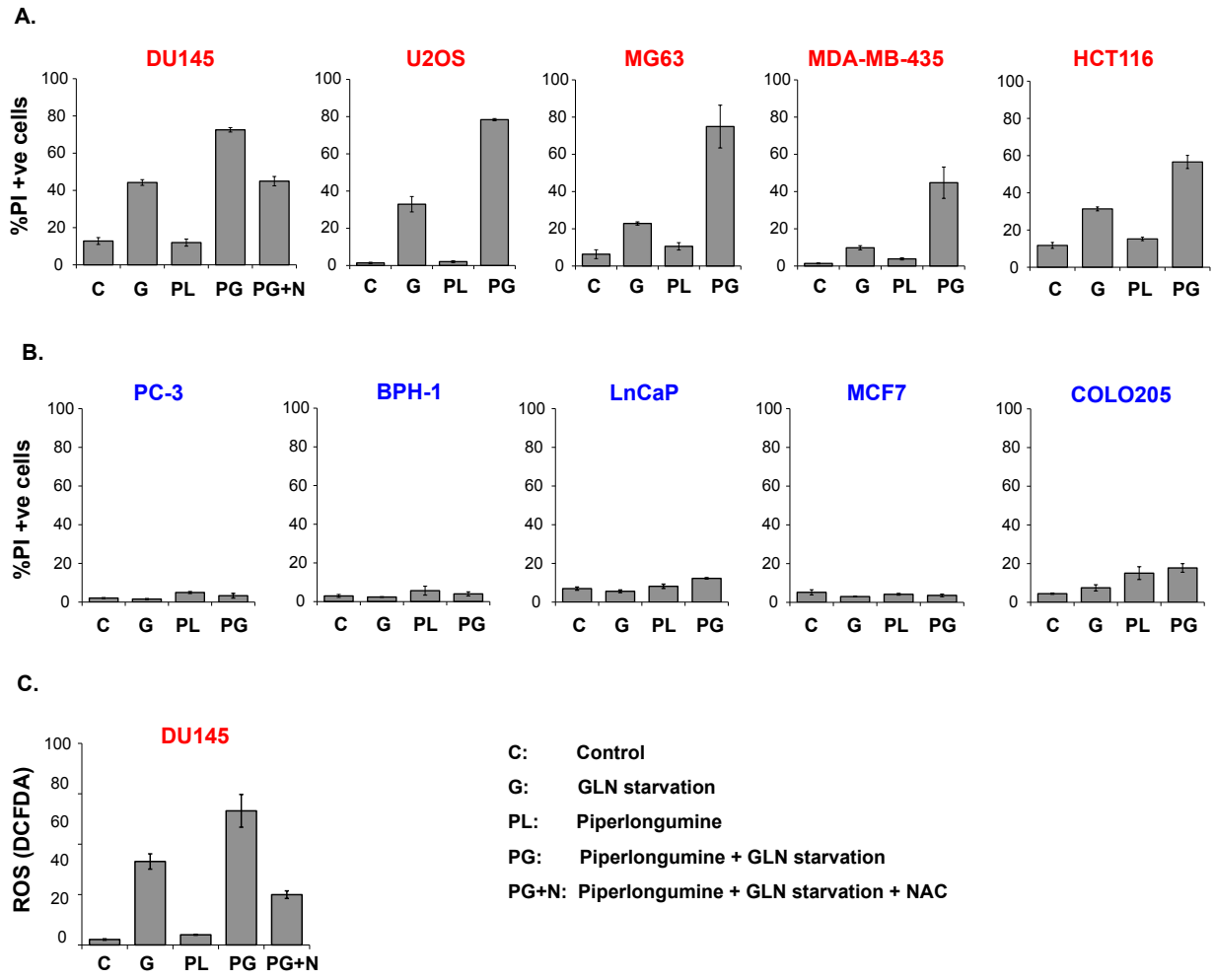

Figure 24. Pro-oxidant reagent piperlongumine synergizes with GLN starvation to kill GLN addicted cells. Effect of 5 μM piperlongumine on GLN starvation-induced cell death in **(A)** GLN addicted and **(B)** GLN independent cells. **C.** Effect of piperlongumine on GLN starvation-induced ROS levels in DU145 cells. Cell death was measured after 48 hours of GLN starvation by PI staining. ROS were measured after 30 hours GLN starvation by DCFDA staining. 5 mM NAC was added where indicated. Error bars represent SD (n=3).

escape this catastrophic cell death presumably by evading the initial ROS increase as well as by regulating glucose uptake and metabolism in the absence of GLN.

GLN was initially viewed as nitrogen and carbon source for cancer cells for synthesis of macromolecules and energy and therefore GLN starvation-induced cell death was associated with energetic crisis. Yuneva et al. demonstrated that c-Myc transformation renders cells GLN addicted, but GLN starvation-induced cell death was shown to be independent of GSH depletion and ROS increase in their studies (120). However, a later study reported GSH depletion and ROS increase upon GLN starvation in Myc dependent human cancer cell lines (47). Therefore recent reviews of cancer cell metabolism have implicated GLN as an essential source of GSH synthesis and therefore GLN withdrawal-induced cell death has been linked to depletion of GSH pools and increased ROS in human cancer cell lines (52, 59). Here we show that GLN starvation-induced GSH depletion and ROS elevation are not common features of human cancer cells and establish a correlation between GLN-starvation-induced cell death and ROS elevation. GLN starvation depletes antioxidant pools (GSH and NADPH) only in GLN addicted cells, suggesting that some cells do not rely solely on GLN and are able compensate by perhaps using another source, such as glucose to maintain their antioxidant pools. Accordingly, we expected that GLN independent cells take up more glucose under GLN starvation as compared to the GLN addicted cells. On the contrary, we found that GLN addicted cells increase glucose uptake markedly, whereas the GLN independent cells maintain or even decrease it in the absence of GLN. Incubation of GLN addicted cells with GSH or Glu under GLN starvation blocks the increase of glucose uptake, indicating that GLN starvation first increases ROS

levels, leading to a striking increase in glucose uptake. Unexpectedly, GLN addicted cells have less ROS and survive better in the absence of GLN when glucose concentration is vanishingly low, suggesting that high glucose concentration either causes increased ROS production or inhibits a survival pathway under GLN deplete conditions. Inhibition of mitochondrial metabolism reverses the rescue of GLN addicted cells by low glucose concentration in the absence of GLN and induces massive cell death. This implies that in an attempt to better deal with ROS burden imposed by GLN deprivation, cells increase glucose uptake, however, high glucose concentration somehow inhibits mitochondrial metabolism in GLN addicted cells when GLN is absent.

It has been proposed before that GLN starvation induces cell death by reducing glutaminolysis and restricting glucose uptake by increasing TXNIP expression (115). This view was based on the findings that TXNIP expression is repressed in the presence of GLN and GLN withdrawal de-represses it resulting in inhibition of glucose uptake. However, in that study authors did not provide any information whether their model cell line (BxPC-3) is GLN dependent for survival. Contrary to what has been proposed, our results demonstrate that GLN addicted cells are deficient in TXNIP induction upon GLN starvation and GLN starvation increases TXNIP expression and inhibits glucose uptake elevation only in the GLN independent cells. Down regulation of TXNIP increases glucose uptake in GLN independent cells regardless of GLN availability, however it does not render these cells dependent on GLN for survival. This could be due to several reasons. First, the results introduced in 3.3.6 (Fig.14) demonstrate a ROS-dependent elevation of glucose uptake in GLN addicted cells after GLN starvation. It is possible that induction of ROS by GLN starvation must precede

elevation of glucose uptake. Since GLN starvation does not induce ROS in the GLN independent cells, increased glucose uptake alone may not be sufficient to cause oxidative stress and cell death without GLN. Second, due to the inhibitory effect of TXNIP on the antioxidant activity of TRX (116, 117), reducing TXNIP expression may promote an enhanced TRX antioxidant activity preventing ROS increase.

Glucose can be metabolized in the pentose phosphate pathway and/or the TCA cycle to produce NADPH and Glu (precursor of GSH) respectively. Hence, it is paradoxical that GLN addicted cells cannot maintain their antioxidant pools and suppress ROS despite the surge of glucose in the absence of GLN. We initially presumed that high glucose concentration might signal for proliferation, which would lead to a catastrophic cell death in the absence of the major nutrient GLN. However, cell proliferation as well as the NADPH and energy consuming lipid synthesis were suppressed in GLN addicted cells under GLN starvation. Thus, it is unclear why the antioxidant pools are depleted and ROS are elevated when there is ample supply of glucose. One possibility is the inability of the GLN addicted cells to use glucose efficiently. Although GLN independent cells do not increase glucose uptake with GLN starvation, they may be able to shunt it to right pathways to compensate for GLN depletion. For instance, pyruvate carboxylase has been shown to confer GLN independence by facilitating OAA formation from glucose-derived pyruvate (96). This OAA can then be used in NADPH generating pathways, as well as in GSH synthesis after conversion to Glu via TCA cycle. Our findings support this premise. Inhibition of mitochondrial pyruvate transporters by the specific inhibitor UK-5099 leads to depletion

of GSH and, and to increased oxidative stress and cell death in the GLN independent MCF7 cells under GLN starvation.

Several studies demonstrated vulnerability of cancer cells to ROS-inducing molecules (16, 74, 75). Our results show that GLN starvation, combined with the ROS-inducing compound piperlongumine at the sub-toxic concentration when GLN is present, triggers massive cell death in GLN addicted cells. Interestingly, when GLN is present piperlongumine does not cause ROS increase at the concentration used, however, it augments ROS levels in the absence of GLN. Both cell death and ROS induction is inhibited by NAC indicating that the observed effects are ROS dependent. These findings suggest that GLN addicted cells depend on GLN to cope with both endogenous and exogenous oxidative stress, highlighting combined treatment of GLN depletion and oxidants as a potentially efficient strategy for treatment of GLN dependent tumors. However, usefulness of this strategy will likely depend on identification of biomarkers for GLN addiction phenotype, as GLN independent cells are not sensitive to this treatment.

Chapter 4: GLN Addicted Cells Respond to Oxidative Stress by Increasing GLN Uptake via AMPK-Mediated Upregulation of the GLN Transporter ASCT2 Expression

4.1 Background and Rationale

The results obtained from the studies given in Chapter 3 established that GLN addicted cells depend on GLN for survival to manage intracellular ROS, as well as to cope with toxic effects of oxidative-stress inducing compound piperlongumine. Considering the critical role of GLN in the maintenance of antioxidant pools, we hypothesized that treatment of GLN addicted cells with oxidants may increase GLN uptake. In this chapter we tested this hypothesis and investigated the possible mechanisms that mediate this response.

We found that GLN starvation sensitizes GLN addicted cells to exogenous oxidants, and addition of antioxidants completely prevents this sensitivity suggesting absolute requirement of GLN for anti-oxidative activity in GLN addicted cells. Supporting our hypothesis, GLN addicted cells increase GLN uptake in response to oxidative stress treatment. Several different amino acid transporters, including SLC38A1, SLC38A2, SLC38A3, SLC38A5, and ASCT2 (SLC1A5) are known to mediate transport of GLN into cells depending on the tissue or cell type (56). Among these, ASCT2 is the primary transporter expressed in rapidly proliferating normal and tumor cells in culture (121). We show that oxidative stress treatment increases GLN uptake by upregulating

specifically the major GLN transporter ASCT2 expression. Finally we demonstrate that this response is mediated by AMPK pathway, which is a master regulator of cellular metabolism. Inhibition of ASCT2 or AMPK expression by siRNAs also sensitizes GLN addicted cells to oxidative stress, suggesting that AMPK-mediated upregulation of ASCT2 expression confers resistance to oxidative stress.

4.2 Methods

Cell culture, reagents, siRNA transfection. Cell culture and siRNA transfections were performed as described in Chapter 3.2. GLN-free medium was supplemented with 1 mM sodium pyruvate (Invitrogen) before H_2O_2 treatment. H_2O_2, sodium arsenite solution, compound C were purchased from Sigma. JNK (SB600125), p38 (In Solution SB203580), and MEK1/2 (PD-325901) inhibitors were from EMD Biosciences. Final concentrations of inhibitors used were: 30 μM (JNK inhibitor), 15 μM (p38 inhibitor), 3 μM (MEK1/2 inhibitor). siRNAs were purchased from Dharmacon (Thermo Fisher). siRNA sequences are given in table 1. Smart pools of siRNAs specific for α1 and α2 isoforms of AMPK α-subunits were pooled for efficient down regulation. Stealth RNAi™ siRNA Luciferase Reporter Control (Invitrogen) was used as control siRNA (Scr).

Cell death and ROS measurements. Cell death and ROS were measured using PI or DCFDA staining respectively followed by flow cytometry as described in Chapter 2.2.

Table 1. siRNA sequences used in the Chapter 4 RNA interference experiments.

ASCT2 (pooled)
GCAAGGAGGUGCUCGAUUC
GCCUUUCGCUCAUACUCUA
AMPK α1 (SmartPool)
CCAUACCCUUGAUGAAUUA
GCCCAGAGGUAGAUAUAUG
GAGGAUCCAUCAUAUAGUU
ACAAUUGGAUUAUGAAUGG
AMPK α2 (SmartPool)
CGACUAAGCCCAAAUCUUU
GAGCAUGUACCUACGUUAU
GACAGAAGAUUCGCAGUUU
GUCUGGAGGUGAAUUAUUU
NRF2 (NFE2L2)
GAGUUACAGUGUCUUAAUA
MYC
AACGUUAGCUUCACCAACA
ATF2
GGAAGUACCAUUGGCACAA
JUN
GAGCGGACCUUAUGGCUAC
FOXO3
CGAAUCAGCUGACGACAGU

Table 2. Primer pairs used for amplification of ASCT2, SLC38A5, and GAPDH mRNAs.

ASCT2 (SLC1A5)
Forward: GAGCTGCTTATCCGCTTCTTC
Reverse: GGGGCGTACCACATGATCC
SLC38A5
Forward: GCGCTTCTGTCGTCCTACTC
Reverse: GCTCGGATGCCTGCAATAC
GAPDH
Forward: AAGGTGAAGGTCGGAGTCAAC
Reverse: GGGGTCATTGATGGCAACAATA

^{14}C-GLN uptake. GLN uptake assays were performed as described in Chapter 2.2.

Western blots and antibodies. Western blots were done as in Chapter 2.2. ASCT2, GAPDH, Akt, AMPKα, phospho-AMPKα (Thr172), ACC, phospho-ACC (Ser79), JNK, phospho-JNK (Thr183/Tyr185), Jun, phospho-Jun (Ser63), ATF2, Myc, Foxo3, phospho-Foxo3 (Ser413) antibodies were from Cell Signaling. Actin and NRF2 antibodies were from Santa Cruz. ASCT2 antibody recognizes nonglycosylated and glycosylated forms of human ASCT2.

Semi-quantitative RT-PCR. After indicated treatments total RNA was extracted from the cells using RNeasy RNA extraction kit (Qiagen). RNA concentrations were determined by nanodrop and normalized to 10 ng/µL RNA. 120 ng RNA was used for reverse transcription (Quantitech RT-PCR kit, Qiagen) in a total reaction volume of 20 µL. cDNA was diluted by addition of 10 µL ultrapure water (Gibco). Semi-quantitative RT-PCR was performed using Fast SYBR® Green Master Mix (Invitrogen). Primer sequences are given in table 2.

Statistical analysis. Statistical significance was determined using a two-tailed student's t-test.

4.3 Results

4.3.1 GLN addicted cells are more sensitive to exogenous ROS in the absence of GLN

Because GLN addicted cells depend on GLN to manage intracellular ROS levels, we predicted that these cells might be more sensitive to exogenous ROS when deprived of GLN as well. To test this, we starved a number of GLN addicted and GLN independent cells from GLN and challenged them with H_2O_2 treatment. H_2O_2 treatment induced massive cell death in the GLN addicted cells (U2OS and DU145) in the absence of GLN, whereas no significant cell death was observed when the cells were supplemented with GLN (Fig. 25A). Addition of catalase in culture medium blocked H_2O_2-induced cells death in the absence of GLN. Similarly, both GSH and Glu rescued

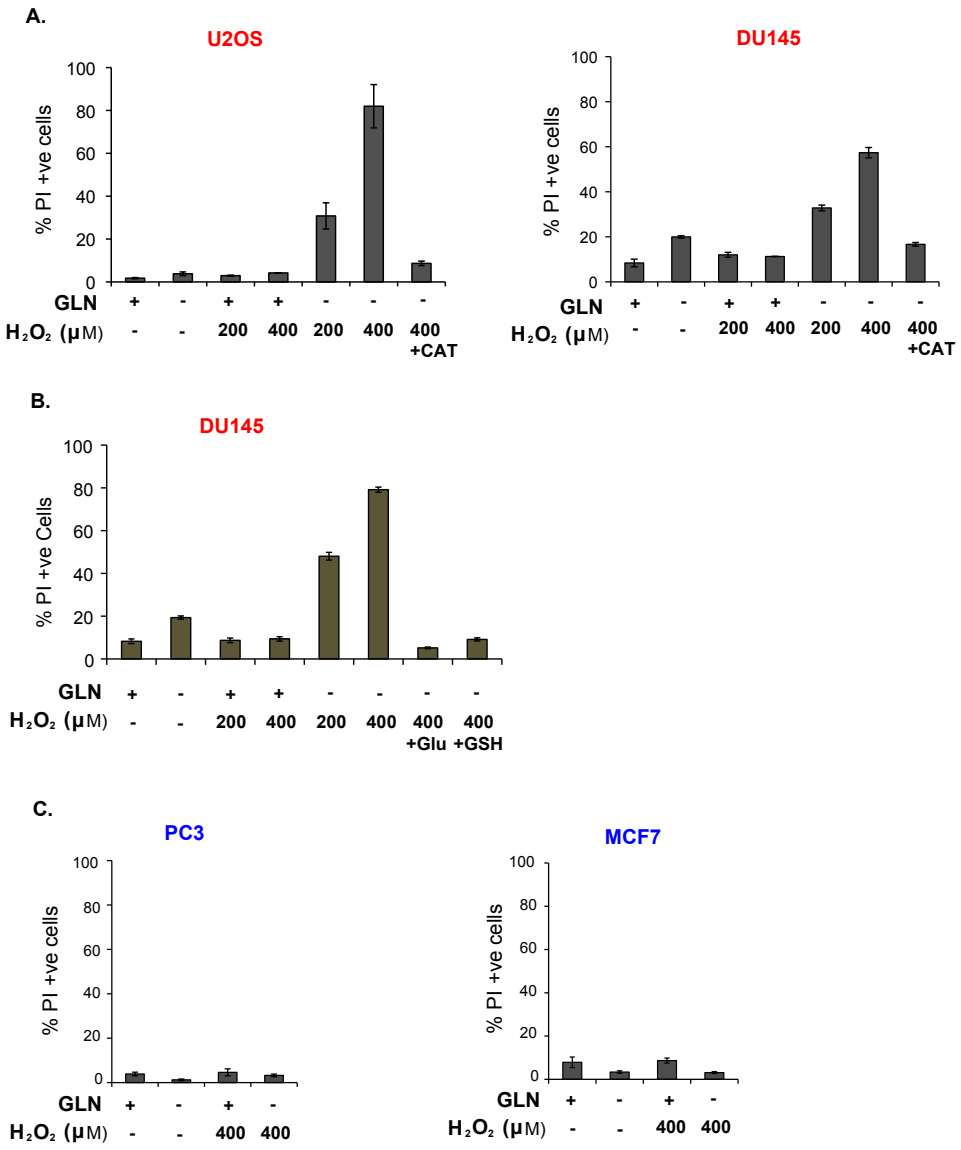

Figure 25. GLN addicted cells are more sensitive to H_2O_2 treatment in the absence of GLN. A. GLN starvation sensitizes GLN addicted cells to H_2O_2 treatment, and catalase (CAT, 100 units/mL) reverses this effect. **B.** Glu (5 mM) or GSH (3 mM) addition abrogates sensitivity of DU145 cells to H_2O_2 treatment under GLN starvation. **C.** H_2O_2 treatment does not induce cell death in GLN independent PC3 and MCF7 cells regardless of GLN presence. H_2O_2 was added after 8 hours of GLN starvation and cells were incubated for another 20 hours. Cell death was determined by PI staining followed by flow cytometry and given as %PI positive (+ve) cells. Error bars represent SD (n=3).

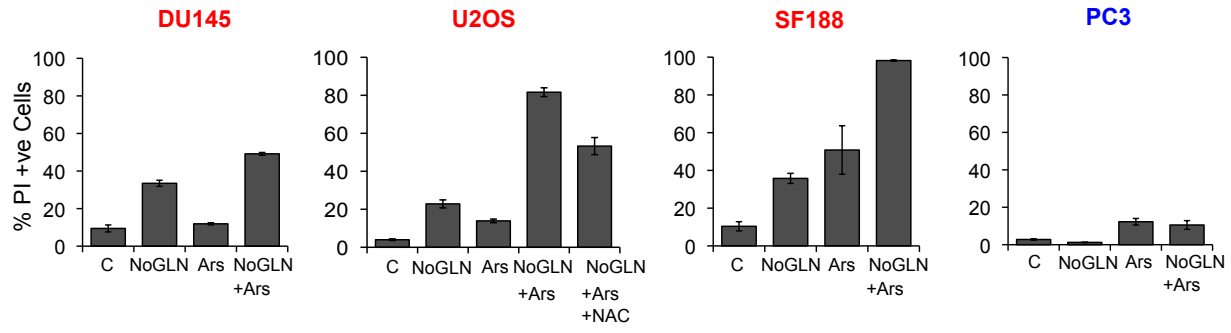

Figure 26. GLN addicted cells are more sensitive to arsenite treatment in the absence of GLN. GLN addicted (DU145, U2OS, SF188) and GLN independent (PC3) cells were starved from GLN for 8 hours and incubated with 10 μM arsenite (Ars) for another 26 hours. Cell death was determined by PI staining followed by flow cytometry and given as %PI positive (+ve) cells. Error bars represent SD (n=3).

H_2O_2-induced cell death in the absence of GLN in DU145 cells (Fig. 25B). By sharp contrast, GLN independent cells (PC3 and MCF7) were not sensitive to H_2O_2 treatment at the concentrations used regardless of GLN presence (Fig. 25C). Similar results were obtained with arsenite treatment, another oxidative stress inducing agent (122) (Fig. 26). Together these results suggest that GLN addicted cells require GLN to cope with both endogenous and exogenous oxidative stress, whereas, GLN independent cells do not depend solely on GLN for redox balance.

4.3.2 Oxidative stress increases GLN uptake in GLN addicted cells

As explained in 1.1.2, in order to block oxidative stress, cells must engage their antioxidant pathways involving the antioxidants GSH and NADPH. Because GLN

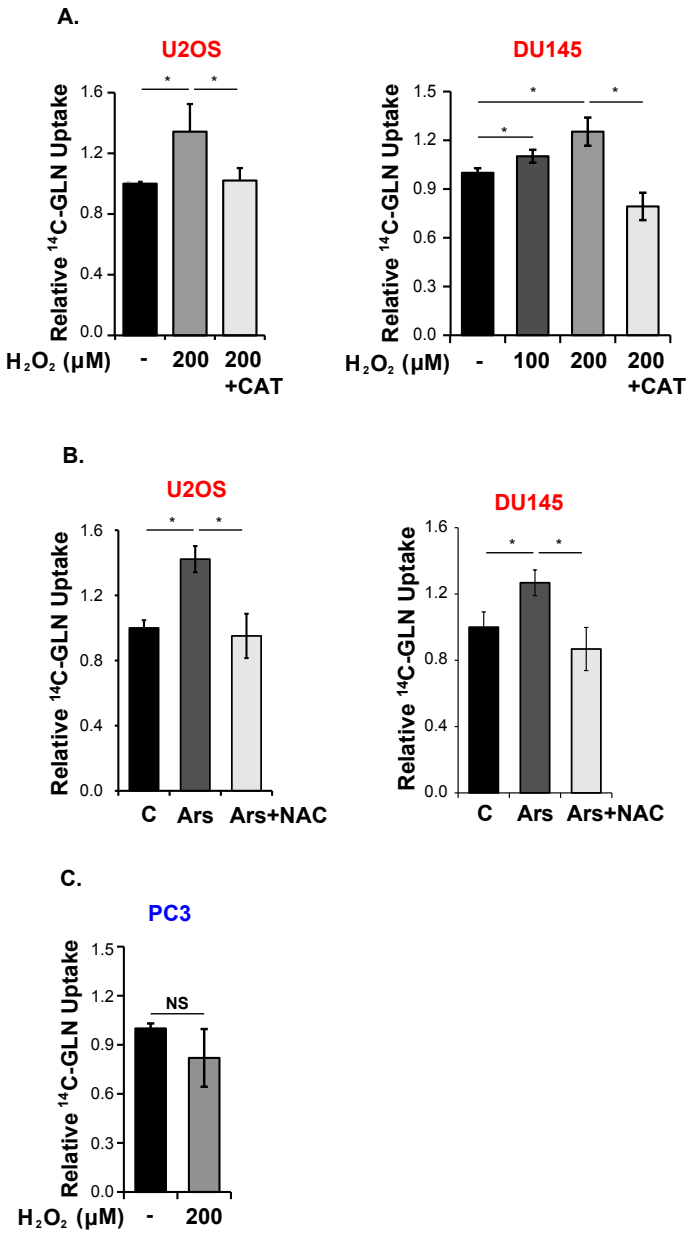

Figure 27. **Oxidative stress increases GLN uptake in GLN addicted cells. A**.^{14}C-GLN uptake assay in GLN addicted U2OS and DU145 cells after 18 hours of H_2O_2 treatment. 100 units/mL catalase (CAT) was added to reverse the effect of H_2O_2. **B.** ^{14}C-GLN uptake assay in GLN addicted U2OS and DU145 cells after 18 hours of arsenite treatment. 5 μM NAC was added to reverse the effect of arsenite. **C.** ^{14}C-GLN uptake assay in GLN independent PC3 cells after 18 hours of H_2O_2 treatment. Error bars represent SD (n=3). *P<0.05.

addicted cells depend on GLN to maintain sufficient levels of these two vital antioxidants molecules, we predicted that oxidative stress treatment of the cells might increase GLN uptake to prevent oxidative damage. Indeed, H_2O_2 treatment increased GLN uptake in the GLN addicted U2OS and DU145 cells, which was reversed by addition of catalase in culture medium (Fig. 27A). Arsenite treatment also increased GLN uptake in U2OS and DU145 cells (Fig. 27B), indicating that GLN addicted cells respond to various types of oxidative stress by upregulating GLN uptake. In contrast, GLN uptake by GLN independent PC3 cells was not changed by H_2O_2 treatment (Fig. 27C), which is in agreement with above results that these cells do not depend on GLN to manage oxidative stress.

4.3.3 Oxidative stress increases GLN uptake by increasing the GLN transporter ASCT2 expression

To determine if GLN addicted cells respond to oxidative stress treatment at the genetic level, we measured mRNA levels of the major GLN transporters ASCT2 and another neutral amino acid transporter (including GLN) SLC38A5 in GLN addicted cells with/without oxidative stress treatment. As shown in figure 28A, 28B, both H_2O_2 and Arsenite treatment increased specifically the ASCT2 mRNA levels in GLN addicted U2OS and DU145 cells. SLC38A5 mRNA levels were slightly increased in the U2OS cells, however to a lesser extend. There were no changes in the mRNA levels of neither of the GLN transporters in GLN independent PC3 cells with oxidative stress treatment (Fig. 28C). Consistent with the changes in mRNA levels, ASCT2 protein levels were

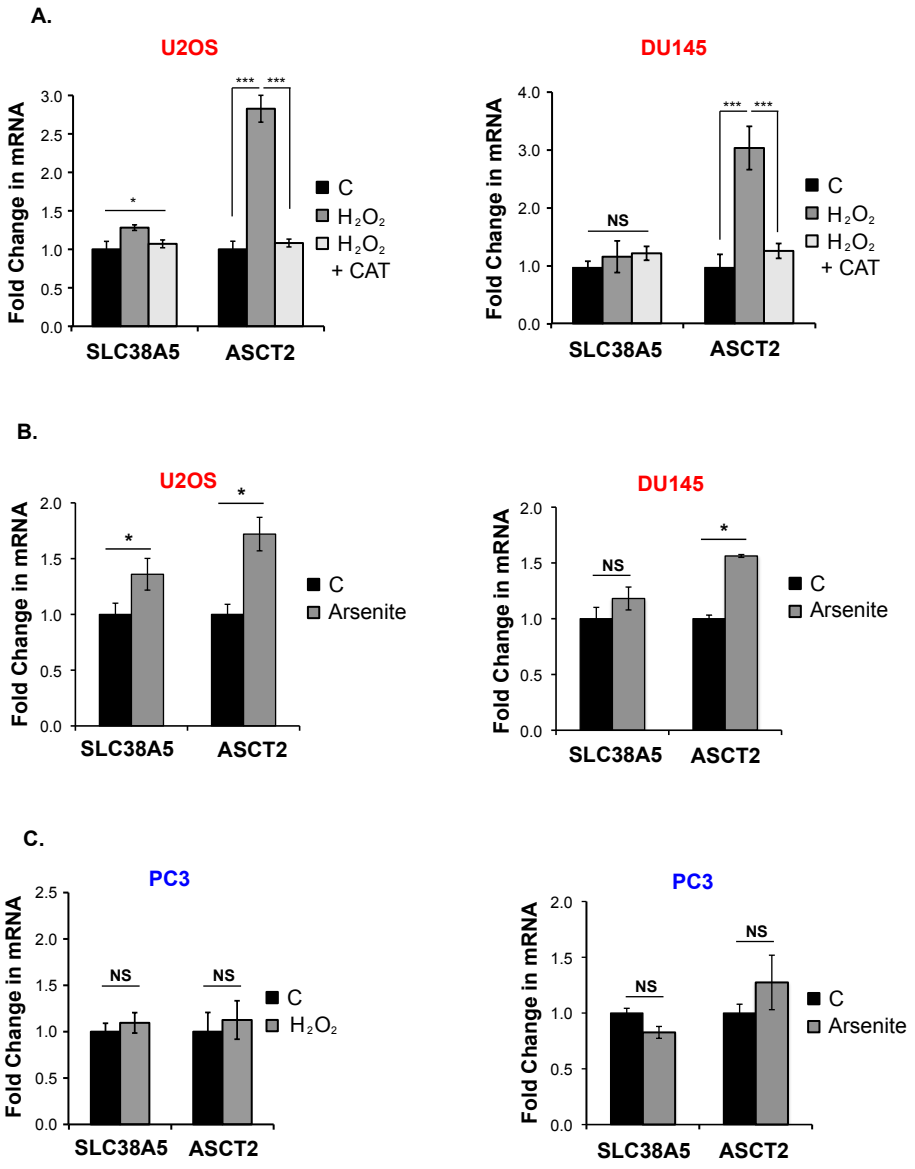

Figure 28. Oxidative stress increases ASCT2 expression. A. Effect of 200 μM H_2O_2 treatment on the expression of GLN transporters SLC38A5 and ASCT2 in GLN addicted U2OS and DU145 cells**.** 100 units/mL catalase (CAT) was used to reverse the effect of H_2O_2 treatment. **B.** Effect of 10 μM arsenite treatment on the expression of GLN transporters SLC38A5 and ASCT2 in GLN addicted U2OS and DU145 cells**. C.** SLC38A2 and ASCT expression analysis in GLN independent PC3 cells with/without 200 μM H_2O_2 or 10 μM arsenite treatment. Error bars represent SD (n=3). **P*<0.05, ****P*<0.001.

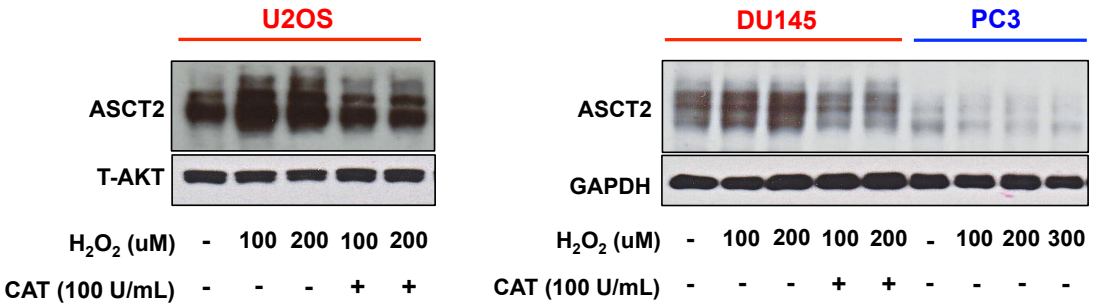

Figure 29. Oxidative stress increases ASCT2 protein in GLN addicted cells. Western blot analysis of ASCT2 protein in GLN addicted U2OS and DU145 cells and GLN independent PC3 cells treated with increasing concentrations of H_2O_2. Catalase (CAT) was used to inhibit H_2O_2 effect.

markedly increased with H_2O_2 treatment in the GLN addicted cells, but not in the GLN independent cells (Fig. 29). To verify that the oxidative stress increases GLN uptake in GLN addicted cells specifically by increasing ASCT2 expression, we down regulated ASCT2 using specific siRNAs and measured GLN uptake in the presence or absence of oxidative stress treatment. Cells treated with ASCT2-specific siRNAs exhibited significant reduction in GLN uptake and H_2O_2 treatment failed to increase it in these cells (Fig. 30). ASCT2 down regulation was confirmed by Western blot analysis. These findings provide strong evidence that oxidative stress increases GLN uptake in GLN addicted cells by upregulating ASCT2 expression.

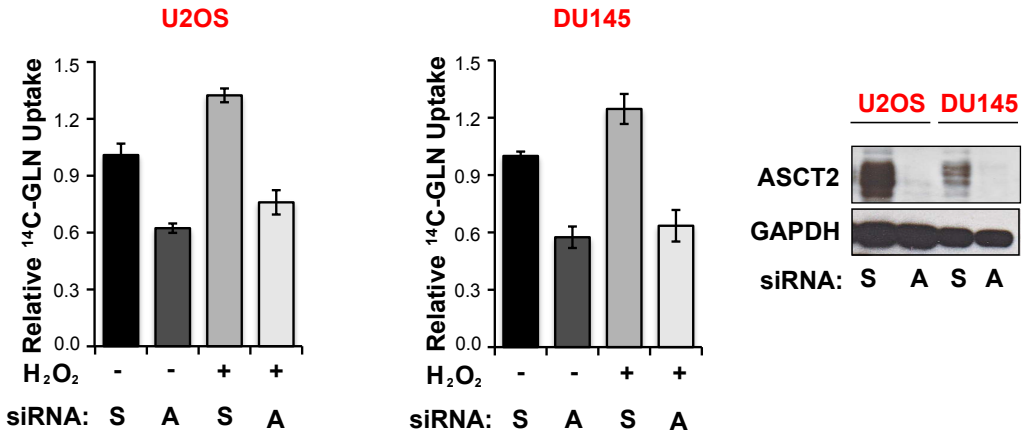

Figure 30. Oxidative stress increases GLN uptake via ASCT2. Effect of ASCT2 knock down on GLN uptake in U2OS and DU145 cells. Cells were treated with 20 nM control (S) or ASCT2 (A) siRNAs. Cells were cultured for 48 hours after siRNA treatments, and incubated with 300 μM H_2O_2 for another 16 hours. ASCT2 knock down was confirmed by Western blot analysis. Error bars represent SD (n=3).

4.3.4 Identification of a signaling pathway mediating oxidative stress-induced increase of ASCT2 expression and GLN uptake

ROS and oxidative stress activate several signaling pathways, including MAPK (mitogen activated protein kinases), MEK, JNK, and p38 cascades (3, 123). While the MAPK pathway promotes proliferation and survival in response to low levels of ROS, activation of the JNK and p38 pathways by high levels of ROS (oxidative stress) has been strongly associated with cell death (124-126). However, more recent reports suggest a protective role for JNK and p38 signaling under stress conditions (127-130). We therefore evaluated the effect of MEK, JNK, and p38 inhibition on the oxidative stress-induced upregulation of ASCT2 in U2OS and DU145 cells by qPCR. As shown in

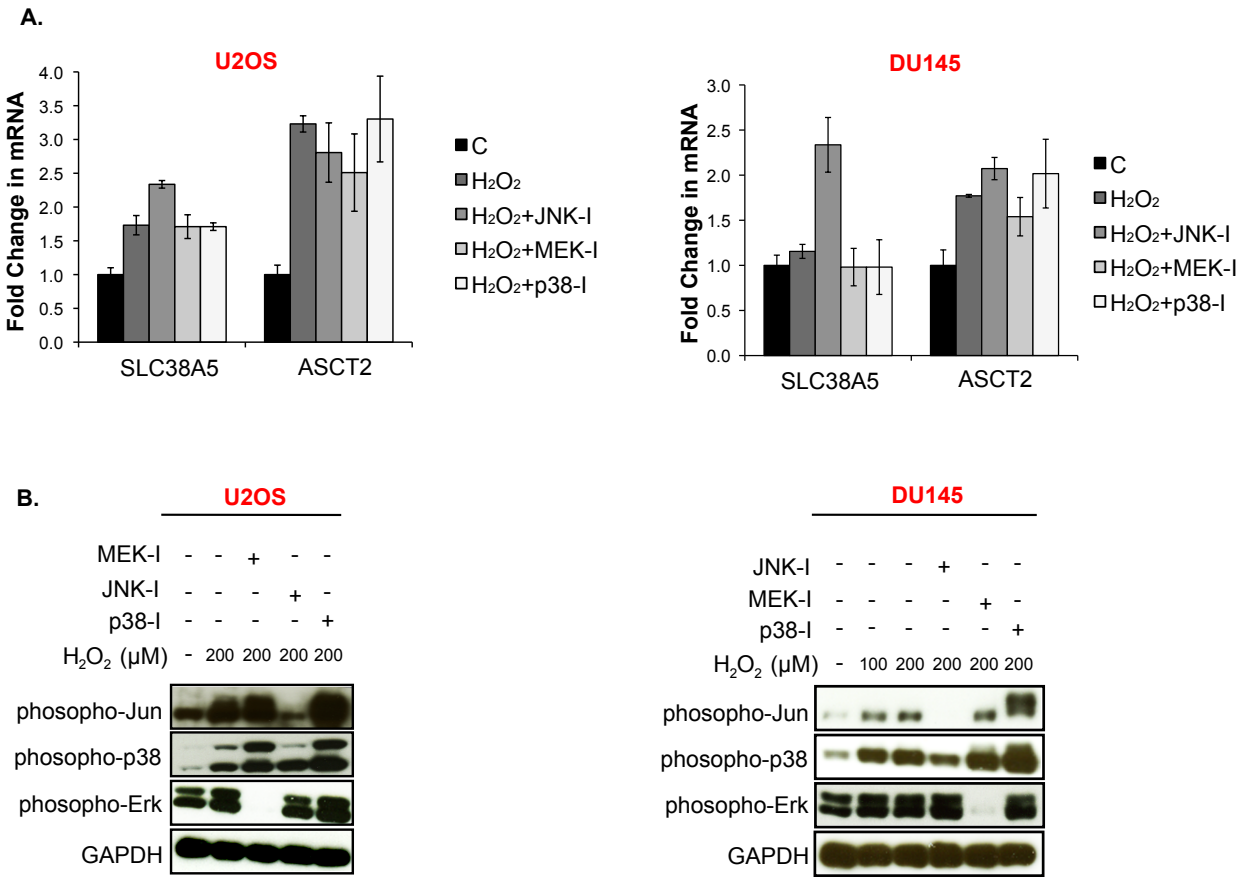

Figure 31. Oxidative stress-induced ASCT2 upregulation is not mediated by JNK, MEK, or p38 pathways. A. Effect of 30 μM JNK inhibitor (JNK-I), 3 μM MEK 1/2 inhibitor (MEK-I), or 15 μM p38 inhibitor (p38-I) on SLC38A5 and ASCT2 expression in GLN addicted U2OS and DU145 cells treated with 200 μM H_2O_2. Cells were first treated with the inhibitors for 30-60 minutes and after addition of H_2O_2, cells incubated for 16 hours. **B.** JNK, MEK, and p38 activation by H_2O_2 treatment (100-200 μM, 3 hours) and efficacy of their specific inhibitors were assessed by Western blot analyses of phospho-Jun, phospho-Erk, and phospho-p38 levels. GAPDH was used as loading control. Error bars represent SD (n=3).

figure 31A, inhibition of these pathways using specific inhibitors did not prevent H_2O_2-

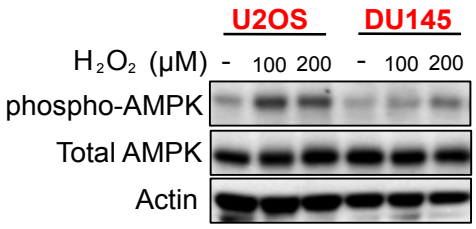

Figure 32. Oxidative stress activates AMPK pathway. U2OS and DU145 cells were treated with 100-200 μM H_2O_2 for 3 hours and AMPK activation was assessed by Western blot analyses of cell lysates using phospho-AMPK antibody. Total AMPK and Actin were used as loading controls.

induced upregulation of ASCT2 mRNA. We also confirmed the activation of these pathways by H_2O_2 treatment, as well as the efficacy of the inhibitors by Western blot analysis (Fig. 31B). H_2O_2 treatment increased phosphorylation of Erk1/2 and c-Jun, that are downstream substrates of MEK and JNK respectively, and the inhibitors reversed this effect. Although increased with H_2O_2 treatment, p38 phosphorylation was not reduced by p38 inhibitor. Therefore we used increased c-Jun phosphorylation as readout for p38 inhibition (131, 132). Treatment with p38 inhibitor significantly increased c-Jun phosphorylation, indicating efficient inhibition of p38 signaling as well. These findings demonstrate that despite induction of MEK, JNK and p38 signaling by H_2O_2 treatment, none of these pathways mediate the observed ASCT2 upregulation. We then considered the involvement of other pathways activated by ROS.

AMPK pathway is emerging as a critical mediator of resistance to various stress conditions in cancer cells (106, 133, 134). Pertinent to our studies, oxidative stress has been shown to activate AMPK directly by oxidation of Cys304 residue in the catalytic α-

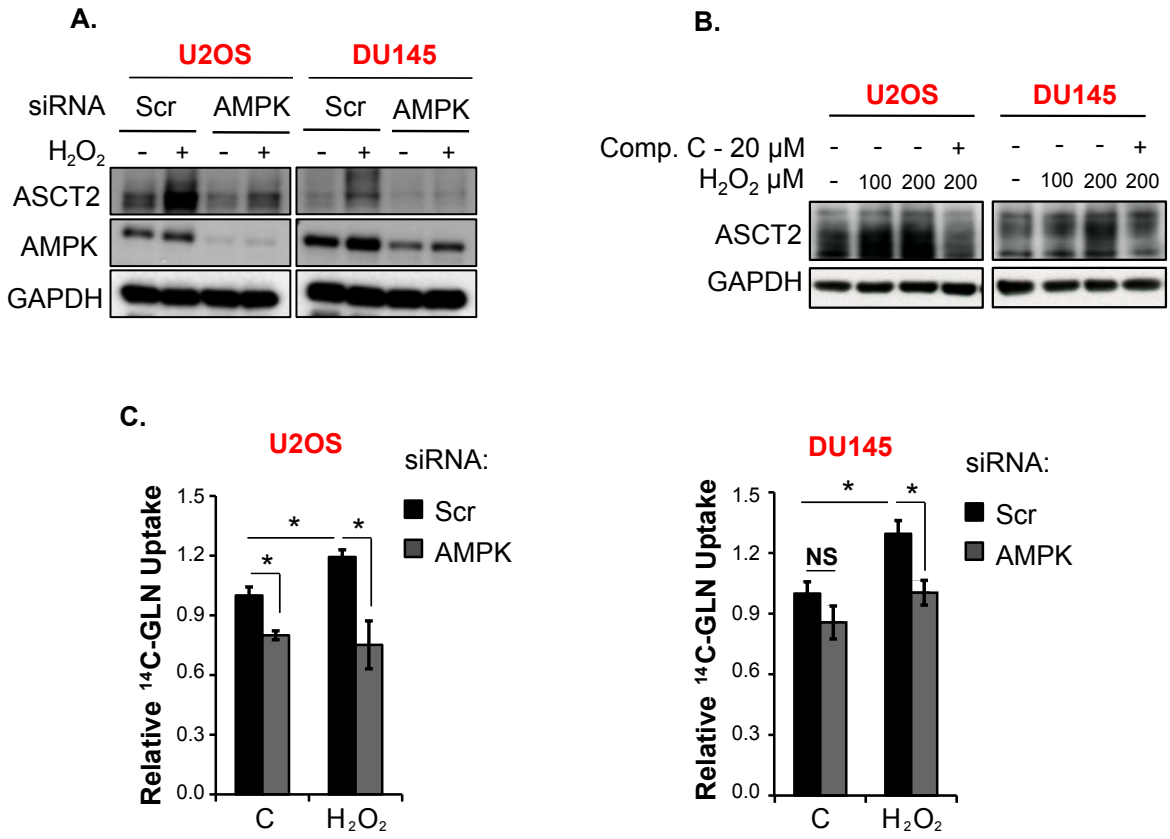

Figure 33. AMPK pathway mediates oxidative stress-induced upregulation of ASCT2 and GLN uptake. A. Western blot analyses of ASCT2 protein levels in U2OS and DU145 cells treated with 40 nM control (Scr) or AMPK α1 (20 nM) and α2 (20 nM) siRNAs. Cells were cultured for 48 hours after siRNA treatments, and incubated with 300 μM H_2O_2 for another 16 hours. **B.** Effect of 20 μM AMPK inhibitor compound C on ASCT2 protein levels. After treatment with compound C for 40 minutes, 100-200 μM H_2O_2 was added and cells were incubated for another 16 hours. **C.** Effect of AMPK down regulation with siRNAs on GLN uptake in U2OS and DU145 cells. After siRNA treatments, cells were cultured for 48 hours and incubated for another 16 hours with 300 μM H_2O_2. Error bars represent SD (n=3). * $P< 0.05$.

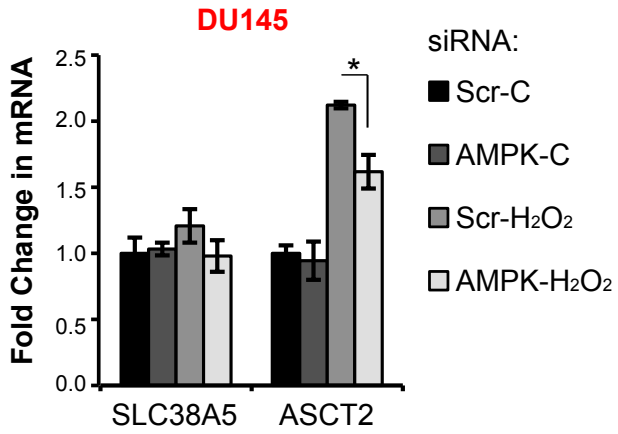

Figure 34. AMPK pathway mediates oxidative stress-induced upregulation of ASCT2 mRNA. qPCR analyses of SLC38A5 and ASCT2 mRNA levels in DU145 cells treated with 40 nM control (Scr) or AMPK α1 (20 nM) and α2 (20 nM) siRNAs. Cells were cultured for 48 hours after siRNA treatments, and incubated with 300 μM H_2O_2 for another 16 hours. Error bars represent SD (n=3). * $P< 0.05$.

subunit (135). Therefore we tested if AMPK mediates upregulation of ASCT2 and GLN uptake in GLN addicted cells. H_2O_2 treatment of the U2OS and DU145 cells resulted in an increase in AMPK phosphorylation (Fig. 32). Down regulating AMPK expression using specific siRNAs blocked H_2O_2-mediated upregulation of ASCT2 protein levels in both U2OS and DU145 cells (Fig. 33A). Chemical inhibition of AMPK using compound C also completely blocked upregulation of ASCT2 protein upon H_2O_2 treatment (Fig. 33B). In parallel, siRNA-mediated downregulation of AMPK inhibited the increase of GLN uptake by the H_2O_2-treated U2OS and DU145 cells (Fig. 33C). Consistent with these findings, down regulation of AMPK by siRNAs reduced ASCT2 mRNA levels in H_2O_2-treated DU145 cells (Fig. 34). These findings collectively implicate AMPK as a

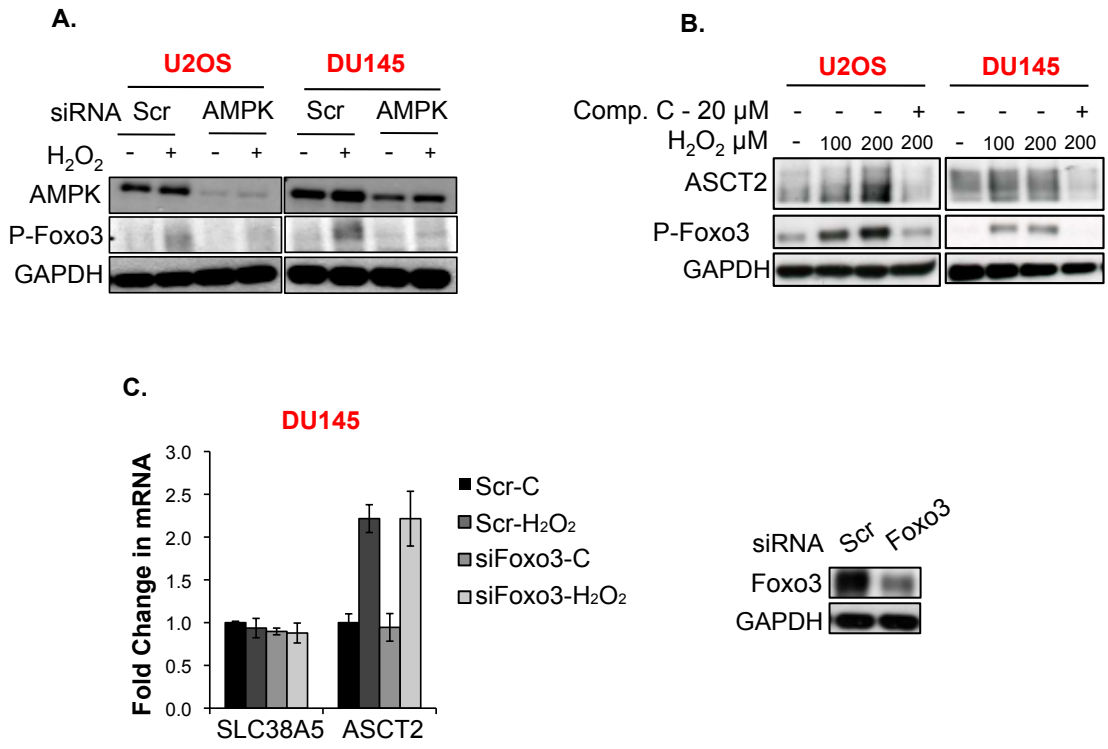

Figure 35. Foxo3 does not mediate oxidative stress-induced upregulation of ASCT2. A. Western blot analysis of Foxo3 phosphorylation status in U2OS and DU145 cells treated with 40 nM control (Scr) or AMPK α1 (20 nM) and α2 (20 nM) siRNAs. Cells were cultured for 48 hours after siRNA treatments, and incubated with 300 μM H_2O_2 for another 16 hours. **B.** Effect of 20 μM AMPK inhibitor compound C on Foxo3 phosphorylation. After treatment with compound C for 40 minutes, 100-200 μM H_2O_2 was added and cells were incubated for another 16 hours. ASCT2 Western blot was included to show the correlation between ASCT2 protein levels and phospho-Foxo3. GAPDH was used as loading control. **C.** Effect of Foxo3 down regulation by siRNAs on SLC38A5 and ASCT2 mRNA levels in DU145 cells. After siRNA treatments, cells were cultured for 48 hours and incubated for another 16 hours with 300 μM H_2O_2. Error bars represent SD (n=3). Foxo3 down regulation was confirmed by Western blot analysis.

mediator of H_2O_2-induced upregulation of ASCT2 and GLN uptake in GLN addicted cells.

4.3.5 Investigation of the potential transcription factors that control ASCT2 mRNA induction in response to oxidative stress

Because oxidative stress increases ASCT2 mRNA levels, we investigated the involvement of possible transcription factors that might increase ASCT2 expression in response to oxidative stress. Considering the role of AMPK in H_2O_2-mediated ASCT2 upregulation, we first focused on the transcription factors that are known to be activated by AMPK under stress conditions. Foxo3 is a known AMPK substrate under energetic stress (136-138). Foxo transcription factors orchestrate expression of a myriad of genes involved in metabolic and oxidative stress response (137). Greer et al. demonstrated that AMPK directly phosphorylates Foxo3 at least at 3 different serine residues, including Ser413 (138). Using a commercially available antibody against phospho-Foxo3 (Ser413), we confirmed induction of Foxo3 phosphorylation by H_2O_2 treatment. Perturbation of AMPK pathway by compound C (AMPK inhibitor) or specific siRNAs for AMPK α1 and α2 subunits abrogated H_2O_2-induced Foxo3 phosphorylation (Fig. 35A) pointing Foxo3 as the potential transcription factor that might link AMPK pathway to increased ASCT2 expression under oxidative stress. However, down regulation of Foxo3 by specific siRNAs did not prevent H_2O_2-induced increase of ASCT2 mRNA (Fig. 35B). This prompted us to evaluate other transcription factors that are known to be activated by oxidative stress.

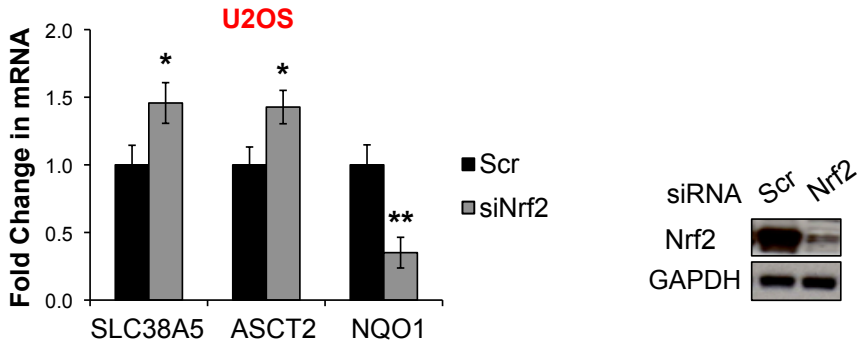

Figure 36. Nrf2 does not mediate oxidative stress-induced upregulation of ASCT2. qPCR analysis of SLC38A2, ASCT2 and NQO1 expression in U2OS cells treated with control (Scr) or Nrf2 siRNAs. Cells were cultured for 48 hours after siRNA transfection, and incubated with 300 μM H_2O_2 for another 16 hours. Nrf2 down regulation was confirmed by Western blots. Error bars represent SD (n=3). * $P < 0.05$, ** $P < 0.005$.

Nrf2 is perhaps the most well-known transcription factor that responds to oxidative stress by transcribing genes necessary for redox balance and survival (139). To test whether Nrf2 regulates ASCT2 expression in response to oxidative stress we used specific siRNAs to inhibit Nrf2 expression in U2OS cells and quantitated ASCT2 expression after exposure to H_2O_2. We used NQO1, an established Nrf2 target gene (70), as a positive control for reduced Nrf2 activity. Interestingly, both SLC38A5 and ASCT2 mRNA levels were significantly increased with Nrf2 knock-down (perhaps due to even higher levels of oxidative stress), whereas NQO1 mRNA levels were decreased by more than 60% (Fig. 36A), excluding Nrf2 as ASCT2 regulator under oxidative stress.

We then tested the role of other transcription factors, including c-Myc and AP-1 members c-Jun and ATF2. Myc has been recently shown to regulate ASCT2 expression

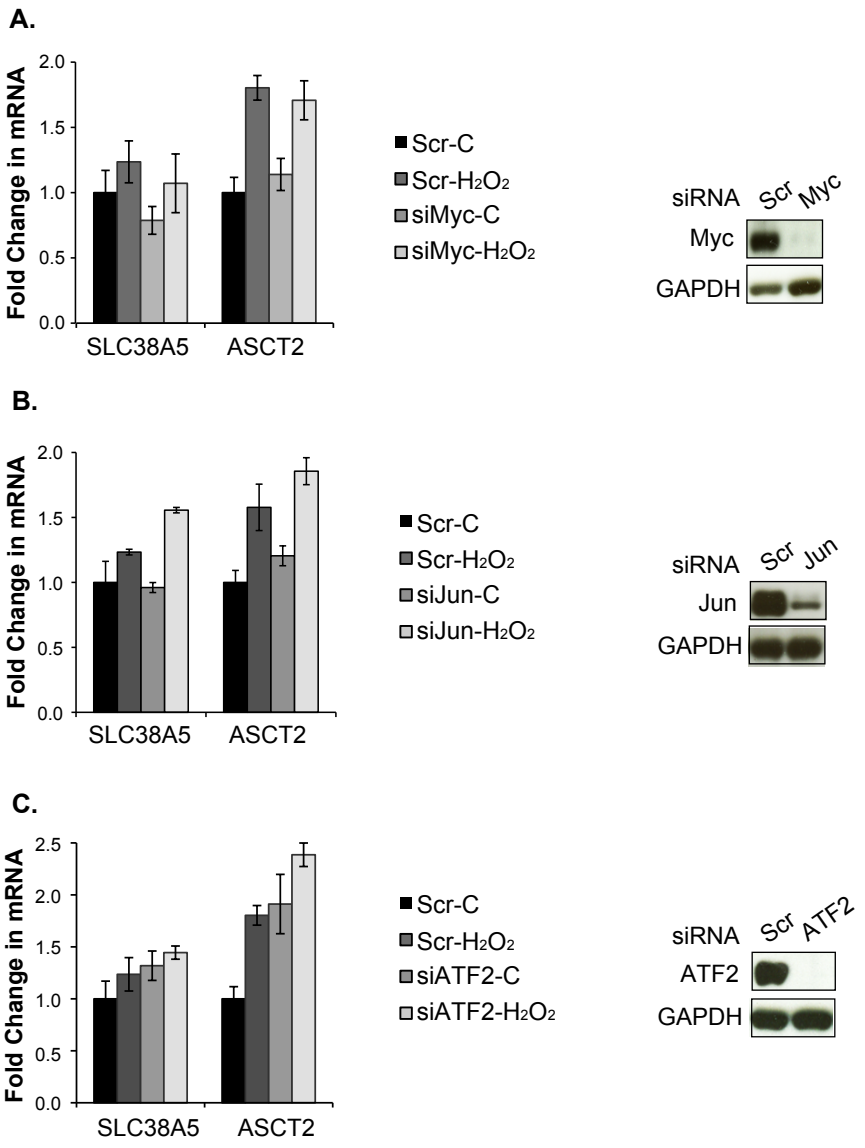

Figure 37. Myc, Jun, or ATF2 are not involved in oxidative stress-induced upregulation of ASCT2. Effect of **A.** Myc, **B.** Jun, and **C.** ATF2 down regulation on SLC38A2 and ASCT2 expression in DU145 cells. Cells were cultured for 48 hours after siRNA transfection, and incubated with 300 μM H_2O_2 for another 16 hours. Down regulation of Myc, Jun, and ATF2 were confirmed by Western blots. Error bars represent SD (n=3).

in SF188 glioblastoma cells under ambient conditions (48). siRNA-mediated knock down of Myc in DU145 cells did not result in a decrease in ASCT2 levels with/without H_2O_2 treatment (Fig. 37A). Both c-Jun and ATF2 transcription factors are activated by oxidative stress (140, 141), however, their down regulation in DU145 cells by specific siRNAs did not inhibit ASCT2 mRNA levels in response to H_2O_2 treatment (Fig. 37B, 37C). These findings suggest that regulation of ASCT2 under oxidative stress may be complex and perhaps a more systemic approach is required to elucidate the precise mechanisms involved in this process, which will be discussed in the discussion section of this chapter.

4.3.6 Down regulation of ASCT2 and AMPK expression sensitizes GLN addicted cells to oxidative stress

Results of the studies introduced in this chapter so far demonstrate that GLN addicted cells respond to oxidative stress by increasing ASCT2 expression and GLN uptake in an AMPK dependent manner. To determine if this mechanism is protective against oxidative stress, we down regulated ASCT2 or AMPK expression using siRNAs, which inhibit H_2O_2-induced increase of GLN uptake (Chapter 4.3.3, 4.3.4), and challenged the cells with 400 μM of H_2O_2 exposure. Both U2OS and DU145 cells exhibited increased sensitivity to H_2O_2 treatment when ASCT2 or AMPK were down regulated (Fig. 38A). To show that this is due to decreased capacity of these cells to manage oxidative stress, we treated the cells with 300 μM of H_2O_2 for 16 hours and incubated the cells in fresh medium for 1 hour to allow for recovery from oxidative

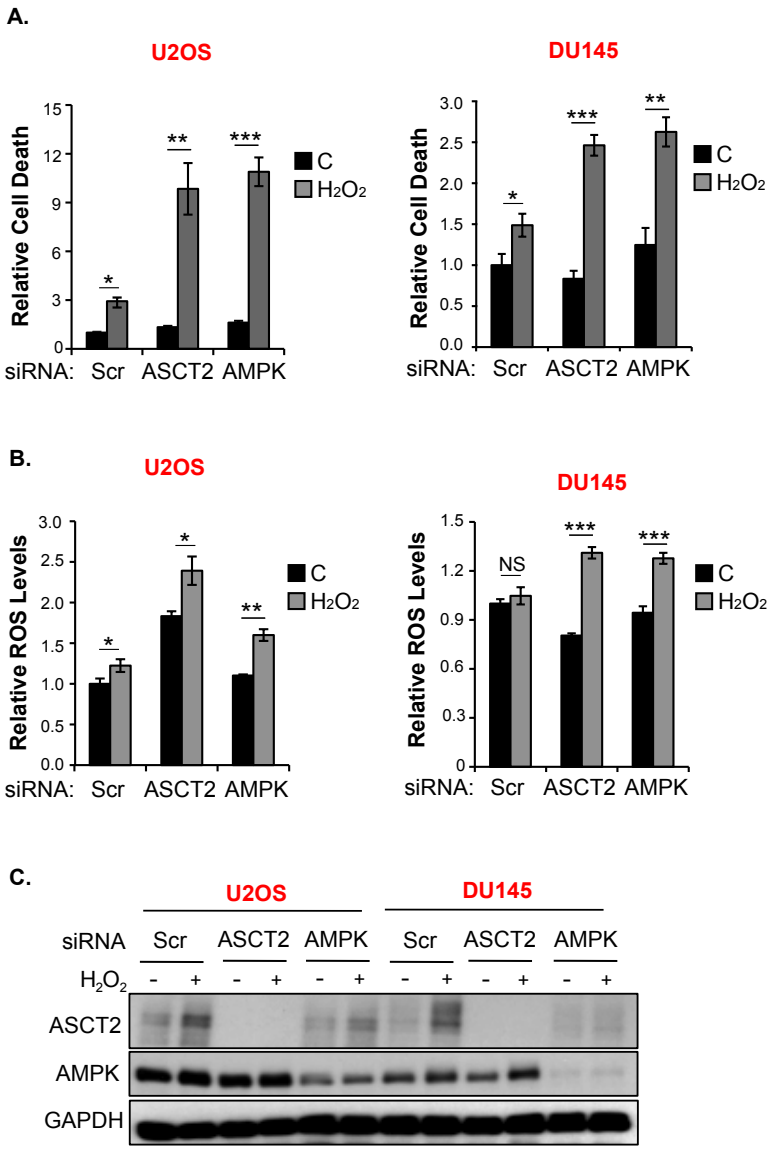

Figure 38. Down regulation of ASCT2 and AMPK sensitizes GLN addicted cells to oxidative stress. Effect of ASCT2 or AMPK down regulation on **A.** cell death, **B.** ROS levels in U2OS and DU145 cells treated with. After 48 hours of siRNA treatments, cells were incubated with 400 μM H_2O_2 for 18 hours and cell death was measured by propidium iodide staining. For ROS analysis, cells were incubated with 300 μM H_2O_2 for 16 hours, and culture medium was replaced with fresh media to allow the cells recover form oxidative stress for 1 hour and ROS levels were measured by DCFDA staining. **C.** Down regulation of ASCT2 and AMPK were confirmed by Western blots. Error bars represent SD (n=3). * $P < 0.05$, ** $P < 0.005$, *** $P < 0.001$.

stress. ROS measurements using DCFDA staining revealed that ASCT2 or AMPK knock down resulted in increased ROS levels in both U2OS and DU145 cells after H_2O_2 treatment (Fig. 38B). We confirmed the successful knock down of ASCT2 and AMPK by Western blot analyses (Fig. 38C). These results collectively suggest that ASCT2 and AMPK confer resistance to oxidative stress in GLN addicted cells.

4.4 Discussion

GLN serves as precursor for synthesis of the antioxidant GSH, as well as for production of NADPH, which is indispensible for regeneration of reduced GSH from its oxidized form. In this chapter, we showed that GLN addicted cells exhibit extreme sensitivity to exogenous oxidants in the absence of GLN. Addition of catalase, Glu, or GSH voids this sensitivity reflecting the absolute requirement of GLN in anti-oxidative processes. GLN addicted cells respond to oxidative challenge by increasing GLN uptake, which involves AMPK-mediated upregulation of the major GLN transporter ASCT2. Inhibition of ASCT2 or AMPK expression by siRNAs renders the GLN addicted cells sensitive to oxidative stress.

GLN can be transported by the cells via several different amino acid transporters, including SLC38A1, SLC38A2, SLC38A3, SLC38A5, and ASCT2 (SLC1A5) depending on the tissue or cell type (56). Among these, ASCT2 is the primary transporter expressed in rapidly proliferating normal and tumor cells in culture (121). Down regulation of ASCT2 in SK-Hep hepatoma cells results in apoptosis (142). Furthermore, a recent study showed that ASCT2 is expressed in majority of the lung cancer tissue

examined, and that ASCT2 is required for growth of lung cancer cells (143). Although ASCT2 expression in cancers is appreciated, how ASCT2 is regulated at the molecular level is not well understood. The oncogenic Myc was shown to directly bind to the ASCT2 promoter to regulate its transcription (48). Another study reported that GLN availability increases ASCT2 expression (144). However, ASCT2 regulation in response to stress has not been reported before. In this chapter, we showed unambiguously that oxidative stress upregulates ASCT2 levels to increase GLN uptake and identified the signaling pathway that mediates this response.

AMPK is a sensor of energy levels, and thus a critical regulator of cellular and organismal metabolism (136, 145). When energy levels are low, AMPK senses the high AMP/ATP or ADP/ATP ratios and reprograms metabolic pathways to promote ATP producing catabolic activity and to inhibit ATP consuming anabolic activity. AMPK exists as a heterodimer of a catalytic subunit (α), and two regulatory subunits (β and γ). AMP or ADP binding to the regulatory γ subunit causes AMPK to assume an obligatory conformation that exposes Thr172 in the activation loop to the upstream kinases, leading to AMPK activation. AMPK is known to increase glucose uptake in various tissue and cell types by upregulating/activating the glucose transporters (GLUTs) under energetic stress (146, 147). However, AMPK regulation of GLN uptake has not been reported before. In this chapter, we provided considerable evidence for the regulatory role of AMPK in ASCT2 expression and GLN uptake in GLN addicted cells in response to oxidative stress. Of note, AMPK seems to regulate ASCT2 levels and GLN uptake in U2OS cells under ambient conditions (Fig. 33A, 33C), implying a regulatory role for AMPK in basal GLN metabolism in some cell types. Furthermore, our findings implicate

AMPK in oxidative stress resistance as reducing AMPK levels by siRNAs impairs the cells' ability to clear ROS and leads to cell death after H_2O_2 treatment (Fig. 38). Despite the increasing evidence that AMPK confers resistance to various stress conditions in cancer cells (106, 133, 134), a protective role for AMPK in oxidative stress resistance is not well defined. Snf1, the *Saccharomyces cerevisiae ortholog* of AMPK, was recently reported to be critical for yeast survival upon exposure to selenite and to GSH oxidizing reagents, associating AMPK with oxidative stress resistance (148). On the other hand, Chen et al. reported that AMPK mediates H_2O_2-induced apoptosis in neuronal cells (149). Considering the diversity of the pathways AMPK participates in different systems, it is highly likely that outcome of AMPK activity under oxidative stress conditions may be context dependent.

AMPK activation by oxidative stress has been documented in the literature (135, 150, 151) however, the route of activation remains contentious. The initial study by Choi et al. suggested an indirect activation due to inhibition of mitochondrial ATP synthesis by high ROS, resulting in an increased AMP and ADP levels (151). On the other hand, more recent studies reported a direct activation of AMPK by ROS via oxidation of two conserved cysteine residues in the catalytic α-subunit (135, 152). Nevertheless, our findings are consistent with the literature reports that ROS activates AMPK, which is apparent from the increased Thr172 phosphorylation (Fig. 32). The precise mechanism of AMPK activation by ROS is beyond the scope of this thesis studies and will not be discussed here any further.

In addition to GLN, ASCT2 also transports alanine, serine, cysteine, asparagine, and other small neutral amino acids (121, 153), but the effects of ASCT2 down

regulation on cancer cell growth and viability is usually attributed to reduced GLN transport. However, we did not observe any significant cell death due to ASCT2 down regulation by siRNAs. This can be explained by only ~50% reduction in GLN uptake after treatment with ASCT2 siRNAs (Fig. 30). This is consistent with the results obtained using lung cancer cells, in which ASCT2 accounted for 50% of GLN uptake (143). Rest of the GLN taken up by cells is most likely mediated by the other transporters (e.g. SLC38A5). Since there is still a substantial amount of GLN available for the cells, ASCT2 down regulation is not expected to induce cell death under ambient conditions. On the other hand, under certain stress conditions, a threshold of GLN concentration may be important for cell survival, and therefore it may be beneficial for the cells to increase GLN uptake to maintain it at a certain concentration. This idea is supported by our findings that, oxidative stress treatment of the cells increase GLN uptake by increasing ASCT2 expression and only under oxidative stress the cells become dependent upon ASCT2 for survival.

Although we showed that AMPK mediates the oxidative stress-induced increase of ASCT2 and GLN uptake, we were not able to identify a transcription factor that links AMPK pathway to ASCT2 induction despite several attempts. Taking into account the important role of GLN in antioxidant pathways, it is possible that there is more than one transcription factor that can regulate ASCT2 transcription and cells may compensate for the loss of one transcription factor by engaging an alternative one to ensure adequate GLN concentration. Therefore identification of the transcription factor(s) will likely require a more systemic approach using siRNA pools. Furthermore, the qPCR experiments do not necessarily suggest that ASCT2 is regulated at the transcriptional

level. For instance, we did not rule out the possibility that oxidative stress stabilizes ASCT2 mRNA in an AMPK-dependent manner. Therefore future studies should aim to establish ASCT2 promoter activity and mRNA stability under oxidative stress conditions.

It is intriguing that oxidative stress does not increase ASCT2 expression in GLN independent cells. It is not clear from the current studies if this is because oxidative stress does not activate AMPK, or the yet unknown downstream effector of AMPK in GLN addicted cells is defective or does not serve as an AMPK substrate in the GLN independent cells. In a previous study, oxidative stress increased cysteine uptake by specifically upregulating the SLC38A1 expression in freshly isolated rat cardiomyocytes without having an effect on ASCT2 expression (154). This supports our findings that ASCT2 induction by oxidative stress is not common across all cell types and that some cells (e.g. GLN addicted cells) have adopted this mechanism for protection against oxidative stress. Yet, it remains to be determined if and how GLN addiction and ASCT2 regulation are intertwined.

Chapter 5: Conclusion and Future Directions

The aim of this thesis was to characterize the relationship between GLN metabolism and ROS to better understand the GLN addiction phenotype of cancer cells. The research was divided into three sections. In the first section (Chapter 2) ROS-dependent GLN addiction concept was investigated in a simple system, in which the tumor suppressor Hace1 with a ROS inhibiting function was deleted. Findings of Chapter 2 studies demonstrated for the first time that increased ROS levels resulting from loss of a tumor suppressor lead to GLN addiction. These studies were expanded to several different types of human cancer cell lines in the second section (Chapter 3), and a correlation between GLN-dependent redox balance and GLN addiction phenotype was established. In addition, a mechanism for GLN starvation-induced cell death involving ROS-dependent elevation of glucose uptake and augmentation of GLN starvation-induced ROS was uncovered. Studies in the third section (Chapter 4) approached the research topic from a different angle and identified a protective mechanism in GLN addicted cells that involves upregulation of the GLN transporter ASCT2 expression and GLN uptake in an AMPK pathway dependent manner in response to oxidative stress.

GLN is the most abundant amino acid in the plasma and it is consumed by tumors at rates much greater than that of any other amino acid. Akin to glucose, GLN is a major precursor for ATP synthesis. In addition to satisfying bioenergetic needs, GLN has many important functions in a variety of key processes in proliferating cells, including synthesis of proteins, nucleic acids, lipids, hexosamines, and GSH. Not

surprisingly most proliferating cells require GLN for growth and certain oncogenes have been shown to influence GLN metabolism in the context of cell proliferation. Moreover, a considerable number of cancer cell lines depend on GLN for survival, a phenomenon known as GLN addiction. However, the reasons why some cells are GLN addicted and some are not have been elusive. Our initial hypothesis was that transformed cells with increased ROS levels depend on GLN to cope with oxidative stress, and are therefore GLN addicted. Results of the studies with Hace1 deficient cells (Chapter 2) supported this hypothesis, that Hace1 loss results in increased ROS levels thereby predisposes the cells to GLN addiction. However, studies in Chapter 3 revealed that dependency on GLN for survival does not correlate with basal ROS levels in cancer cells. Instead, dependency on GLN for redox balance defines GLN addiction phenotype. Chapter 4 studies further attest to this premise that only GLN addicted cells require GLN to cope with oxidative stress posed by exogenous oxidants.

While the studies in this thesis identified novel aspects of GLN metabolism and ROS regulation, they also raised several questions that remain to be addressed. As described in Chapter 2, Hace1 deficient cells, with increased ROS levels, exhibit GLN dependence for survival, increased GLN uptake and metabolism. While exogenous antioxidants inhibit ROS and void GLN addiction phenotype of Hace1 deficient cells, it is not known whether antioxidant treatment decreases GLN uptake and metabolism to the levels observed with Hace1-expressing cells. Therefore future studies could address this issue to clarify the potential role of intracellular ROS generation in GLN uptake and metabolism.

An unexpected result revealed by the studies in Chapter 3 is that GLN addicted cells increase glucose uptake in the absence of GLN, whereas the GLN independent cells maintain it at basal levels. TXNIP is an established regulator of glucose uptake and is known to be induced by GLN deprivation to inhibit glucose uptake. Our results demonstrate that this notion is valid only for GLN independent cells. Unlike GLN addicted cells, GLN independent cells are able to increase TXNIP protein levels upon GLN starvation providing an explanation for why elevation of glucose uptake is inhibited in GLN independent cells. However, despite a marked increase in glucose uptake, down regulation of TXNIP using specific siRNAs results in only a slight increase in ROS and cell death in GLN independent cells in the absence of GLN. This suggests that increased glucose uptake in the absence of GLN is not sufficient to predispose cells to GLN addiction. Therefore the contribution of TXNIP to GLN independence phenotype of cancer cells needs to be further investigated.

The Chapter 3 studies further demonstrate that increased glucose uptake is a consequence of ROS induction upon GLN starvation, but appears to exacerbate deleterious effects of GLN depletion as GLN addicted cells can survive in the absence of GLN when glucose concentration in the culture medium is vanishingly low. These results are unexpected for two reasons. First, in sharp contrast to GLN addicted cells, GLN independent cells can preserve their antioxidant pools in the absence of GLN and are therefore presumed to exhibit increased dependence on glucose as an alternative source for antioxidants, and hence increased glucose uptake. Second, increased glucose uptake by GLN addicted cells in the absence of GLN is expected to be compensatory for managing redox state. On the contrary, despite the surge of glucose,

GLN addicted cells cannot use it efficiently, whereas GLN independent cells are able to compensate for GLN loss by shunting glucose into antioxidant generating pathways. Inhibition of mitochondrial pyruvate transport significantly increases oxidative stress and cell death in GLN independent cells in the absence of GLN. More importantly, it markedly depletes reduced GSH levels under GLN starvation, strongly suggesting that GLN independent cells are able to use glucose-derived pyruvate in the TCA cycle to maintain GSH pools. However, this idea is currently only speculative, and its validation requires metabolic labeling experiments using ^{13}C-glucose, which would allow for tracing of the glucose carbons and for comparing the fate of glucose between GLN addicted and GLN independent cells under GLN deplete conditions.

Another question raised by the studies in Chapter 3 is that whether GLN starvation increases ROS by triggering ROS generation or reducing ROS elimination or both. Findings of the studies in Chapter 4 clarify this issue to a certain extend. GLN addicted cells respond to exogenous oxidative stress by increasing GLN uptake via a specific mechanism involving upregulation of the GLN transporter ASCT2, which is necessary to manage ROS levels. This suggests that GLN addicted cells meet the challenge posed by exogenous oxidants by increasing GLN uptake, presumably to maintain sufficient pools of antioxidants. It is therefore more likely that GLN deprivation first depletes antioxidants in GLN addicted cells leading to ROS increase.

It is intriguing that ASCT2 expression and GLN uptake are not affected by oxidative stress in GLN independent cells. This may be due to the failure of AMPK activation by oxidative stress, which mediates upregulation of ASCT2 and GLN uptake in GLN addicted cells. Future studies could take advantage of AMPK activating

compounds, such as the AMP mimetic AICAR (5-aminoimidazole-4-carboximide-1-β-D-ribofuranoside) to determine whether they can trigger ASCT2 induction and GLN uptake in GLN independent cells. Another potential explanation is that the yet unknown downstream effector of AMPK that links AMPK to ASCT2 expression in response to oxidative stress might be defective in GLN independent cells. Nevertheless, clarification of this issue warrants more detailed studies.

Perhaps the most significant contribution of this thesis to the cancer cell metabolism field is the identification of a potential therapeutic strategy that combines GLN deprivation with oxidizing reagents for effective killing of GLN addicted cells. Our results demonstrate that GLN starvation combined with the pro-oxidant small molecule piperlongumine selectively kills GLN addicted cells. However, GLN independent cells are impervious to these treatments, raising the issue that this strategy will not work in all cancer types and argue the necessity for identification of biomarkers for GLN addiction. Furthermore these *in vitro* findings remain to be validated by *in vivo* studies.

Taken together, this thesis established the reciprocal regulation of GLN metabolism and ROS by characterizing the link between ROS and GLN addiction phenotype of cancer cells. More importantly, these studies identified combination of GLN deprivation and pro-oxidant reagents as a potentially effective therapeutic strategy for elimination of GLN addicted cancer cells.

References

1. Trachootham D, Alexandre J, & Huang P (2009) Targeting cancer cells by ROS-mediated mechanisms: a radical therapeutic approach? *Nature reviews. Drug discovery* 8(7):579-591.
2. D'Autreaux B & Toledano MB (2007) ROS as signalling molecules: mechanisms that generate specificity in ROS homeostasis. *Nature reviews. Molecular cell biology* 8(10):813-824.
3. Trachootham D, Lu W, Ogasawara MA, Nilsa RD, & Huang P (2008) Redox regulation of cell survival. *Antioxidants & redox signaling* 10(8):1343-1374.
4. Sena LA & Chandel NS (2012) Physiological roles of mitochondrial reactive oxygen species. *Molecular cell* 48(2):158-167.
5. Lambeth JD (2004) NOX enzymes and the biology of reactive oxygen. *Nature reviews. Immunology* 4(3):181-189.
6. Block K & Gorin Y (2012) Aiding and abetting roles of NOX oxidases in cellular transformation. *Nature reviews. Cancer* 12(9):627-637.
7. Bae YS*, et al.* (1997) Epidermal growth factor (EGF)-induced generation of hydrogen peroxide. Role in EGF receptor-mediated tyrosine phosphorylation. *The Journal of biological chemistry* 272(1):217-221.
8. Bae YS*, et al.* (2000) Platelet-derived growth factor-induced H(2)O(2) production requires the activation of phosphatidylinositol 3-kinase. *The Journal of biological chemistry* 275(14):10527-10531.

9. Sundaresan M, Yu ZX, Ferrans VJ, Irani K, & Finkel T (1995) Requirement for generation of H2O2 for platelet-derived growth factor signal transduction. *Science* 270(5234):296-299.

10. Lee SR*, et al.* (2002) Reversible inactivation of the tumor suppressor PTEN by H2O2. *The Journal of biological chemistry* 277(23):20336-20342.

11. Kwon J*, et al.* (2004) Reversible oxidation and inactivation of the tumor suppressor PTEN in cells stimulated with peptide growth factors. *Proceedings of the National Academy of Sciences of the United States of America* 101(47):16419-16424.

12. Leslie NR*, et al.* (2003) Redox regulation of PI 3-kinase signalling via inactivation of PTEN. *The EMBO journal* 22(20):5501-5510.

13. Rhee SG*, et al.* (2005) Intracellular messenger function of hydrogen peroxide and its regulation by peroxiredoxins. *Current opinion in cell biology* 17(2):183-189.

14. Szatrowski TP & Nathan CF (1991) Production of large amounts of hydrogen peroxide by human tumor cells. *Cancer research* 51(3):794-798.

15. Toyokuni S, Okamoto K, Yodoi J, & Hiai H (1995) Persistent oxidative stress in cancer. *FEBS letters* 358(1):1-3.

16. Trachootham D*, et al.* (2006) Selective killing of oncogenically transformed cells through a ROS-mediated mechanism by beta-phenylethyl isothiocyanate. *Cancer cell* 10(3):241-252.

17. Irani K*, et al.* (1997) Mitogenic signaling mediated by oxidants in Ras-transformed fibroblasts. *Science* 275(5306):1649-1652.

18. Rodrigues MS, Reddy MM, & Sattler M (2008) Cell cycle regulation by oncogenic tyrosine kinases in myeloid neoplasias: from molecular redox mechanisms to health implications. *Antioxidants & redox signaling* 10(10):1813-1848.

19. Brandon M, Baldi P, & Wallace DC (2006) Mitochondrial mutations in cancer. *Oncogene* 25(34):4647-4662.

20. Ishikawa K*, et al.* (2008) ROS-generating mitochondrial DNA mutations can regulate tumor cell metastasis. *Science* 320(5876):661-664.

21. Achanta G*, et al.* (2005) Novel role of p53 in maintaining mitochondrial genetic stability through interaction with DNA Pol gamma. *The EMBO journal* 24(19):3482-3492.

22. Vafa O*, et al.* (2002) c-Myc can induce DNA damage, increase reactive oxygen species, and mitigate p53 function: a mechanism for oncogene-induced genetic instability. *Molecular cell* 9(5):1031-1044.

23. Murphy MP (2009) How mitochondria produce reactive oxygen species. *The Biochemical journal* 417(1):1-13.

24. Dang CV, Li F, & Lee LA (2005) Could MYC induction of mitochondrial biogenesis be linked to ROS production and genomic instability? *Cell cycle* 4(11):1465-1466.

25. Morrish F & Hockenbery D (2003) Myc's mastery of mitochondrial mischief. *Cell cycle* 2(1):11-13.

26. Indo HP*, et al.* (2007) Evidence of ROS generation by mitochondria in cells with impaired electron transport chain and mitochondrial DNA damage. *Mitochondrion* 7(1-2):106-118.

27. Carew JS*, et al.* (2003) Mitochondrial DNA mutations in primary leukemia cells after chemotherapy: clinical significance and therapeutic implications. *Leukemia* 17(8):1437-1447.

28. Taylor RW & Turnbull DM (2005) Mitochondrial DNA mutations in human disease. *Nat Rev Genet* 6(5):389-402.

29. Achanta G & Huang P (2004) Role of p53 in sensing oxidative DNA damage in response to reactive oxygen species-generating agents. *Cancer research* 64(17):6233-6239.

30. Sablina AA*, et al.* (2005) The antioxidant function of the p53 tumor suppressor. *Nature medicine* 11(12):1306-1313.

31. Vousden KH & Lane DP (2007) p53 in health and disease. *Nature reviews. Molecular cell biology* 8(4):275-283.

32. Giorgio M, Trinei M, Migliaccio E, & Pelicci PG (2007) Hydrogen peroxide: a metabolic by-product or a common mediator of ageing signals? *Nature reviews. Molecular cell biology* 8(9):722-728.

33. Cooke MS, Evans MD, Dizdaroglu M, & Lunec J (2003) Oxidative DNA damage: mechanisms, mutation, and disease. *FASEB journal : official publication of the Federation of American Societies for Experimental Biology* 17(10):1195-1214.

34. Avery SV (2011) Molecular targets of oxidative stress. *The Biochemical journal* 434(2):201-210.

35. Behrend L, Henderson G, & Zwacka RM (2003) Reactive oxygen species in oncogenic transformation. *Biochem Soc Trans* 31(Pt 6):1441-1444.

36. Hu Y*, et al.* (2005) Mitochondrial manganese-superoxide dismutase expression in ovarian cancer: role in cell proliferation and response to oxidative stress. *The Journal of biological chemistry* 280(47):39485-39492.

37. Takahashi A*, et al.* (2006) Mitogenic signalling and the p16INK4a-Rb pathway cooperate to enforce irreversible cellular senescence. *Nature cell biology* 8(11):1291-1297.

38. Young TW*, et al.* (2004) Activation of antioxidant pathways in ras-mediated oncogenic transformation of human surface ovarian epithelial cells revealed by functional proteomics and mass spectrometry. *Cancer research* 64(13):4577-4584.

39. Benassi B*, et al.* (2006) c-Myc phosphorylation is required for cellular response to oxidative stress. *Molecular cell* 21(4):509-519.

40. Yoo MH, Xu XM, Carlson BA, Gladyshev VN, & Hatfield DL (2006) Thioredoxin reductase 1 deficiency reverses tumor phenotype and tumorigenicity of lung carcinoma cells. *The Journal of biological chemistry* 281(19):13005-13008.

41. DeNicola GM*, et al.* (2011) Oncogene-induced Nrf2 transcription promotes ROS detoxification and tumorigenesis. *Nature* 475(7354):106-109.

42. Cantor JR & Sabatini DM (2012) Cancer cell metabolism: one hallmark, many faces. *Cancer discovery* 2(10):881-898.

43. DeBerardinis RJ, Lum JJ, Hatzivassiliou G, & Thompson CB (2008) The biology of cancer: metabolic reprogramming fuels cell growth and proliferation. *Cell metabolism* 7(1):11-20.

44. Deberardinis RJ, Sayed N, Ditsworth D, & Thompson CB (2008) Brick by brick: metabolism and tumor cell growth. *Current opinion in genetics & development* 18(1):54-61.

45. Warburg O (1956) On respiratory impairment in cancer cells. *Science* 124(3215):269-270.

46. Warburg O (1956) On the origin of cancer cells. *Science* 123(3191):309-314.

47. Gao P*, et al.* (2009) c-Myc suppression of miR-23a/b enhances mitochondrial glutaminase expression and glutamine metabolism. *Nature* 458(7239):762-765.

48. Wise DR*, et al.* (2008) Myc regulates a transcriptional program that stimulates mitochondrial glutaminolysis and leads to glutamine addiction. *Proceedings of the National Academy of Sciences of the United States of America* 105(48):18782-18787.

49. Eagle H (1955) Nutrition needs of mammalian cells in tissue culture. *Science* 122(3168):501-514.

50. DeBerardinis RJ & Cheng T (2010) Q's next: the diverse functions of glutamine in metabolism, cell biology and cancer. *Oncogene* 29(3):313-324.

51. Weinberg F*, et al.* (2010) Mitochondrial metabolism and ROS generation are essential for Kras-mediated tumorigenicity. *Proceedings of the National Academy of Sciences of the United States of America* 107(19):8788-8793.

52. Shanware NP, Mullen AR, DeBerardinis RJ, & Abraham RT (2011) Glutamine: pleiotropic roles in tumor growth and stress resistance. *Journal of molecular medicine* 89(3):229-236.

53. Wise DR & Thompson CB (2010) Glutamine addiction: a new therapeutic target in cancer. *Trends in biochemical sciences* 35(8):427-433.

54. Klimberg VS & McClellan JL (1996) Claude H. Organ, Jr. Honorary Lectureship. Glutamine, cancer, and its therapy. *American journal of surgery* 172(5):418-424.

55. Chen MK, Espat NJ, Bland KI, Copeland EM, 3rd, & Souba WW (1993) Influence of progressive tumor growth on glutamine metabolism in skeletal muscle and kidney. *Annals of surgery* 217(6):655-666; discussion 666-657.

56. McGivan JD & Bungard CI (2007) The transport of glutamine into mammalian cells. *Frontiers in bioscience : a journal and virtual library* 12:874-882.

57. Ahluwalia GS, Grem JL, Hao Z, & Cooney DA (1990) Metabolism and action of amino acid analog anti-cancer agents. *Pharmacol Ther* 46(2):243-271.

58. DeBerardinis RJ*, et al.* (2007) Beyond aerobic glycolysis: transformed cells can engage in glutamine metabolism that exceeds the requirement for protein and nucleotide synthesis. *Proceedings of the National Academy of Sciences of the United States of America* 104(49):19345-19350.

59. Cairns RA, Harris IS, & Mak TW (2011) Regulation of cancer cell metabolism. *Nature reviews. Cancer* 11(2):85-95.

60. Hidalgo M*, et al.* (1998) A Phase I and pharmacological study of the glutamine antagonist acivicin with the amino acid solution aminosyn in patients with advanced solid malignancies. *Clinical cancer research : an official journal of the American Association for Cancer Research* 4(11):2763-2770.

61. Mueller C, Al-Batran, S., Jaeger, B., Bausch, M., Unger, C., and Sethuraman, N. (2008) A Phase IIa study of PEGylated glutaminase (PEG-PGA) plus 6-diazo-5-

oxo-L-norleucine (DON) in patients with advanced refractory solid tumors. *Journal of clinical oncology : official journal of the American Society of Clinical Oncology* 26.

62. Lessner HE, Valenstein S, Kaplan R, DeSimone P, & Yunis A (1980) Phase II study of L-asparaginase in the treatment of pancreatic carcinoma. *Cancer Treat Rep* 64(12):1359-1361.

63. Adam L, Crepin M, Savin C, & Israel L (1995) Sodium phenylacetate induces growth inhibition and Bcl-2 down-regulation and apoptosis in MCF7ras cells in vitro and in nude mice. *Cancer research* 55(22):5156-5160.

64. Samid D*, et al.* (1994) Selective activity of phenylacetate against malignant gliomas: resemblance to fetal brain damage in phenylketonuria. *Cancer research* 54(4):891-895.

65. Harrison LE, Wojciechowicz DC, Brennan MF, & Paty PB (1998) Phenylacetate inhibits isoprenoid biosynthesis and suppresses growth of human pancreatic carcinoma. *Surgery* 124(3):541-550.

66. Moldave K & Meister A (1957) Enzymic acylation of glutamine by phenylacetic acid. *Biochimica et biophysica acta* 24(3):654-655.

67. Brusilow SW*, et al.* (1984) Treatment of episodic hyperammonemia in children with inborn errors of urea synthesis. *N Engl J Med* 310(25):1630-1634.

68. Chang SM*, et al.* (1999) Phase II study of phenylacetate in patients with recurrent malignant glioma: a North American Brain Tumor Consortium report. *Journal of clinical oncology : official journal of the American Society of Clinical Oncology* 17(3):984-990.

69. Qu W*, et al.* (2011) Synthesis of optically pure 4-fluoro-glutamines as potential metabolic imaging agents for tumors. *Journal of the American Chemical Society* 133(4):1122-1133.

70. Kong Q, Beel JA, & Lillehei KO (2000) A threshold concept for cancer therapy. *Medical hypotheses* 55(1):29-35.

71. Lenehan PF*, et al.* (1995) Resistance to oxidants associated with elevated catalase activity in HL-60 leukemia cells that overexpress multidrug-resistance protein does not contribute to the resistance to daunorubicin manifested by these cells. *Cancer Chemother Pharmacol* 35(5):377-386.

72. Trachootham D*, et al.* (2008) Effective elimination of fludarabine-resistant CLL cells by PEITC through a redox-mediated mechanism. *Blood* 112(5):1912-1922.

73. Zhang H*, et al.* (2008) Effective killing of Gleevec-resistant CML cells with T315I mutation by a natural compound PEITC through redox-mediated mechanism. *Leukemia* 22(6):1191-1199.

74. Raj L*, et al.* (2011) Selective killing of cancer cells by a small molecule targeting the stress response to ROS. *Nature* 475(7355):231-234.

75. Shaw AT*, et al.* (2011) Selective killing of K-ras mutant cancer cells by small molecule inducers of oxidative stress. *Proceedings of the National Academy of Sciences of the United States of America* 108(21):8773-8778.

76. DeBerardinis RJ (2008) Is cancer a disease of abnormal cellular metabolism? New angles on an old idea. *Genetics in medicine : official journal of the American College of Medical Genetics* 10(11):767-777.

77. Rajagopalan KN & DeBerardinis RJ (2011) Role of glutamine in cancer: therapeutic and imaging implications. *Journal of nuclear medicine : official publication, Society of Nuclear Medicine* 52(7):1005-1008.

78. Reynolds MR*, et al.* (2013) Control of glutamine metabolism by the tumor suppressor Rb. *Oncogene*.

79. Nicolay BN*, et al.* (2013) Loss of RBF1 changes glutamine catabolism. *Genes & development* 27(2):182-196.

80. Ebi H*, et al.* (2009) Counterbalance between RB inactivation and miR-17-92 overexpression in reactive oxygen species and DNA damage induction in lung cancers. *Oncogene* 28(38):3371-3379.

81. Anglesio MS*, et al.* (2004) Differential expression of a novel ankyrin containing E3 ubiquitin-protein ligase, Hace1, in sporadic Wilms' tumor versus normal kidney. *Human molecular genetics* 13(18):2061-2074.

82. Zhang L*, et al.* (2007) The E3 ligase HACE1 is a critical chromosome 6q21 tumor suppressor involved in multiple cancers. *Nature medicine* 13(9):1060-1069.

83. Hibi K*, et al.* (2008) Aberrant methylation of the HACE1 gene is frequently detected in advanced colorectal cancer. *Anticancer research* 28(3A):1581-1584.

84. Thelander EF*, et al.* (2008) Characterization of 6q deletions in mature B cell lymphomas and childhood acute lymphoblastic leukemia. *Leukemia & lymphoma* 49(3):477-487.

85. Sakata M*, et al.* (2009) Methylation of HACE1 in gastric carcinoma. *Anticancer research* 29(6):2231-2233.

86. Huang Y*, et al.* (2010) Gene expression profiling identifies emerging oncogenic pathways operating in extranodal NK/T-cell lymphoma, nasal type. *Blood* 115(6):1226-1237.

87. Slade I*, et al.* (2010) Constitutional translocation breakpoint mapping by genome-wide paired-end sequencing identifies HACE1 as a putative Wilms tumour susceptibility gene. *Journal of medical genetics* 47(5):342-347.

88. Diskin SJ*, et al.* (2012) Common variation at 6q16 within HACE1 and LIN28B influences susceptibility to neuroblastoma. *Nature genetics* 44(10):1126-1130.

89. Mettouchi A & Lemichez E (2012) Ubiquitylation of active Rac1 by the E3 ubiquitin-ligase HACE1. *Small GTPases* 3(2):102-106.

90. Castillo-Lluva S, Tan CT, Daugaard M, Sorensen PH, & Malliri A (2013) The tumour suppressor HACE1 controls cell migration by regulating Rac1 degradation. *Oncogene* 32(13):1735-1742.

91. Torrino S*, et al.* (2011) The E3 ubiquitin-ligase HACE1 catalyzes the ubiquitylation of active Rac1. *Developmental cell* 21(5):959-965.

92. Cheng G, Diebold BA, Hughes Y, & Lambeth JD (2006) Nox1-dependent reactive oxygen generation is regulated by Rac1. *The Journal of biological chemistry* 281(26):17718-17726.

93. Ueyama T, Geiszt M, & Leto TL (2006) Involvement of Rac1 in activation of multicomponent Nox1- and Nox3-based NADPH oxidases. *Molecular and cellular biology* 26(6):2160-2174.

94. Daugaard M*, et al.* (2013) Hace1 controls ROS generation of vertebrate Rac1-dependent NADPH oxidase complexes. *Nature communications* 4:2180.

95. Wellen KE*, et al.* (2010) The hexosamine biosynthetic pathway couples growth factor-induced glutamine uptake to glucose metabolism. *Genes & development* 24(24):2784-2799.

96. Cheng T*, et al.* (2011) Pyruvate carboxylase is required for glutamine-independent growth of tumor cells. *Proceedings of the National Academy of Sciences of the United States of America* 108(21):8674-8679.

97. Fernandez CA, Des Rosiers C, Previs SF, David F, & Brunengraber H (1996) Correction of 13C mass isotopomer distributions for natural stable isotope abundance. *J Mass Spectrom* 31(3):255-262.

98. Tong X, Zhao F, & Thompson CB (2009) The molecular determinants of de novo nucleotide biosynthesis in cancer cells. *Current opinion in genetics & development* 19(1):32-37.

99. Moldave K & Meister A (1957) Synthesis of phenylacetylglutamine by human tissue. *The Journal of biological chemistry* 229(1):463-476.

100. Li XN*, et al.* (2004) Phenylbutyrate and phenylacetate induce differentiation and inhibit proliferation of human medulloblastoma cells. *Clinical cancer research : an official journal of the American Association for Cancer Research* 10(3):1150-1159.

101. Nicklin P*, et al.* (2009) Bidirectional transport of amino acids regulates mTOR and autophagy. *Cell* 136(3):521-534.

102. Bedard K & Krause KH (2007) The NOX family of ROS-generating NADPH oxidases: physiology and pathophysiology. *Physiological reviews* 87(1):245-313.

103. Roth E*, et al.* (2002) Regulative potential of glutamine--relation to glutathione metabolism. *Nutrition* 18(3):217-221.

104. Flaring UB, Rooyackers OE, Wernerman J, & Hammarqvist F (2003) Glutamine attenuates post-traumatic glutathione depletion in human muscle. *Clinical science* 104(3):275-282.

105. Brennan L*, et al.* (2003) 13C NMR analysis reveals a link between L-glutamine metabolism, D-glucose metabolism and gamma-glutamyl cycle activity in a clonal pancreatic beta-cell line. *Diabetologia* 46(11):1512-1521.

106. Jeon SM, Chandel NS, & Hay N (2012) AMPK regulates NADPH homeostasis to promote tumour cell survival during energy stress. *Nature* 485(7400):661-665.

107. Ros S*, et al.* (2012) Functional metabolic screen identifies 6-phosphofructo-2-kinase/fructose-2,6-biphosphatase 4 as an important regulator of prostate cancer cell survival. *Cancer discovery* 2(4):328-343.

108. Mullen AR*, et al.* (2012) Reductive carboxylation supports growth in tumour cells with defective mitochondria. *Nature* 481(7381):385-388.

109. Deberardinis RJ, Lum JJ, & Thompson CB (2006) Phosphatidylinositol 3-kinase-dependent modulation of carnitine palmitoyltransferase 1A expression regulates lipid metabolism during hematopoietic cell growth. *The Journal of biological chemistry* 281(49):37372-37380.

110. Simbulan-Rosenthal CM, Rosenthal DS, Iyer S, Boulares AH, & Smulson ME (1998) Transient poly(ADP-ribosyl)ation of nuclear proteins and role of poly(ADP-ribose) polymerase in the early stages of apoptosis. *The Journal of biological chemistry* 273(22):13703-13712.

111. Bonner WM*, et al.* (2008) GammaH2AX and cancer. *Nature reviews. Cancer* 8(12):957-967.

112. Loike JD & Horwitz SB (1976) Effect of VP-16-213 on the intracellular degradation of DNA in HeLa cells. *Biochemistry* 15(25):5443-5448.

113. Wozniak AJ & Ross WE (1983) DNA damage as a basis for 4'-demethylepipodophyllotoxin-9-(4,6-O-ethylidene-beta-D-glucopyranoside) (etoposide) cytotoxicity. *Cancer research* 43(1):120-124.

114. Dang CV (2012) Cancer cell metabolism: there is no ROS for the weary. *Cancer discovery* 2(4):304-307.

115. Kaadige MR, Looper RE, Kamalanaadhan S, & Ayer DE (2009) Glutamine-dependent anapleurosis dictates glucose uptake and cell growth by regulating MondoA transcriptional activity. *Proceedings of the National Academy of Sciences of the United States of America* 106(35):14878-14883.

116. Kaimul AM, Nakamura H, Masutani H, & Yodoi J (2007) Thioredoxin and thioredoxin-binding protein-2 in cancer and metabolic syndrome. *Free radical biology & medicine* 43(6):861-868.

117. Junn E*, et al.* (2000) Vitamin D3 up-regulated protein 1 mediates oxidative stress via suppressing the thioredoxin function. *Journal of immunology* 164(12):6287-6295.

118. Patwari P*, et al.* (2009) Thioredoxin-independent regulation of metabolism by the alpha-arrestin proteins. *The Journal of biological chemistry* 284(37):24996-25003.

119. Adams DJ*, et al.* (2012) Synthesis, cellular evaluation, and mechanism of action of piperlongumine analogs. *Proceedings of the National Academy of Sciences of the United States of America* 109(38):15115-15120.

120. Yuneva M, Zamboni N, Oefner P, Sachidanandam R, & Lazebnik Y (2007) Deficiency in glutamine but not glucose induces MYC-dependent apoptosis in human cells. *The Journal of cell biology* 178(1):93-105.

121. Fuchs BC & Bode BP (2005) Amino acid transporters ASCT2 and LAT1 in cancer: partners in crime? *Seminars in cancer biology* 15(4):254-266.

122. Liu SX, Athar M, Lippai I, Waldren C, & Hei TK (2001) Induction of oxyradicals by arsenic: implication for mechanism of genotoxicity. *Proceedings of the National Academy of Sciences of the United States of America* 98(4):1643-1648.

123. Veal EA, Day AM, & Morgan BA (2007) Hydrogen peroxide sensing and signaling. *Molecular cell* 26(1):1-14.

124. Xia Z, Dickens M, Raingeaud J, Davis RJ, & Greenberg ME (1995) Opposing effects of ERK and JNK-p38 MAP kinases on apoptosis. *Science* 270(5240):1326-1331.

125. Tobiume K*, et al.* (2001) ASK1 is required for sustained activations of JNK/p38 MAP kinases and apoptosis. *EMBO reports* 2(3):222-228.

126. Nadeau PJ, Charette SJ, Toledano MB, & Landry J (2007) Disulfide Bond-mediated multimerization of Ask1 and its reduction by thioredoxin-1 regulate H(2)O(2)-induced c-Jun NH(2)-terminal kinase activation and apoptosis. *Molecular biology of the cell* 18(10):3903-3913.

127. Cappellini A*, et al.* (2005) Antiapoptotic role of p38 mitogen activated protein kinase in Jurkat T cells and normal human T lymphocytes treated with 8-methoxypsoralen and ultraviolet-A radiation. *Apoptosis : an international journal on programmed cell death* 10(1):141-152.

128. Wagner EF & Nebreda AR (2009) Signal integration by JNK and p38 MAPK pathways in cancer development. *Nature reviews. Cancer* 9(8):537-549.

129. Shi GX, Jin L, & Andres DA (2011) A rit GTPase-p38 mitogen-activated protein kinase survival pathway confers resistance to cellular stress. *Molecular and cellular biology* 31(10):1938-1948.

130. Cai W*, et al.* (2011) An evolutionarily conserved Rit GTPase-p38 MAPK signaling pathway mediates oxidative stress resistance. *Molecular biology of the cell* 22(17):3231-3241.

131. Lahti A, Sareila O, Kankaanranta H, & Moilanen E (2006) Inhibition of p38 mitogen-activated protein kinase enhances c-Jun N-terminal kinase activity: implication in inducible nitric oxide synthase expression. *BMC pharmacology* 6:5.

132. Muniyappa H & Das KC (2008) Activation of c-Jun N-terminal kinase (JNK) by widely used specific p38 MAPK inhibitors SB202190 and SB203580: a MLK-3-MKK7-dependent mechanism. *Cellular signalling* 20(4):675-683.

133. Ng TL*, et al.* (2012) The AMPK stress response pathway mediates anoikis resistance through inhibition of mTOR and suppression of protein synthesis. *Cell death and differentiation* 19(3):501-510.

134. Leprivier G*, et al.* (2013) The eEF2 Kinase Confers Resistance to Nutrient Deprivation by Blocking Translation Elongation. *Cell* 153(5):1064-1079.

135. Zmijewski JW*, et al.* (2010) Exposure to hydrogen peroxide induces oxidation and activation of AMP-activated protein kinase. *The Journal of biological chemistry* 285(43):33154-33164.

136. Hardie DG, Ross FA, & Hawley SA (2012) AMPK: a nutrient and energy sensor that maintains energy homeostasis. *Nature reviews. Molecular cell biology* 13(4):251-262.

137. Eijkelenboom A & Burgering BM (2013) FOXOs: signalling integrators for homeostasis maintenance. *Nature reviews. Molecular cell biology* 14(2):83-97.

138. Greer EL*, et al.* (2007) The energy sensor AMP-activated protein kinase directly regulates the mammalian FOXO3 transcription factor. *The Journal of biological chemistry* 282(41):30107-30119.

139. Sporn MB & Liby KT (2012) NRF2 and cancer: the good, the bad and the importance of context. *Nature reviews. Cancer* 12(8):564-571.

140. Gupta S, Campbell D, Derijard B, & Davis RJ (1995) Transcription factor ATF2 regulation by the JNK signal transduction pathway. *Science* 267(5196):389-393.

141. Hayakawa J*, et al.* (2004) Identification of promoters bound by c-Jun/ATF2 during rapid large-scale gene activation following genotoxic stress. *Molecular cell* 16(4):521-535.

142. Fuchs BC, Perez JC, Suetterlin JE, Chaudhry SB, & Bode BP (2004) Inducible antisense RNA targeting amino acid transporter ATB0/ASCT2 elicits apoptosis in human hepatoma cells. *American journal of physiology. Gastrointestinal and liver physiology* 286(3):G467-478.

143. Hassanein M*, et al.* (2013) SLC1A5 mediates glutamine transport required for lung cancer cell growth and survival. *Clinical cancer research : an official journal of the American Association for Cancer Research* 19(3):560-570.

144. Bungard CI & McGivan JD (2004) Glutamine availability up-regulates expression of the amino acid transporter protein ASCT2 in HepG2 cells and stimulates the ASCT2 promoter. *The Biochemical journal* 382(Pt 1):27-32.

145. Mihaylova MM & Shaw RJ (2011) The AMPK signalling pathway coordinates cell growth, autophagy and metabolism. *Nature cell biology* 13(9):1016-1023.

146. Kurth-Kraczek EJ, Hirshman MF, Goodyear LJ, & Winder WW (1999) 5' AMP-activated protein kinase activation causes GLUT4 translocation in skeletal muscle. *Diabetes* 48(8):1667-1671.

147. Barnes K*, et al.* (2002) Activation of GLUT1 by metabolic and osmotic stress: potential involvement of AMP-activated protein kinase (AMPK). *Journal of cell science* 115(Pt 11):2433-2442.

148. Perez-Sampietro M, Casas C, & Herrero E (2013) The AMPK family member Snf1 protects Saccharomyces cerevisiae cells upon glutathione oxidation. *PloS one* 8(3):e58283.

149. Chen L*, et al.* (2010) Hydrogen peroxide inhibits mTOR signaling by activation of AMPKalpha leading to apoptosis of neuronal cells. *Laboratory investigation; a journal of technical methods and pathology* 90(5):762-773.

150. Hawley SA*, et al.* (2010) Use of cells expressing gamma subunit variants to identify diverse mechanisms of AMPK activation. *Cell metabolism* 11(6):554-565.

151. Choi SL*, et al.* (2001) The regulation of AMP-activated protein kinase by H(2)O(2). *Biochemical and biophysical research communications* 287(1):92-97.

152. Emerling BM*, et al.* (2009) Hypoxic activation of AMPK is dependent on mitochondrial ROS but independent of an increase in AMP/ATP ratio. *Free radical biology & medicine* 46(10):1386-1391.

153. Christensen HN, Liang M, & Archer EG (1967) A distinct Na+-requiring transport system for alanine, serine, cysteine, and similar amino acids. *The Journal of biological chemistry* 242(22):5237-5246.

154. King N, Lin H, & Suleiman MS (2011) Oxidative stress increases SNAT1 expression and stimulates cysteine uptake in freshly isolated rat cardiomyocytes. *Amino acids* 40(2):517-526.